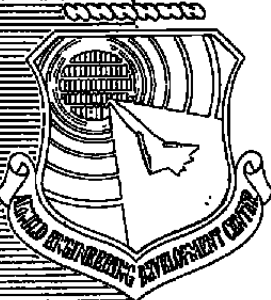


AEDC-TR-80-30

C.1

ARCHIVE COPY
DO NOT LOAN



Infrared Optical Properties of Solid Mixtures of Molecular Species at 20°K

K. F. Palmer
Westminster College
Fulton, Missouri

and

B. E. Wood and J. A. Roux
ARO, Inc.

January 1981

Final Report for Period October 1, 1979 — February 1, 1980

Approved for public release; distribution unlimited.

Property of U. S. Air Force
AEDC LIBRARY
F40600-81-C-0004

ARNOLD ENGINEERING DEVELOPMENT CENTER
ARNOLD AIR FORCE STATION, TENNESSEE
AIR FORCE SYSTEMS COMMAND
UNITED STATES AIR FORCE



NOTICES

When U. S. Government drawings, specifications, or other data are used for any purpose other than a definitely related Government procurement operation, the Government thereby incurs no responsibility nor any obligation whatsoever, and the fact that the Government may have formulated, furnished, or in any way supplied the said drawings, specifications, or other data, is not to be regarded by implication or otherwise, or in any manner licensing the holder or any other person or corporation, or conveying any rights or permission to manufacture, use, or sell any patented invention that may in any way be related thereto.

Qualified users may obtain copies of this report from the Defense Technical Information Center.

References to named commercial products in this report are not to be considered in any sense as an indorsement of the product by the United States Air Force or the Government.

This report has been reviewed by the Office of Public Affairs (PA) and is releasable to the National Technical Information Service (NTIS). At NTIS, it will be available to the general public, including foreign nations.

APPROVAL STATEMENT

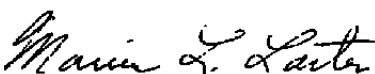
This report has been reviewed and approved.



KENNETH H. LENERS, Captain, USAF
Project Manager
Directorate of Technology

Approved for publication:

FOR THE COMMANDER



MARION L. LASTER
Director of Technology
Deputy for Operations

UNCLASSIFIED

REPORT DOCUMENTATION PAGE		READ INSTRUCTIONS BEFORE COMPLETING FORM
1 REPORT NUMBER AEDC-TR-80-30	2 GOVT ACCESSION NO.	3 RECIPIENT'S CATALOG NUMBER
4 TITLE (and Subtitle) INFRARED OPTICAL PROPERTIES OF SOLID MIXTURES OF MOLECULAR SPECIES AT 20°K		5 TYPE OF REPORT & PERIOD COVERED Final Report-October 1, 1979 to February 1, 1980
		6 PERFORMING ORG REPORT NUMBER
7 AUTHOR(s) K. F. Palmer, Westminster College, Fulton, Missouri, and B. E. Wood and J. A. Roux, ARO, Inc., a Sverdrup Corporation Company		8. CONTRACT OR GRANT NUMBER(s)
9 PERFORMING ORGANIZATION NAME AND ADDRESS Arnold Engineering Development Center/DOT Air Force Systems Command Arnold Air Force Station, Tennessee 37389		10. PROGRAM ELEMENT, PROJECT, TASK AREA & WORK UNIT NUMBERS Program Element 65807F
11 CONTROLLING OFFICE NAME AND ADDRESS Arnold Engineering Development Center/DOS Air Force Systems Command Arnold Air Force Station, Tennessee 37389		12 REPORT DATE January 1981
14 MONITORING AGENCY NAME & ADDRESS (if different from Controlling Office)		13. NUMBER OF PAGES 132
		15 SECURITY CLASS (of this report) UNCLASSIFIED
		15a DECLASSIFICATION/DOWNGRADING SCHEDULE N/A
16 DISTRIBUTION STATEMENT (of this Report) Approved for public release; distribution unlimited.		
17 DISTRIBUTION STATEMENT (of the abstract entered in Block 20, if different from Report)		
18 SUPPLEMENTARY NOTES Available in Defense Technical Information Center (DTIC).		
19 KEY WORDS (Continue on reverse side if necessary and identify by block number) infrared spectra refractive index thin films least squares method cryogenics mathematical models Fourier spectrometers Kramers-Kronig method		
20 ABSTRACT (Continue on reverse side if necessary and identify by block number) Infrared transmittance spectra were measured by a Fourier transform spectrometer for 200K cryofilms of homogeneous mixtures of N ₂ , Ar, NH ₃ , CO, CO ₂ , and H ₂ O molecules. Such cryofilms may contaminate cryogenic optical surfaces of spacecraft or aircraft. The films, cryopumped onto a 200K germanium substrate, varied from 0.24 to 13 μm thick. The spectral domain ranged from 500 to 3700 cm ⁻¹ . For all films, the complex refractive index ($\hat{n} = n + ik$)		

UNCLASSIFIED

UNCLASSIFIED

20. ABSTRACT (Continued)

was determined at each wavenumber by fitting the experimental behavior of the transmittance with film thickness to a lamellate model of the film and substrate. The model accounts for beam reflection losses as well as attenuation caused by passing the beam through the film and substrate materials. A Kramers-Kronig (KK) technique for obtaining the n values is compared with the thin-film determination of n.

PREFACE

The work reported herein was conducted by the Arnold Engineering Development Center (AEDC), Air Force Systems Command (AFSC). The results were obtained by ARO, Inc., AEDC Division (a Sverdrup Corporation Company), operating contractor for the AEDC, AFSC, Arnold Air Force Station, Tennessee, under ARO Project No. P32K-13. The project manager was Dr. Herman E. Scott. The manuscript was submitted for publication on July 1, 1980.

CONTENTS

	<u>Page</u>
1.0 INTRODUCTION	7
2.0 INSTRUMENTATION	8
3.0 PROCEDURE	8
4.0 TRANSMITTANCE OF CRYOFILMS ON A 20°K GERMANIUM SUBSTRATE	
4.1 Films Containing NH₃	11
4.2 20°K Films Containing Only N₂, CO, or CO₂	12
4.3 20°K Films Containing H₂O	15
5.0 THE INFRARED (IR) OPTICAL PROPERTIES OF CRYOFILMS	
5.1 Analytical Model of the Film and Substrate Interactions with a Normally Incident IR Beam	19
5.2 Computation of the Optical Constants	23
6.0 SUMMARY	28
7.0 REFERENCES	28

ILLUSTRATIONS

Figure

1. Schematic of the Infrared Optical Transmission Chamber (IROTC) with FTS-14 Interferometer Spectrometer	33
2. Plan and Elevation Views of Cryogenically Cooled Window Holder	34
3. Gas Deposition System	35
4. Transmittance of 1.43-μm-Thick Solid NH₃ on 20°K Germanium	36
5. Transmittance of 4.97-μm-Thick Solid NH₃/N₂ Mixture (20%/80%) on 20°K Germanium	36
6. Transmittance of 4.97-μm-Thick Solid NH₃/N₂ Mixture (20%/80%) after Warmup from 20 to 59°K on Germanium	37
7. Transmittance of Pure CO on 20°K Germanium	37
8. Transmittance of 4.765-μm-Thick Solid N₂/CO Mixture (79%/20%) on 20°K Germanium	38
9. Transmittance of 3.88-μm-Thick Solid CO₂ on 20°K Germanium	39
10. Transmittance of 4.74-μm-Thick Solid CO₂/N₂ Mixture (20%/80%) on 20°K Germanium	39

<u>Figure</u>	<u>Page</u>
11. Transmittance of 13.16- μm -Thick Solid CO ₂ /CO Mixture (50%/50%) on 20°K Germanium	40
12. Transmittance of 13.16- μm -Thick Solid CO ₂ /CO Mixture (50%/50%) after Warmup from 20 to 50°K on Germanium	40
13. Transmittance of 6.602- μm -Thick Solid N ₂ /CO/CO ₂ Mixture (64%/23%/13%) on 20°K Germanium	41
14. Transmittance of 1.00- μm -Thick Solid H ₂ O on 20°K Germanium	42
15. Transmittance of 3.49- μm -Thick Solid H ₂ O/CO ₂ Mixture (61%/36%) on 20°K Germanium	42
16. Transmittance of 3.49- μm -Thick Solid H ₂ O/CO ₂ Mixture (61%/36%) after Warmup from 20 to 153°K on Germanium	43
17. Transmittance of 6.78- μm -Thick Solid N ₂ /H ₂ O/CO ₂ Mixture (86%/13%/1%) on 20°K Germanium	43
18. Transmittance of 5.75- μm -Thick Solid Ar/H ₂ O Mixture (93%/6%) on 20°K Germanium	44
19. Transmittance of 6.54- μm -Thick Solid CO/H ₂ O Mixture (91%/9%) on 20°K Germanium	45
20. Transmittance of 6.54- μm -Thick Solid CO/H ₂ O Mixture (91%/9%) after Warmup from 20 to 105°K on Germanium	45
21. Transmittance of 6.72- μm -Thick Solid Simulated Plume Mixture 1 on 20°K Germanium	46
22. Transmittance of 6.72- μm -Thick Solid Simulated Plume Mixture after Warmup of Germanium from 20 to 96°K	46
23. Geometry Depicting Analytical Model for a Thin Film Formed on a Thick Film	47
24. Refractive Index of Solid N ₂ /NH ₃ Mixture (85%/15%) on 20°K Germanium	48
25. Absorption Index of Solid N ₂ /NH ₃ Mixture (85%/15%) on 20°K Germanium	49
26. Comparison of the Data with the Nonlinear Least-Squares Fit for N ₂ /NH ₃ Films (85%/15%) at 1038, 2850, and 3386 cm ⁻¹	50
27. Refractive Index of Solid N ₂ /CO Mixture (79%/20%) on 20°K Germanium	51
28. Absorption Index of Solid N ₂ /CO Mixture (79%/20%) on 20°K Germanium	52
29. Refractive Index of Solid N ₂ /CO ₂ Mixture (75%/25%) on 20°K Germanium	53
30. Absorption Index of Solid N ₂ /CO ₂ Mixture (75%/25%) on 20°K Germanium	54

<u>Figure</u>	<u>Page</u>
31. Refractive Index of Solid CO/CO ₂ Mixture (50%/50%) on 20°K Germanium	55
32. Absorption Index of Solid CO/CO ₂ Mixture (50%/50%) on 20°K Germanium	56
33. Refractive Index of Solid N ₂ /CO/CO ₂ Mixture (64%/23%/13%) on 20°K Germanium	57
34. Absorption Index of Solid N ₂ /CO/CO ₂ Mixture (64%/23%/13%) on 20°K Germanium	58
35. Refractive Index of Solid H ₂ O/CO ₂ Mixture (61%/36%) on 20°K Germanium	59
36. Absorption Index of Solid H ₂ O/CO ₂ Mixture (61%/36%) on 20°K Germanium	60
37. Refractive Index of Solid N ₂ /H ₂ O Mixture (87%/12%) on 20°K Germanium	61
38. Absorption Index of Solid N ₂ /H ₂ O Mixture (87%/12%) on 20°K Germanium	62
39. Refractive Index of Solid Ar/H ₂ O Mixture (93%/6%) on 20°K Germanium	63
40. Absorption Index of Solid Ar/H ₂ O Mixture (93%/6%) on 20°K Germanium	64
41. Refractive Index of Solid CO/H ₂ O Mixture (91%/9%) on 20°K Germanium	65
42. Absorption Index of Solid CO/H ₂ O Mixture (91%/9%) on 20°K Germanium	66
43. Refractive Index of Solid Simulated Plume Mixture N ₂ /H ₂ O/CO ₂ /CO (50%/23%/17%/10%) on 20°K Germanium	67
44. Absorption Index of Solid Simulated Plume Mixture N ₂ /H ₂ O/CO ₂ /CO (50%/23%/17%/10%) on 20°K Germanium	68

TABLES

1. Physical Properties of 20°K Cryofilms	69
2. Locations of Absorption Bands of Molecular Species in 20°K Cryofilms (cm ⁻¹)	70
3. Optical Constants of 20°K N ₂ /NH ₃	72
4. Optical Constants of 20°K N ₂ /CO	78
5. Optical Constants of 20°K N ₂ /CO ₂	82
6. Optical Constants of 20°K CO/CO ₂	87
7. Optical Constants of 20°K N ₂ /CO/CO ₂	93

<u>Figure</u>	<u>Page</u>
8. Optical Constants of 20°K H ₂ O/CO ₂	99
9. Optical Constants of 20°K N ₂ /H ₂ O	105
10. Optical Constants of 20°K Ar/H ₂ O	113
11. Optical Constants of 20°K CO/CO ₂	120
12. Optical Constants of 20°K Simulated Plume Mixture	128

1.0 INTRODUCTION

Cryogenic surfaces within infrared (IR) optical devices on spacecraft and on high-altitude aircraft can be contaminated by the condensation of engine exhaust and atmospheric gases. The degradation in performance of these optical devices by absorption and interference effects depends on the optical characteristics of the contaminating cryofilm. The optical properties are conveniently summarized by the complex index of refraction: $\hat{n} = n + ik$, where n is the (real) refraction index and k is the absorption index. The "plus" symbol in this definition is appropriate for plane wave electromagnetic radiation with a time dependence proportional to $\exp(-i\omega t)$.

Roux et al. (Refs. 1, 2, and 3) have identified common molecular contaminants from exhausts and in the atmosphere. These include the IR-active molecular species CO₂, H₂O, NH₃, CO, NO, CH₄, HCl, and N₂O; unburned fuels such as MMH and N₂H₄, oxidizer N₂O₄, and the IR-inactive species N₂, Ar, and O₂. The IR transmittance spectra and optical constants of pure CO₂, H₂O, and NH₃ films on a 20°K germanium (Ge) substrate are given in Ref. 1, along with the transmittance spectra of several mixtures (also on a 20°K Ge substrate): N₂/CO₂, N₂/H₂O, N₂/NH₃, Ar/H₂O, and H₂O/CO₂. The transmittance spectrum of a simulated plume mixture (N₂/H₂O/CO₂/CO) appears in Ref. 4. In this report the optical properties of these mixtures are tabulated and discussed along with the spectra and optical properties of N₂/CO, CO₂/CO, N₂/CO/CO₂, and CO/H₂O cryofilms on 20°K Ge. Of particular interest are the changes in the optical properties of cryofilms as the proportions of their molecular constituents are varied. Changes in intermolecular interactions are shown in Section 4.0 to be dependent on the type of molecular association (e.g., Van der Waals, or hydrogen bonding) and the concentrations of molecular species in the cryofilm.

Several means can determine the optical properties of film materials, including transmittance and reflectance measurements, internal reflection spectroscopy (IRS), and polarimetry methods such as ellipsometry. Kramers-Kronig (KK) dispersion analysis of data has been commonly used to extract $n(\nu)$ and $k(\nu)$ (Refs. 5 and 6), and computer programs have been used for KK analysis in this report.

The next two sections briefly describe the experiment. References 7 and 1 may be consulted for further details: Ref. 7 details the experimental apparatus and procedure used in this report, and Ref. 1 summarizes the experimental details.

2.0 INSTRUMENTATION

Figure 1 shows the path followed by the IR beam from the IR interferometer (Digilab Model FTS-14), through the 4-mm-thick Ge substrate (or window) of the Infrared Optical Transmission Chamber (IROTC), to the pyroelectric detector. The interferometer is capable of 0.5 cm^{-1} resolution; its wavenumber accuracy is 0.02 cm^{-1} . A liquid-nitrogen (LN_2)-cooled liner allowed a vacuum of 10^{-8} torr to be achieved in the IROTC.

The window holder (Fig. 2) cools the Ge substrate with use of either gaseous He (20°K) or LN_2 (80°K). For all of the measurements described in this report, the temperature of the Ge substrate was 20°K .

The contaminant gases to be condensed on the Ge window entered the evacuated chamber through a toroidal header, as indicated in Fig. 3. A quartz crystal microbalance (QCM) adjacent to the Ge window monitored the surface density (mass per unit area) of the condensed gases. The film surface density and the interference patterns from the two laser beams shown in Fig. 1 were used to calculate the film index of refraction at $0.6328 \mu\text{m}$, the film thickness, and the film density as explained in the next section. The films formed on the Ge window were uniformly thick and nearly undetectable in visible light unless fractured or shattered (Ref. 1).

3.0 PROCEDURE

When the LN_2 liner was filled and the cryostat was used to cool the Ge window, the holder, and the transfer line at nearly 20°K , the chamber pressure was in the low 10^{-8} torr range. After pressure and thermal equilibriums were reached, a reference IR power spectrum was recorded and stored by the interferometer while the Ge window was out of the IR beam. Before a Fourier transform was done, 16 interferograms at 4 cm^{-1} were usually co-added to ensure obtaining a large signal-to-noise ratio. The process was repeated with the Ge window in the IR beam path for zero and nonzero film thicknesses. The ratio of the reference power spectrum to the sample power spectrum (the absolute transmittance) was computed every 2 cm^{-1} and then plotted.

Research grade CO_2 , CO, NH_3 or Ar gas in lecture bottles was introduced at the gas supply (Fig. 3). Before entering the chamber, water vapor, boiled off from distilled water in a vacuum, was purified further by a mechanical pump that removed foreign gases. For contaminant films of more than one constituent, the nominal mole fractions of a molecular species were found from the gas partial pressures. The Chemical Laboratory at AEDC revised these estimates of the mole fractions using chromatography methods on samples of the original gas mixture.

As the gases condensed onto the Ge substrate, the intensity changes (due to thin film interference) of two helium-neon laser beams reflected from the film were monitored. The rays had incident angles of θ_a and θ_b (typically 18 deg and 68 deg). The refractive index at $\lambda = 0.6328 \mu\text{m}$ was calculated from (Ref. 8)

$$n = \left[(\sin^2 \theta_b - \beta^2 \sin^2 \theta_a) / (1 - \beta^2) \right]^{\frac{1}{2}} \quad (1)$$

where β is the ratio of the period of the interference pattern at θ_b to that at θ_a . The film thickness, d_i , was found for each experiment from the relation

$$m \lambda = 2d_i (n^2 - \sin^2 \theta)^{\frac{1}{2}} \quad (2)$$

where m is the order of the interference maximum at incident angle θ . In practice, θ_a was the incident angle used in Eq. (2) because of its smaller periods. The orders m were usually integer, except for the occasional half-integral values used for highly absorbing films.

The surface mass density measurements provided by the QCM were used along with the film thickness measurements to find the volume mass density of the contaminant film. The precise measurement of film density is especially important in computing mole fractions from optical data.

At a given wavenumber, mathematical determination of the optical constants n and k requires transmittance measurements of at least two film thicknesses. However, in this work, measurements from more than two thicknesses were used to overdetermine n and k with a nonlinear least-squares computational technique so that more accurate constants could be obtained. Since some films fractured or shattered more easily than others at large thicknesses, the number of film thicknesses at which transmittance measurements were made varied from film to film. For example, because of the film's shattering, Roux et al. (Ref. 1) were able to see a pure 20°K H₂O film 1 μm thick, whereas most of the films in this report were invisible even at thicknesses greater than 5 μm .

4.0 TRANSMITTANCE OF CRYOFILMS ON A 20°K GERMANIUM SUBSTRATE

For condensed phases, intermolecular interactions affect the intramolecular interactions of the atomic constituents within a molecule. The optical spectra of condensed phases show shifts in the positions of molecular absorptions, different intensities, and new absorptions due to lattice or multimer movements when compared to the gas phase spectra. These effects usually increase as the strengths of the intermolecular interactions increase. For the weaker Van der Waals interaction, the changes in the vibrational band positions and intensities are

not drastic, although rotational and translational motion may be severely restricted. Interactions among Ar, CO, and CO₂ molecules are Van der Waals type interactions.

However, for hydrogen-containing molecules, which are subject to the stronger hydrogen bonding with neighboring molecules, the spectral changes between gas and condensed phases can be spectacular. A noteworthy example is the H₂O molecule. When H₂O is hydrogen-bonded with other H₂O molecules — as in pure H₂O films or in films in which H₂O is the major constituent — the well defined gas phase bands at 3151 cm⁻¹ ($2\nu_2$), 3652 cm⁻¹ (ν_1) and 3756 cm⁻¹ (ν_3) are seen in the films as one broad band centered near 3300 cm⁻¹ with an integrated absorption intensity an order of magnitude greater than the sum of the corresponding gas phase intensities (Ref. 7). NH₃ also forms hydrogen bonds which affect its spectra.

Roux et al. (Ref. 1) discuss the transmittance spectra for cryofilms deposited on 20°K Ge for pure NH₃, pure CO₂, pure H₂O, and the mixtures 85% N₂/12% H₂O/(1% CO₂), 93% Ar/6% H₂O/(0.5% CO₂), 61% H₂O/36% CO₂/(2% N₂), and 91% CO₂/9% H₂O. Reference 4 contains a discussion of the spectrum of a simulated plume mixture, 50% N₂/23% H₂O/17% CO₂/10% CO. Some of the details on these spectra that are not given in this work are included in those references. This report also gives the previously unpublished transmittance spectra of 79% N₂/20% CO/ (< 0.5% CO₂), 49.8% CO₂/49.5% CO, 64% N₂/23% CO/13% CO₂, and 91% CO/9% H₂O.

Table 1 lists values for some physical properties of the films that are mixtures of molecular species; the spectra and the optical constants are given in this report. The percent mole fraction values are from the analysis that the Chemical Laboratory performed on a sample of the original gas mixture taken from the mixing chamber ahead of the gas jets in the IROTC. The index of refraction at the He-Ne (helium-neon) laser wavelength (0.6328 μm) was found from Eq. (1), and was used to calculate film thicknesses and the mass densities in the manner explained in Section 3.0. The calculation of the optical indices n and k (Section 5.0) included transmittance measurements from the number of film thicknesses given in the table. Thicknesses ranged from zero to the tabulated maximum thickness.

The locations of those absorptions in the 20°K cryofilms that can be attributed to a certain molecular species are contained in Table 2. For the pure molecular species, the vapor phase molecular band locations are those given in Ref. 10, and the solid phase positions are those extracted from the measurements included in Ref. 1, except for the CO absorptions. The CO positions, which were obtained from the data of Refs. 3 and 11, agree with the locations given for pure CO in Ref. 12. The values in parentheses indicate molecular species present in the cryofilms in amounts less than 1 percent mole fraction.

4.1 FILMS CONTAINING NH₃

Figures 4 and 5 show the transmittance spectra of the pure NH₃ film and that of the 85% N₂/15% NH₃ film. Both figures show the maxima and minima attributable to thin-film interference, which is termed "channel spectra." A comparison of Figs. 4 and 5 indicates that the N₂/NH₃ film has several absorptions not found in the spectra of pure NH₃ films and that it has shifted band positions (Ref. 1). The broad weak absorptions at 770 and 850 cm⁻¹ and much of the stronger absorption below 700 cm⁻¹ are attributable to the Ge substrate. Because these Ge absorptions appear in the transmittance data for all films, all the measurements below 700 cm⁻¹ are unreliable.

Table 2 assigns the prominent absorptions of the pure NH₃ film at 1075, 1627, 3210, 3295 and 3376 cm⁻¹ to the low-lying intramolecular vibrational modes of the NH₃ molecule. The table also lists the locations of the corresponding absorptions of the N₂/NH₃ film. The large shifts in band positions from those of the pure vapor phase of NH₃ are less drastic in the solid N₂/NH₃ film than in the pure solid NH₃ film. This difference can be attributed to a lesser degree of hydrogen bonding among NH₃ molecules in the N₂/NH₃ film than in pure solid NH₃.

The ν_2 and ν_4 vibrational bands of NH₃ each have two components in the N₂/NH₃ mixture. Splitting of absorption bands of a molecular species trapped in a matrix often occurs; this splitting is usually attributable to differences in the types of substitutional sites occupied by the trapped molecules. This probably explains the splitting of the ν_4 band. However, because of "inversion doubling," the ν_2 band is split into two components in the vapor phase (Ref. 10). Because there are two equilibrium positions for the N nucleus on either side of the H₃ plane, the symmetrical vibrational mode energy levels, ν_1 and ν_2 , are split into two components: one component associated with a change in the N nucleus equilibrium position during a vibration, and the other with no change. (The ν_1 splitting is very small in gaseous NH₃ and in our spectra.) Thus the two components of the ν_2 band seen at 988 and 1050 cm⁻¹ in the N₂/NH₃ film could result entirely from inversion doubling.

The pure NH₃ band at 524 cm⁻¹, among strong Ge substrate absorptions, is attributable to lattice movements, i.e., motions of large aggregates of NH₃ molecules. The lattice band does not appear in the N₂/NH₃ transmittance spectra.

Many studies of the weaker absorptions of molecular species trapped in an inert matrix, such as N₂, have indicated the self-association of the trapped molecules into dimers, trimers, and higher multimers. In those studies the concentration of trapped species was normally much lower than in the present work. The quality of the data in this report allowed a similar

analysis of the weaker absorptions of the N₂/NH₃ mixture as well for some of the other films presented below. In this work, the multimer absorptions were often blended with the stronger monomer absorptions. To discern the multimer absorptions, transmittance spectra were used and the corresponding absorption index (k) spectra, taken from the appropriate tables discussed in Section 5.0, which were plotted on graphs with scales greatly expanded from those in this report.

Suzuki et al. (Ref. 13), using Ar matrices, have assigned the more prominent bands appearing in our expanded scale N₂/NH₃ spectra at 972 and 3243 cm⁻¹, and the less prominent absorptions at 1005, 1647, and 3310 cm⁻¹ (which is coincident with ν_1) to hydrogen bonded dimers of NH₃. Bands appearing in our expanded scale spectra at 1015, 1035, 3364, and 3650 cm⁻¹ are attributed to NH₃ trimers or higher multimers. These self-associations of NH₃ molecules are evidence of some degree of local order in 20°K N₂/NH₃ films, but the absence of absorption, or the presence of extremely low absorption attributable to NH₃ lattice movements (at 525 cm⁻¹ in pure NH₃), suggests that the degree of crystallinity in N₂/NH₃ films is small.

When the film is warmed to 59°K, the absorptions of the N₂/NH₃ film (Fig. 6) more closely resemble those of pure NH₃ in their relative intensities. (Compare Figs. 4, 5, and 6.) This result is consistent with the explanation that at 59°K, most of the N₂ had sublimated (at approximately 10⁻⁶ torr) and that most of the remaining NH₃ molecules formed hydrogen bonds, as in the pure NH₃ film. Thus, their spectra are similar, except that the thin-film interference extrema, indicating a scattering film in the path of the IR beam, are missing in the 59°K film.

4.2 20°K FILMS CONTAINING ONLY N₂, CO, OR CO₂

Transmittance measurements were obtained for 20°K films of pure CO (Refs. 3 and 11), pure CO₂ (Ref. 1), and four mixtures containing CO and/or CO₂: 79.3% N₂/20.3% CO/(0.1% CO₂), 75% N₂/25% CO₂ (Ref. 1), 49.8% CO₂/49.5% CO, and 64.3% N₂/23.3% CO/13.2% CO₂. The presence of any of these molecular species had little effect on either the shape or the location of the very narrow absorptions that were attributable to CO or CO₂.

4.2.1 Pure CO and 79.3% N₂/20.3% CO/(0.1% CO₂) Films

Figure 7 shows the transmittance spectra of a solid film of pure CO at 20°K (from Ref. 3). The narrow 1→0 bands appear at 2092 cm⁻¹ for ¹³CO and at 2140 cm⁻¹ for ¹²CO. There is also a region of broader absorption near 2200 cm⁻¹ that is attributed to a combination of

the ^{12}CO 1-0 band with a lattice band (Ref. 12). The line positions of peaks within this region — 2184 (shoulder), 2202, 2212, and 2226 cm^{-1} (shoulder) — agree with the values given by Ewing and Pimentel (Ref. 12).

The transmittance spectra of the 79.3% N_2 /20.3% CO/ (0.1% CO_2) film in Fig. 8 show little change from the shape or line positions in the pure CO spectra, except for the 1-0 + lattice absorption near 2200 cm^{-1} . In the N_2/CO film there are two peaks at 2200 and 2210 cm^{-1} that also occur in the pure CO spectra, but the absorptions at 2180 and 2190 cm^{-1} that also occur in the pure CO spectra, but the absorptions at 2180 and 2190 cm^{-1} (which are on a shoulder in the pure CO spectra) have increased in their relative intensities and become distinct peaks for the lower CO concentration of the N_2/CO film. The reduction in the intensity of the 2200 cm^{-1} band in the N_2/CO film, in relation to its intensity in pure CO, indicates that the band in N_2/CO is due to the association of a CO molecule with neighboring CO molecules, rather than with neighboring N_2 molecules.

The N_2/CO spectrum in Fig. 8 is that of a 4.76- μm -thick film formed in layers approximately 0.26 μm thick. The spectrum of a 4.76- μm N_2/CO film formed in a continuous deposition process was identical to Fig. 8, indicating that the effects of deposition migration on the IR spectra are negligible.

4.2.2 Pure CO_2 and 74.7% N_2 /25.3% CO_2 Films

The pure CO_2 transmittance spectra (Fig. 9) from Ref. 1 show the narrow absorptions of $^{12}\text{CO}_2$ and $^{13}\text{CO}_2$ listed in Table 2 for the ν_2 , ν_3 , and $2\nu_2 + \nu_3$ vibrational modes. Not shown is the $\nu_1 + \nu_3$ band of $^{12}\text{CO}_2$ at 3710 cm^{-1} which is in Fermi resonance with the $2\nu_2 + \nu_3$ band at 3602 cm^{-1} (Ref. 10). As expected, both bands have about the same intensity. (Because the low signal-to-noise ratios of the IR spectrometer produce unreliable data for wavenumbers greater than 3700 cm^{-1} , the data are not presented for any film discussed in this report.) The strong $^{12}\text{CO}_2$ ν_3 band at 2347 cm^{-1} has a pronounced high wavenumber shoulder caused by very far IR lattice bands in combination with the ν_3 vibrational mode. The ν_3 band of $^{13}\text{CO}_2$ at 2284 cm^{-1} shows little asymmetry. The ν_2 band of $^{13}\text{CO}_2$ at 630 cm^{-1} is blended with the ν_2 band of $^{12}\text{CO}_2$ at 660 cm^{-1} .

There is a very weak absorption at 1285 cm^{-1} , and there are broader ones at 1450 and 1740 cm^{-1} that are apparent only when the spectra are plotted on graphs with greatly expanded scales (as explained in Section 4.1). In Table 2 we have tentatively assigned the 1285 cm^{-1} band to the $2\nu_2$ vibrational mode, which appears at 1286 cm^{-1} only in the Raman spectra of vapor phase CO_2 molecules. Its appearance in the solid IR spectra could be caused by a distortion of the symmetry of the CO_2 molecule by neighboring molecules (Ref. 14).

The 1450 and 1740 cm^{-1} absorptions are tentatively assigned to lattice bands in combination with $2\nu_4$. The stronger absorptions with a peak at 2460 cm^{-1} are more confidently labeled as lattice bands in combination with the $^{12}\text{CO}_2 \nu_3$ band. A weak absorption at 2316 cm^{-1} is identified with the corresponding lattice combination band with ν_3 of $^{13}\text{CO}_2$. Lattice combination band features are also observed on the high wavenumber side of the $2\nu_2 + \nu_3$ band of $^{12}\text{CO}_2$ at 3602 cm^{-1} .

The transmittance spectra of the 20°K 74.7% $\text{N}_2/25.3\%$ CO_2 film (Fig. 10) are very similar to the pure CO_2 film spectra. The asymmetry of the $^{12}\text{CO}_2 \nu_3$ band in N_2/CO_2 is reduced from what it was in pure CO_2 , yet its presence indicates a remaining degree of crystallinity of CO_2 molecules. In expanded scale plots, the broad absorption at 1450 cm^{-1} in pure CO_2 is intensified and is even broader in N_2/CO_2 relative to the vibrational bands. Also, the $\nu_3 +$ lattice band of $^{12}\text{CO}_2$ is divided into two broad peaks (at 2390 and 2430 cm^{-1}) in N_2/CO_2 . In comparison to the pure CO_2 spectrum, these differences may indicate non-negligible interactions occurring between CO_2 and N_2 molecules, like those found by Perchard et al. (Ref. 15) between HCl and N_2 molecules.

4.2.3 49.8% $\text{CO}_2/49.5\%$ CO and 64.3% $\text{N}_2/23.3\%$ CO/ 13.2% CO_2 Films

When CO and CO_2 molecules are mixed, very slight changes occur in the positions of the molecular normal vibrational modes relative to their positions in pure CO and CO_2 films (Table 2). The transmittance spectra of 49.8% $\text{CO}_2/49.5\%$ CO (Fig. 11) look like a superimposition of the corresponding spectra of pure CO and pure CO_2 . The very small interaction of CO with CO_2 molecules is a consequence both of their small electric dipole moments (which preclude noticeable dipole-dipole effects) and of the fact that these molecules cannot hydrogen-bond to one another.

The asymmetry of the ν_3 band of $^{12}\text{CO}_2$, noted above for the pure CO_2 and N_2/CO_2 films, is also present in the CO/ CO_2 film. The CO_2/CO film also exhibits the lattice combination bands at 2225 and 2412 cm^{-1} that are associated with the $1\leftarrow 0$ band of ^{12}CO and the ν_3 band of $^{12}\text{CO}_2$, respectively, and that respectively appear in the pure CO and N_2/CO films, and in the pure CO_2 and N_2/CO_2 films.

A new but very weak absorption — more easily seen in an expanded scale plot — appears in CO_2/CO (at 2110 cm^{-1}) in the high wavenumber wing of the $1\leftarrow 0$ band of ^{13}CO . Also in contrast to the pure CO and N_2/CO films, a shoulder appears on the $1\leftarrow 0$ ^{12}CO band in CO_2/CO at 2138 cm^{-1} . Such splittings of the $1\leftarrow 0$ bands are observed in Ar/CO films (Ref. 16). Extremely weak absorptions near 1400 cm^{-1} are unassigned and may be spurious.

Upon warming to 50°K and then recooling to 20°K, the transmittance spectra of the CO₂/CO film show reduced CO absorption and a distortion of the channel spectra (Fig. 12). Both effects can be attributed to the greater sublimation of CO molecules at the higher temperatures. Sublimation of CO from the deposit would produce voids within the deposit. These voids would cause radiation scattering that would be expected to be more pronounced at the higher wavenumbers, as is seen in Fig. 12.

The N₂/CO/CO₂ film has nearly identical spectral positions and band shapes as have the spectra of the CO₂/CO film (Fig. 13). The ν_3 band of ¹²CO₂ is asymmetric (as it is in all films containing significant amounts of CO₂) indicating that the CO₂ lattice effects are still noticeable. Lattice combination absorptions occur at the same locations in both N₂/CO/CO₂ and CO₂/CO, but their intensities are smaller in N₂/CO/CO₂. Thus, as expected, smaller numbers of CO or CO₂ molecules form crystals of like species in N₂ matrices.

4.3 20°K FILMS CONTAINING H₂O

H₂O molecules have large electric dipole moments and readily form hydrogen bonds with neighboring H₂O or other hydrogen-containing molecules. The propensity of H₂O molecules to form hydrogen bonds accounts for many of the unique properties of water including the fact that ice I is less dense at 273°K and atmospheric pressure than is liquid water. When the IR spectra of a pure hydrogen-bonded molecular species are compared to the gas phase spectra of the species, dramatic shifts in band positions and changes in the relative and absolute intensities of absorptions could appear. The changes are most noticeable for the stretching vibrational modes (Ref. 7). (Changes in the IR spectra of H₂O molecules in condensed phases have been noted at the beginning of this section.)

The films containing H₂O can be classified into (1) those in which H₂O is the major or only constituent [pure H₂O and 61% H₂O/36% CO₂/(2% N₂)] and (2) those in which H₂O is a minor constituent [87% N₂/12% H₂O/(1% CO₂), 93% Ar/6% H₂O]/(< 0.5% CO₂), 91% CO/9% H₂O, and the simulated plume mixture 50.3% N₂/22.5% H₂O/17.2% CO₂/10.0% CO)]. The effects of hydrogen bonding are shown below to be much greater in the first category.

4.3.1 Pure H₂O and 61% H₂O/36% CO₂/(2% N₂) Films

The transmittance spectra (Fig. 14) of pure 20°K H₂O (with a trace of CO₂) exhibit the high degree of hydrogen bonding by H₂O molecules that causes large spectral changes upon variation of temperature and phase. The spectra of liquid- (Ref. 17) and solid-phase H₂O

molecules are very similar. The differences between the spectra of H₂O condensed phases and the spectra of the vapor phase are well documented (Ref. 9). The effects of temperature on the IR spectra of H₂O in the liquid (Ref. 18) and solid (Refs. 1 and 19) phases have also been extensively investigated.

Comparing the ν_2 band positions for pure H₂O vapor (1595 cm⁻¹) and for pure solid H₂O (1660 cm⁻¹) reveals the *upward* shift behavior that is typical of in-plane bending vibrational modes of hydrogen-bonded molecules (Ref. 9). In contrast, the stretching modes of hydrogen-bonded molecules are shifted *downward* in spectral position from their nonbonded (i.e., vapor phase) locations. For H₂O, the vapor phase positions of the ν_1 (3652 cm⁻¹) and ν_3 (3756 cm⁻¹) O-H stretching modes shift downward in solid H₂O by 350 to 450 cm⁻¹, and appear with $2\nu_2$ as one very strong, broad, and slightly asymmetric absorption centered near 3300 cm⁻¹. A hindered translation lattice band, ν_T , may be in combination with the $2\nu_2$ vibrational mode and may also contribute to the high wavenumber side of the 3300 cm⁻¹ absorption. Other lattice absorptions in solid pure H₂O are the hindered rotation ("libration") band, ν_L , at 770 cm⁻¹ and a weak "associational" band, ν_X , at 2200 cm⁻¹. (See Ref. 20 for a proposed assignment of the ν_X band.) Near 1420 cm⁻¹, there may also be some lattice effects which extend into the ν_2 absorption region of solid H₂O. As stated in Section 3.0, there are also scattering effects in thick H₂O films that produce an apparent background absorption throughout the spectra.

It was noted at the beginning of this section that the absorption intensities of the O-H bond stretching vibrational modes (ν_1 and ν_3) are much larger in the condensed phases of H₂O than in the non-hydrogen-bonded vapor phase. There may also be some enhancement of the $2\nu_2$ absorption in solid H₂O because of its proximity to the ν_1 vibration. Both bands are type A₁ and can interact through Fermi resonance, which causes "intensity mixing" (Ref. 10). In contrast to the stretching mode intensities, the intensity of the ν_2 (bending) vibrational mode decreases slightly upon the hydrogen bonding of H₂O molecules (Ref. 9).

The transmittance spectra of the 20°K 61% H₂O/36% CO₂/(2% N₂) film (Fig. 15) resembles a superimposition of the spectra for the pure 20°K H₂O film (Fig. 14) and the pure 20°K CO₂ film (Fig. 9). In particular, the broad H₂O band at 3300 cm⁻¹ is present in both the mixture and in the pure film, and the ν_3 band of CO₂ (2345 cm⁻¹) is asymmetric just as it is in the spectra of the films that contained CO₂ (Section 4.2). The H₂O/CO₂ spectra indicate a high degree of hydrogen bonding among the H₂O molecules and show that any interactions between H₂O and CO₂ molecules do not appreciably affect the spectrum of either species.

There are some differences between the H₂O/CO₂ spectra and the spectra of pure H₂O or pure CO₂. The location of the peak of the O-H stretching band of H₂O is at 3340 cm⁻¹ in

the H₂O/CO₂ film, rather than at the pure H₂O film position of 3300 cm⁻¹. Also, there is in H₂O/CO₂ a fairly broad and intense band at 3653 cm⁻¹ that obscures the 2ν₂ + ν₃ band of ¹²CO₂ at 3605 cm⁻¹; this broad band does not appear either in pure H₂O or in pure CO₂ films. These features are probably caused by an appreciable number of monomeric (non-hydrogen-bonded) H₂O molecules that are prevented from forming hydrogen bonds by the presence of the CO₂ molecules. This explanation could also account for the reduction of the H₂O multimer absorption at 3300 cm⁻¹ in H₂O/CO₂. The appearance of the 3653 cm⁻¹ band is presumed caused by O-H bond stretching of H₂O monomers and, possibly, low order multimers. After the H₂O/CO₂ film is warmed to 128°K, the transmittance spectra (Fig. 16) show that the relative intensity of the O-H stretching band has increased and shifted from 3340 cm⁻¹ to lower wavenumbers and that the intensity of the 3653 cm⁻¹ band has been considerably reduced, along with the CO₂ absorptions. Thus, more CO₂ molecules must have sublimated from the film than H₂O molecules, thereby causing the concentration of H₂O monomers to decrease. The overall reduction in the magnitude of the transmittance is attributable to scattering from voids produced by the sublimated CO₂.

Finally, a small absorption at 3703 cm⁻¹ in the H₂O/CO₂ film (not seen in Fig. 16) probably has contributions from H₂O molecules as well as from the ν₁ + ν₃ vibrational mode of ¹²CO₂ (Table 2).

4.3.2 The 20°K 87% N₂/12% H₂O/(1% CO₂), 93% Ar/6% H₂O/(< 0.5% CO₂), and 91% CO/ 9% H₂O/(< 0.5% CO₂) Films

In these three films, H₂O is a minority constituent, and we might expect to see a reduction in the effects of the hydrogen bonding of H₂O molecules. In fact, this does occur, as is shown by the transmittance spectra of 20°K N₂/H₂O (Fig. 17), Ar/H₂O (Fig. 18), and CO/H₂O (Fig. 19), which all show distinct and less intense absorptions in the O-H stretching region than are seen in the pure H₂O spectra (Fig. 14). The spectral effects of hydrogen bonding also become more important as the concentration of H₂O molecules increases; for example, the spectra of the 87% N₂/12% H₂O film are more like the pure solid H₂O spectra than are the 93% Ar/6% H₂O spectra, which bear more similarity to vapor phase H₂O spectra.

Also, in these three films, the absorptions near 3230 cm⁻¹ are attributed in Table 2 to the 2ν₂ vibrational mode of H₂O molecules that are in monomer and multimer associations. Other assignments in the O-H stretching region of H₂O are difficult to make because even at these relatively low H₂O concentrations, the absorptions attributed to monomers, dimers, and other low order multimers are often obscured by absorptions of higher order multimers. The dimer and higher multimer assignments of Table 2 agree with those given for H₂O by Huong and Cornut (Ref. 21).

There are less dramatic changes from the pure H₂O spectra in the ν_2 region of H₂O near 1600 cm⁻¹. At low H₂O concentrations in solid N₂ or rare gas matrices, the ν_2 band has several spectral components that can be seen in expanded scale spectra (Section 4.1). In our Ar/H₂O spectra, for example, there are peaks at 1593, 1602, 1613, and 1625 cm⁻¹ that are in excellent agreement with the bands observed by Ayers and Pullin (Ref. 22) at 1593, 1602, 1611, and 1623 cm⁻¹. Ayers and Pullin attribute the 1593 and 1611 cm⁻¹ absorptions to H₂O dimers and the others to H₂O multimers.

The ν_2 band of H₂O has just two major components in our CO and N₂ matrices. In the CO/H₂O film, the lower wavenumber component (1603 cm⁻¹) has a greater intensity than the higher (1638 cm⁻¹), while in the N₂/H₂O film, with a greater H₂O concentration, the higher wavenumber component (1637 cm⁻¹) has the greater intensity. This growth in intensity and the corresponding shift in wavenumber by the higher wavenumber components of the H₂O ν_2 band have been monitored as a function of H₂O concentration in N₂ matrices by Van Thiel et al. (Ref. 23), Tursi and Nixon (Ref. 24), and Huong and Cornut (Ref. 21). This effect has been observed in Ar and other rare gas matrices by Catalano and Milligan (Ref. 25), Glasel (Ref. 26), Ayers and Pullin (Ref. 22), and Huong and Cornut (Ref. 21). The effect is ascribed to a decrease in the relative number of monomer H₂O molecules (absorbing at 1603 cm⁻¹), compared to the number of H₂O dimers (absorbing at 1620 cm⁻¹) and higher multimers (absorbing at 1633 cm⁻¹ and higher), as the concentration of H₂O molecules in a matrix increases.

Figure 20 shows the transmittance spectra of the CO/H₂O film after warming to 105°K. The CO absorptions and interference extrema are absent and the spectra look like the spectra of a very thin but nonuniform film of H₂O (with a trace of CO₂). In particular, the O-H stretching region has grown more intense and shifted toward 3300 cm⁻¹ after warming. Analogous results appear in the warm spectra of N₂/H₂O and Ar/H₂O (Ref. 1). However, in the N₂/H₂O film the O-H stretching band becomes highly asymmetric toward the lower wavenumbers. Perhaps this is due to differences between amorphous and crystalline forms of H₂O multimers (Ref. 27). However, in none of these three films is there any evidence of appreciable interactions between the matrix and H₂O molecules which affect the spectra in Figs. 17-19.

4.3.3 The 20°K 50.3% N₂/22.5% H₂O/17.2% CO₂/10.0% CO Film (Simulated Plume Mixture)

The 50.3% N₂/22.5% H₂O/17.2% CO₂/10.0% CO film is a mixture with its constituents in the approximate proportion of their stoichiometric concentrations (neglecting hydrogen) after the combustion of MMH and N₂O₄ (Ref. 4). As indicated in the

transmittance spectra of the plume mixture (Fig. 21), the film belongs to the latter group of H₂O-containing films in which hydrogen bonding of H₂O molecules is less pronounced. Other spectral features are similar to those in films discussed previously. For instance, the CO and CO₂ absorptions are again very narrow and have shifted very little in position, and the ν₃ band of ¹²CO₂ is still asymmetric. However, in the plume mixture the 1-0 band of ¹²CO has an asymmetry not observed in the other films containing CO. The feature might be attributable to H₂O lattice vibrations such as ν_X.

After the simulated plume mixture is warmed to 96°K, the transmittance spectra (Fig. 22) show decreased H₂O monomer and CO absorptions. There is also the same type of asymmetry of the O-H stretching band observed for the N₂/H₂O film (Ref. 1) (Section 4.3.2). The broad and very pronounced absorptions throughout the plume spectra may, in fact, be due to scattering effects caused by shattering (Ref. 1).

5.0 THE IR OPTICAL PROPERTIES OF CRYOFILMS

The effects of contaminant cryofilms upon surfaces that are part of the optical trains of IR instruments can be determined from a knowledge of the complex index of refraction, $\hat{n}(\nu) = n(\nu) + ik(\nu)$ (Ref. 1). At any wavenumber, the optical constants n and k of a given cryofilm are dependent not only on its molecular components but also on its physical properties, including density, temperature, thickness, variances in thickness, and the degree of homogeneity of the film constituents. Density is affected by all of the other properties and is the most important. The complex index, \hat{n} , of a film material with density, ρ , is related to the index, \hat{n}' , of the same material with density, ρ' , through the complex Lorentz-Lorenz equation,

$$\frac{\rho^{-1}(\hat{n}^2 - 1)}{(\hat{n}^2 + 2)} = \frac{\rho'^{-1}(\hat{n}'^2 - 1)}{(\hat{n}'^2 + 2)} \quad (3)$$

5.1 ANALYTICAL MODEL OF THE FILM AND SUBSTRATE INTERACTIONS WITH A NORMALLY INCIDENT IR BEAM

The model used to interpret the normal absolute transmittance of cryofilms deposited on a substrate is pictured in Fig. 23, and has been discussed in detail in Refs. 1 and 28. The film is considered to be homogeneous, uniform in thickness, d_1 , and deposited on a homogeneous substrate having a uniform but much greater thickness, D, than the film. The degree of coherence of the normally incident IR beam is assumed to allow thin-film interference in the cryofilm (Ref. 29) but not in the substrate. The infinite number of rays reflected from the 2-3 interface in Fig. 23 undergoes thin-film interference in the contaminant. The intensities of the rays transmitted through the interface add (convergent series) to a finite sum (Refs. 1 and 28).

The absolute transmittance at normal incidence, $T(\nu)$, of the film plus substrate can be written as (Ref. 30)

$$T(\nu) = \hat{t}^*(\nu) \hat{t}(\nu) \quad (4)$$

Thus,

$$\hat{t}(\nu) = [T(\nu)]^{1/2} \exp [i \phi(\nu)] \quad (5)$$

where \hat{t} is the complex normal transmission coefficient of the film and substrate, and ϕ is the change of phase suffered by the IR beam as it travels through the entire film and substrate. Analysis of the model in Fig. 23 gives

$$\hat{t} = \frac{\hat{t}_{23} |\hat{t}_{012} \exp (-\beta_2 D)}{\left[1 - |\hat{r}_{23}|^2 |\hat{r}_{210}|^2 \exp (-i\beta_2 D) \right]^{1/2}} \quad (6)$$

where

$$\hat{t}_{ij} = \frac{2\hat{n}_j}{\hat{n}_i + \hat{n}_j} \quad (7)$$

and

$$\hat{r}_{ij} = \frac{\hat{n}_i - \hat{n}_j}{\hat{n}_i + \hat{n}_j} \quad (8)$$

are the complex Fresnel relations for normal incidence on the i-j interface

$$\hat{t}_{012} = \frac{\left[\hat{r}_{01} \hat{r}_{12} \exp (2i \hat{\gamma}_1 d_1) \right]}{\left[1 - \hat{r}_{01} \hat{r}_{12} \exp (2i \hat{\gamma}_1 d_1) \right]} \quad (9)$$

$$\hat{r}_{210} = \frac{\left[\hat{r}_{21} + \hat{r}_{10} \exp (2i \hat{\gamma}_1 d_1) \right]}{\left[1 - \hat{r}_{21} \hat{r}_{10} \exp (2i \hat{\gamma}_1 d_1) \right]} \quad (10)$$

$$\beta_2 = 2\pi\nu k_1 \quad (11)$$

and

$$\gamma_1 = 2 \pi \nu \hat{n}_1 \quad (12)$$

[According to Eq. (8), $\hat{r}_{ij} = -\hat{f}_{ji}$; therefore, the denominators of Eqs. (9) and (10) are equal. Also, k in Eq. (11) is the absorption index of the film (medium 1).] The main difference between the form of the absolute normal transmittance given in Eqs. (4) and (6) and that given in the equations for T in Refs. 1 and 28 is that Eqs. (4) through (12) preserve the phase relationships. The phase relationships are necessary for the development of a Kramers-Kronig analysis of the normal transmittance of a single film thickness. These relationships are also easier to code in computer languages such as FORTRAN IV that can make complex number manipulations.

At a given wavenumber ν , the model contained in Eqs. (4) through (12) depends on 10 parameters: both the real and the imaginary parts for the indices \hat{n}_0 , \hat{n}_1 , \hat{n}_2 , and \hat{n}_3 , and the film and substrate thickness, d_1 and D . In the experiments performed for the present work, media 0 and 3 were considered to be vacuums (i.e., $n_0 = n_3 = 1$), D was 4 mm, and the substrate (medium 2) was 20°K Ge. The Ge substrate had an index $\hat{n}_2(\nu) = n_g(\nu) + ik_g(\nu)$ where, at 20°K and between 700 and 3700 cm⁻¹ (Refs. 1 and 28),

$$n_g(\nu) = A + BL + CL^2 + D\nu^{-2} + E\nu^{-4} \quad (13)$$

where

$$A = 3.99931$$

$$B = 0.391707 \text{ cm}^2$$

$$C = 0.163492 \text{ cm}^4$$

$$D = 0.000006 \text{ cm}^2$$

$$E = 0.000000053 \text{ cm}^4$$

$$L = (\nu^{-2} - 0.028 \text{ cm}^2)^{-1}$$

and

$$k_g(\nu) = 0 \quad (14)$$

It was assumed that the unknown n and k values of the film did not depend on the remaining parameter d_1 , the film thickness, which was, experimentally, the easiest parameter to change and measure. The optical constants were found at a given wavenumber by a match of the model in Eqs. (4) through (14) to the observed behavior of the normal absolute transmittance as a function of film thickness. Since neither Eq. (4) nor (6) can be solved in closed form for n_1 , the nonlinear least-squares algorithm of Marquardt (Ref. 31) was used to extract the indices.

Approximate values of the indices are often useful, especially in least-squares algorithms. It is possible to make assumptions that are valid near strong absorptions and to obtain a closed form (approximate) solution for k in the following manner. Near the strong cryofilm absorptions, the effects of thin-film interference diminish greatly because the rays within the film are rapidly attenuated. (The distortion of the interference extrema near strong absorptions can be seen in the transmittance spectra of the cryofilms in Figs. 1 through 22.) Thus, if the attenuation is sufficient, the entire IR beam can be considered to pass through the film just once.

We may consider that the change in the transmittance values for the two cases (1) substrate only and (2) film plus substrate is attributable entirely to the passage of the IR beam through a thickness, d_1 , of the film. The transmittance, T_s , of the substrate alone is given by

$$T_s = \hat{t}_s * \hat{t}_s \quad (15)$$

where

$$\hat{t}_s = \frac{|\hat{r}_{23}| |\hat{r}_{02} \exp(-\beta_2 D)|}{[1 - |\hat{r}_{23}|^2 |\hat{r}_{02}|^2 \exp(-4\beta_2 D)]^{1/2}} \quad (16)$$

a result that can be obtained heuristically by eliminating the "1" subscript from Eq. (6). The observed ratio, I_3/I_0 , of the transmitted beam power, I_3 , to the incident beam power, I_0 , *when a film is present* is then, approximately, $|n_3/n_0| T_s \exp(-\alpha_1 d_1)$, where the Lambert absorption coefficient $-\alpha_1 = 4\pi\nu k$. Equating I_3/I_0 with $|n_3/n_0| T_s \exp(-\alpha_1 d_1)$ and solving for k gives

$$k(\nu) \approx \frac{\ln [|n_3/n_0| T_s / (I_3/I_0)]}{(4\pi\nu d_1)} \quad (17)$$

which has only known quantities on the right-hand side.

5.2 COMPUTATION OF THE OPTICAL CONSTANTS

The reliable data domain lay between 700 and 3700 cm^{-1} . For wavenumbers less than 700 cm^{-1} , the absorptions attributable to the substrate are large. Actually, k_g is not precisely equal to zero [Eq. (13)] near 760 or 850 cm^{-1} , either. These weak Ge absorptions cause fictitious contributions of approximately 5×10^{-3} to the absorption index of the films, and should be regarded as spurious. At wavenumbers greater than 3700 cm^{-1} , the low signal-to-noise ratio of the interferometer makes the transmittance data inaccurate. Measurements of the transmittance were obtained by interferometer every 2 cm^{-1} in the wavenumber domain from 500 to 4000 cm^{-1} . Least-squares computations of the optical constants of the cryofilms were normally made every 10 cm^{-1} between 700 to 3700 cm^{-1} , although the wavenumber domain was often extended to include absorption features slightly beyond the endpoints of the 700 to 3700 cm^{-1} domain. However, only the values between 700 and 3700 cm^{-1} are reported. The computations were normally performed every 2 cm^{-1} near noticeable absorptions.

In the nonlinear least-squares algorithm, estimated values of the optical constants were required at every wavenumber; the values used were usually the converged values of the preceding calculation. As noted by Roux et al. (Ref. 1), the least-squares values of k were more reliable than the n values, especially near strong absorptions, such as the narrow $^{12}\text{CO}_2$ ν_3 band, at which the optical constants changed rapidly with wavenumber. This changing can be explained by the fact that portions of the IR beam pass through the film many times so that changes in the beam's attenuation are more strongly influenced by molecular absorptions, which determine k , than by reflection losses, which determine n . For example, in the transmittance spectra of pure CO_2 (Fig. 9), molecular absorption, as a function of wavenumber, changes much more noticeably near 2350 cm^{-1} than do the reflection losses, which cause the channel spectra.

As a consequence, there are many pairs of n and k values that, if introduced into Eqs. (4) through (12), can yield transmittance values within the experimental uncertainties of the observed values for a given film thickness. [This phenomenon was observed in CdS films in the visible range (Ref. 32).] The calculated n values ranged from near 0 to 10 in strong narrow absorptions, but k was much better determined, typically having a range of ± 10 percent of the mean value. Occasionally, especially near the peak of a strong narrow absorption, the converged value of n given by the nonlinear least-squares algorithm was far out of line with the surrounding n values. Usually, the algorithm converged to a more acceptable value of n when the initial estimate of k was given by Eq. (17), and a reasonable guess was made for n .

The uncertainties in the least-squares n values mentioned above have led Roux et al. (Refs. 1 through 4) and others to use Kramers-Kronig (KK) techniques to compute n from the least-squares values of k. In this work, the subtractive Kramers-Kronig (SKK) relation

$$n(\nu) = n(\nu_0) + \frac{2(\nu^2 - \nu_0^2)}{\pi} P \int_0^\infty \frac{\nu' k(\nu') d\nu'}{(\nu^2 - \nu'^2)(\nu_0^2 - \nu'^2)} \quad (18)$$

is also used to find n(ν). Here, the real index n(ν_0) is that found at wavenumber ν_0 by a separate measurement, and P denotes that the Cauchy principle value of the integral is to be taken. The reference wavenumber ν_0 was always chosen from a region where there were no strong absorptions and where n was very slowly varying. The least-squares determined value of n(ν_0) was used in the SKK computation. [One of the advantages of the SKK treatment of data is that an error of Δ in n(ν_0) merely shifts *all* of the computed n values by the same amount Δ , preserving the shape of the n curve.] Usually, the data domain in the SKK calculation ranged from 700 to 3700 cm⁻¹; however, if prominent features lay just beyond this domain, then these data were also included. The additional data, even if inaccurate, help make the SKK determinations more precise near 700 and 3700 cm⁻¹. In every case, k was assumed always to be zero outside the data domain.

The least-squares values and the SKK values of n agreed except, as noted above, near the peaks of strong narrow absorptions. In all cases, the plotted SKK n values gave smoother curves than did the least-squares values, and the ranges of the SKK n values in regions of anomalous dispersion were not as large as the ranges of the least-squares values. As in Refs. 1, 2, and 3, the tabulated values of n are from the SKK computation, and the given k values are those from the nonlinear least-squares determination from the normal transmittance data.

5.2.1 Optical Constants of 85% N₂/15% NH₃ Films

The optical indices of the 20°K 85% N₂/15% NH₃ cryofilms are given in Table 3 and plotted in Figs. 24 and 25. As noted in Table 1, the least-squares indices were determined from the transmittance of 18 films having a maximum thickness of 5.00 μm. Figure 26 shows the small deviations of the least-squares fit of the data relative to the original data points, at three widely spaced wavenumbers. The data at 1038 cm⁻¹ are near the strongest NH₃ absorptions, and the decreasing transmittance can be seen superimposed on the interference extrema. This is less noticeable for the 3386 cm⁻¹ data, and not at all for the data at 2850 cm⁻¹, which is far from any absorptions. The standard deviations of the fitting procedure were typically near 0.01 for all of the films studied. Our confidence in the essential accuracy of the model contained in Eqs. (4) through (12) is increased by the fact that the model contains just two fitted parameters, n and k.

The reference wavenumber ν_0 in the SKK determination of the n values was 2180 cm^{-1} , and the refractive index was determined to be 1.24 from the least-squares fit. This n value is near the n values in the visible region, as is the case for all films presented here. The SKK calculation included only data in the $700\text{-}3700\text{-cm}^{-1}$ wavenumber domain. As in all of the plots of n, both the SKK and the least-squares curves are coincident at ν_0 ; the SKK plot is smoother with its extremal values within the least-squares maxima and minima (Fig. 24). A large discrepancy between the curves occurs at the strong absorption at 970 cm^{-1} . The small absorption index peaks in Fig. 25 at 760 and 850 cm^{-1} (seen in all k spectra) are fictitious as explained earlier.

Comparisons of the present data with the data of other researchers can only be qualitative because almost all work concerning NH_3 in N_2 matrices has been done at much lower NH_3 concentrations. Also, in almost all cases, only relative absorption intensities are given, and the real index is not reported at all (Ref. 13).

5.2.2 Optical Constants of 79.3% $\text{N}_2/20.3\%$ CO/(0.1% CO_2) Films

Figures 27 and 28 are the plots of n and k of the 20°K 79.3% $\text{N}_2/20.3\%$ CO/(0.1% CO_2) cryofilms presented in Table 4. The SKK reference wavenumber ν_0 and its n value were 2300 cm^{-1} and 1.21, respectively, and the domain of the data was from 700 to 3700 cm^{-1} . The difference between the SKK and least-squares n values at the $1 - 0$ ^{12}CO band (2140 cm^{-1}) is striking.

o

As for most of the films, there are few quantitative data available that can be compared to our results for a cryofilm with a large CO concentration compared to concentrations used in matrix isolation studies of CO (Refs. 12, 16, 33, and 34). (Most of the qualitative comparisons that could be made were given in Section 4.2.2.)

5.2.3 Optical Constants of 74.5% $\text{N}_2/25.3\%$ CO_2 Films

Table 5 lists the optical constants of the 20°K 74.7% $\text{N}_2/25.3\%$ CO_2 film which are plotted in Figs. 29 and 30. The reference wavenumber and the corresponding n value are 2144 cm^{-1} and 1.26, respectively. Here, the SKK data domain extended from 602 to 3750 cm^{-1} so that the $^{12}\text{CO}_2$ absorptions at 665 cm^{-1} (ν_2) and at 3710 cm^{-1} ($\nu_1 + \nu_3$) could be included in the calculation of n from the least-squares k values. The agreement of the SKK and the least-squares n values is very good even in the strongly absorbing regions.

Again, few data can be found on the higher CO_2 concentrations in N_2 matrix isolation studies which are useful in comparisons with our work.

5.2.4 Optical Constants of 49.8% CO₂/49.5% CO Films

The optical indices of 20°K 49.8% CO₂/49.5% CO film are included in Table 6. The n and k curves appear in Figs. 31 and 32, respectively. The SKK values were obtained from a calculation in which the reference wavenumber was 2600 cm⁻¹, the reference n value was 1.19, and the domain of the data extended from 610 to 3750 cm⁻¹. For CO₂/CO, the severest discrepancies between the SKK and the least-squares n values occur at low n values near the ¹²CO 1 → 0 band.

These spectra are probably unique in the literature.

5.2.5 Optical Constants of 64% N₂/23% CO/ 13% CO₂ Films

The n curves of 20°K 64% N₂/23% CO/ 13% CO₂ films in Fig. 33 appear nearly identical to the n curves of the CO₂/CO films (Fig. 31) except for the reduced range of n in N₂/CO/CO₂ in the anomalous dispersion regions. Analogous results occur for the k curve of N₂/CO/CO₂ in Fig. 34. The SKK parameters were $\nu_0 = 2600 \text{ cm}^{-1}$, $n(\nu_0) = 1.21$; the data domain lay from 610 to 3750 cm⁻¹. The optical constants derived from the SKK analysis for n and the least-squares analysis for k appear in Table 7.

Again, these data are probably unique in the literature.

5.2.6 Optical Constants of 61% H₂O/36% CO₂/(2% N₂) Films

Table 8 contains the optical constants of 20°K 61% H₂O/36% CO₂/(2% N₂) films which are plotted in Figs. 35 and 36. The reference wavenumber in the SKK determinations of n was 2750 cm⁻¹ where n had the value 1.34. The SKK data domain was from 610 to 3750 cm⁻¹, which included the ν_2 absorption of H₂O that appears at 660 cm⁻¹ in H₂O/CO films. The agreement of the SKK n values with the n values found from the least-squares analysis is poorer, especially near 3300 cm⁻¹, than the agreement seen in other films. Apart from the CO₂ absorptions, the k curve has a shape very similar to that of pure solid H₂O (Ref. 1).

5.2.7 Optical Constants of 87% N₂/12% H₂O/(1% CO₂) Films

The plots of the n values of 20°K 87% N₂/12% H₂O/(1% CO₂) films are given in Fig. 37. The least-squares parameters used are in Table 1, and the parameters needed in the SKK analysis were $\nu_0 = 2500 \text{ cm}^{-1}$, $n(\nu_0) = 1.24$; the data domain extended from 610 to 3750 cm⁻¹. Figure 38 is the k curve plotted from the values listed in Table 9. The complex structure in the O-H stretching region is easily seen in Fig. 38, as well as the CO₂ absorption.

Despite the enormous body of literature concerning H₂O in N₂ matrices (e.g., Refs. 9, 21, 23, and 24), there are no data available for comparison at our high H₂O concentration, except for the qualitative features discussed in Section 4.3.2.

5.2.8 Optical Constants of 94% Ar/6% H₂O/(<0.5% CO₂) Films

The optical constants of 20°K 93% Ar/6% H₂O/(<0.5% CO₂) films are listed in Table 10 and plotted in Figs. 39 and 40. The SKK analysis used a reference wavenumber of 2600 cm⁻¹ where the least-squares n value was 1.25. The SKK data domain extended from 610 to 3800 cm⁻¹. The structure of the O-H stretching band in Fig. 40 is even more complex than for N₂/H₂O films (Fig. 38) because of the increased rotational motion allowed the H₂O molecules in Ar matrices (Ref. 24).

The excellent qualitative agreement of the present Ar/H₂O mixture data with other results (Refs. 21, 22, 25, and 26) has been cited in Section 4.3.2. However, none of the other work has specific quantitative data at the high H₂O concentration of our films. Jiang et al. (Ref. 16) give a value of 1.412 for the refractive index at 1000 cm⁻¹ (away from H₂O absorptions) of pure solid Ar at 30°K. If the density (1.44 gm/cm³) and the n value at 1000 cm⁻¹ (1.249) of our 20°K Ar/H₂O film is assumed to be that of pure Ar, the Lorentz-Lorenz relation [Eq. (3)] yields a density for the pure Ar film of Jiang et al. that is approximately 1.5 times larger. We found the same factor — 1.5 — for the ratio of the pure CO densities as was found by Jiang et al.; this factor represents differences in the deposition procedures.

5.2.9 Optical Constants of 91% CO/9% H₂O/(<0.5% CO₂) Films

In the SKK analysis of the least-squares k values of 20°K 91% CO/9% H₂O/(<0.5% CO₂) (Table 11), the n value 1.25 was used at the reference wavenumber 1900 cm⁻¹. The data domain in the SKK calculations extended from 610 to 3748 cm⁻¹, and the optical constants from the SKK and least-squares analysis are plotted in Figs. 41 and 42. The features attributable to H₂O are much less intense than the 1-0 ¹²CO band, but on the expanded scale in Fig. 42 the H₂O absorptions look more like the k curve of the N₂/H₂O film (Fig. 38) than the k curve for Ar/H₂O. This means that a CO matrix restricts the rotation of H₂O molecules much like an N₂ matrix.

No comparable data exist in the literature.

5.2.10 Optical Constants of 50.3% N₂/22.5% H₂O/17.2% CO₂/10.0% CO (Simulated Plume Mixture) Films

The 20°K optical spectra of the simulated plume mixture of gases, 50.3% N₂/22.5% H₂O/17.2% CO₂/10.0% CO, are shown in Figs. 43 and 44. Table 1 lists the least-squares fitting parameters, and Table 12 gives the resulting k values. A reference wavenumber of 1900 cm⁻¹, a reference index of refraction of 1.23, and a data domain extending from 600 to 3750 cm⁻¹ were used to make the SKK determinations. The SKK n values from Table 12 are shown (Fig. 43) to agree with the least-squares values even at the strong ¹²CO and ¹²CO₂ absorptions. The features attributable to H₂O do not affect the n or k curves very much, indicating that the degree of hydrogen bonding among H₂O molecules is low (Section 4.3.3).

6.0 SUMMARY

Accurate transmittance spectra have been obtained at 20°K for films of N₂/NH₃, N₂/CO, N₂/CO₂, CO₂/CO, N₂/CO/CO₂, N₂/H₂O, Ar/H₂O, H₂O/CO₂, CO/H₂O, and N₂/H₂O/CO₂/CO mixtures. The films were condensed onto a 20°K Ge substrate. Within the observed spectral domain — from 500 to 3700 cm⁻¹ — lie most of the (intramolecular) vibrational mode absorptions as well as many features caused by lattice (intermolecular) motions. Absorption features due to CO or CO₂ varied only slightly from film to film. The very drastic changes occurring in H₂O absorptions and, less spectacularly, in NH₃ features, as concentration or temperature changes were made, can be explained in terms of the degree of hydrogen bonding of these molecules.

The optical constants n and k were obtained from a least-squares fit to a lamellate model of the thin film and substrate. The tabulated n and k values were plotted and compared favorably with the n values obtained from the SKK analysis of k.

REFERENCES

1. Roux, J. A., Wood, B. E., and Smith, A. M. "IR Optical Properties of Thin H₂O, NH₃, and CO₂ Cryofilms." AEDC-TR-79-57 (AD-A074913), September 1979.
2. Roux, J. A., Wood, B. E., and Smith, A. M. "Infrared Optical Properties of Bipropellant Cryocontaminants." AEDC-TR-79-50 (AD-A073186), August 1979.
3. Roux, J. A., Wood, B. E., Smith, A. M. and Plyler, R. R. "Infrared Optical Properties of Thin CO, NO, CH₄, HC1, N₂O, O₂, N₂, Ar, and Air Cryofilms." AEDC-TR-79-81 (AD-A088269), August 1980.

4. Roux, J. A., Wood, B. E., Smith, A. M., Pipes, J. G., and Scott, H. E. "IR Optical Properties of Bipropellant Cryocontaminants." In *Proceedings. USAF/NASA International Spacecraft Contamination Conference.* AFML-TR-78-190, NASA-CA-2039, May 1979.
5. Bowlden, H. J. and Wilmhurst, J. K. "Evaluation of the One-Angle Reflection Technique for the Determination of Optical Constants." *Journal of the Optical Society of America*, Vol. 53, No. 9, September 1963, pp. 1073-1078.
6. Robertson, Charles W., Downing, Harry D., Curnutte, Basil, and Williams, Dudley. "Optical Constants of Solid Ammonia in the Infrared." *Journal of the Optical Society of America*, Vol. 65, No. 4, April 1975, pp. 432-435.
7. Pipes, J. G., Roux, J. A., Smith, A. M., and Scott, H. E. "Infrared Transmission of Contaminated Cryocooled Optical Windows." *AIAA Journal*, Vol. 16, No. 9, September 1978, pp. 984-990.
8. Tempelmeyer, K. E. and Mills, D. W., Jr. "Refractive Index of Carbon Dioxide Cryodeposit." *Journal of Applied Physics*, Vol. 39, No. 6, May 1968, pp. 2968-2969.
9. Pimentel, G. C. and McClellan, A. L. *The Hydrogen Bond*. Freeman, San Francisco, 1960.
10. Herzberg, G. *Infrared and Raman Spectra of Polyatomic Molecules*. D. Van Nostrand Co., Inc., Princeton, N. J., 1954.
11. Newbolt, W. B. "Tests of Two Hypotheses Concerning the Optical Properties of Cryodeposited Gases." Participant's Final Report, 1977 USAF-ASEE Summer Faculty Research Program, AEDC.
12. Ewing, G. E. and Pimentel, G. D. "Infrared Spectrum of Solid Carbon Monoxide." *Journal of Chemical Physics*, Vol. 35, No. 3, September 1961, pp. 925-930.
13. Suzuki, S., Barnes, A. J., Cowieson, D., Mielke, Z., and Purnell, C. J. "Studies of Molecular Complexes by Matrix Isolation Spectroscopy." *Molecular Spectroscopy of Dense Phases — Proceedings of the 12th European Congress on Molecular Spectroscopy*, Strasbourg, France, July 1 — 4, 1975. Elsevier Scientific Publishing Co., Amsterdam, 1976.

14. Wilson, E. Bright, Jr., Decius, J. C., and Cross, Paul C. *Molecular Vibrations: The Theory of Infrared and Raman Vibrational Spectra*. McGraw-Hill, New York, 1955.
15. Schriver, A., Silvi, B., Maillard, D., and Perchard, J. P. "Structure of Water-Hydrochloric Acid Complexes in Argon and Nitrogen Matrices from Infrared Spectra." *Journal of Physical Chemistry*, Vol. 81, No. 22, 3 November 1977, pp. 2095-2102.
16. Jiang, G. J., Person, W. B., and Brown, K. C. "Absolute Infrared Intensities and Band Shapes in Pure Solid CO and CO in Some Solid Matrices." *Journal of Chemical Physics*, Vol. 62, No. 4, 15 February 1975, pp. 1201-1211.
17. Downing, Harry D. and Williams, Dudley. "Optical Constants of Water in the Infrared." *Journal of Geophysical Research*, Vol. 80, No. 12, 20 April 1975, pp. 1656-1661.
18. Pinkley, L. W., Sethna, P. P., and Williams, D. "Optical Constants of Water in the Infrared: Influence of Temperature." *Journal of the Optical Society of America*, Vol. 67, No. 4, April 1977, pp. 494-499.
19. Schaaf, J. W. "The Infrared Reflectance of Ice I." Ph.D. thesis, Kansas State University, 1972.
20. Williams, Dudley. "Frequency Assignments in Infra-red Spectrum of Water." *Nature*, Vol. 210, No. 5032, 9 April 1966, pp. 194-195.
21. Huong, P. V. and Cornut, J. C. "Spectra Infrarouge et Structure de l'Eau dans Les Matrices de Gaz Inertes." *Journal de Chimie Physique*, Vol. 72, No. 4, 1975, pp. 534-536.
22. Ayers, G. P. and Pullin, A.D.E. "The IR Spectra of Matrix Isolated Water Species," Parts 1 through 4. *Spectrochimica Acta*, Vol. 32A, 1976, pp. 1629-1639, 1641-1650, 1689-1693, and 1695-1704.
23. Van Thiel, M., Becker, E. D., and Pimentel, G. C. "Infrared Studies of Hydrogen Bonding of Water by the Matrix Isolation Technique." *Journal of Chemical Physics*, Vol. 26, No. 1, January 1957, pp. 145-150.
24. Tursi, Anthony J. and Nixon, Eugene R. "Matrix Isolation Study of the Water Dimer in Solid Nitrogen." *Journal of Chemical Physics*, Vol. 52, No. 3, 1 February 1970, pp. 1521-1528.

25. Catalano, E. and Milligan, D. E. "Infrared Spectra of H₂O, D₂O, and HDO in Solid Argon, Krypton, and Xenon." *Journal of Chemical Physics*, Vol. 30, No. 1, January 1959, pp. 45-47.
26. Glasel, J. A. "Near-Infrared Absorption Spectra of Ortho- and Para-H₂O in Solid Xenon and Argon." *Journal of Chemical Physics*, Vol. 33, No. 1, July 1960, pp. 252-255.
27. Ritzhaupt, Gary and Devlin, J. Paul. "Infrared Spectrum of D₂O vibrationally Decoupled in Glassy H₂O." *Journal of Chemical Physics*, Vol. 67, No. 10, 15 November 1977, pp. 4779-4780.
28. Pipes, J. G., Roux, J. A., Smith, A. M., and Scott, H. E. "Transmission of Infrared Materials and Condensed Gases at Cryogenic Temperatures." AEDC-TR-77-71 (AD-A044517), September 1977.
29. Heavens, O. S. *Optical Properties of Thin Films*. Dover Publications, Inc., New York, 1965.
30. Maeda, S., Thyagarajan, G., and Schatz, P. N. "Absolute Infrared Intensity Measurements in Thin Films. II. Solids Deposited on Halide Plates." *Journal of Chemical Physics*, Vol. 39, No. 12, December 1963, pp. 3474-3481.
31. Marquardt, D. W. "An Algorithm for Least-Squares Estimation of Nonlinear Parameters." *Journal of the Society for Industrial and Applied Mathematics*, Vol. 11, No. 2, June 1963, pp. 431-441.
32. Wohlgemuth, J. H. and Brodie, D. E. "A Method for Calculating the Index of Refraction of Thin Films." *Canadian Journal of Physics*, Vol. 53, No. 18, 15 September 1975, pp. 1737-1742.
33. Maki, A. G. "Infrared Spectra of Carbon Monoxide as a Solid and in Solid Matrices." *Journal of Chemical Physics*, Vol. 35, No. 3, September 1961, pp. 931-935.
34. Hallam, H. E., ed. *Vibrational Spectroscopy of Trapped Species: Infrared and Raman Studies of Matrix-Isolated Molecules, Radicals, and Ions*. J. Wiley and Sons, New York, 1973.
35. Palmer, K. F. "Methods to Quantify Constituents in Binary Cryodeposits." Participant's Final Report, 1976 USAF-ASEE Summer Faculty Research Program, AEDC.

1. Pyroelectric detector and collection optics.
2. Stainless steel high vacuum chamber, 85 cm tall by 70 cm in diameter (33.5 in. by 27.5 in. in diameter).
3. Cryogenically cooled infrared window; germanium, 4 mm thick by 70 mm square (0.158 in. by 2.76 in.) and QCM.
4. Helium-neon laser ($0.6328 \mu\text{m}$) beam (one of two shown) employed to measure cryofilm thickness.
5. Infrared beam, 38 mm in diameter (1.5 in.).
6. 2-mw He-Ne laser.
7. Michelson interferometer.
8. Infrared source and collimator mirror.

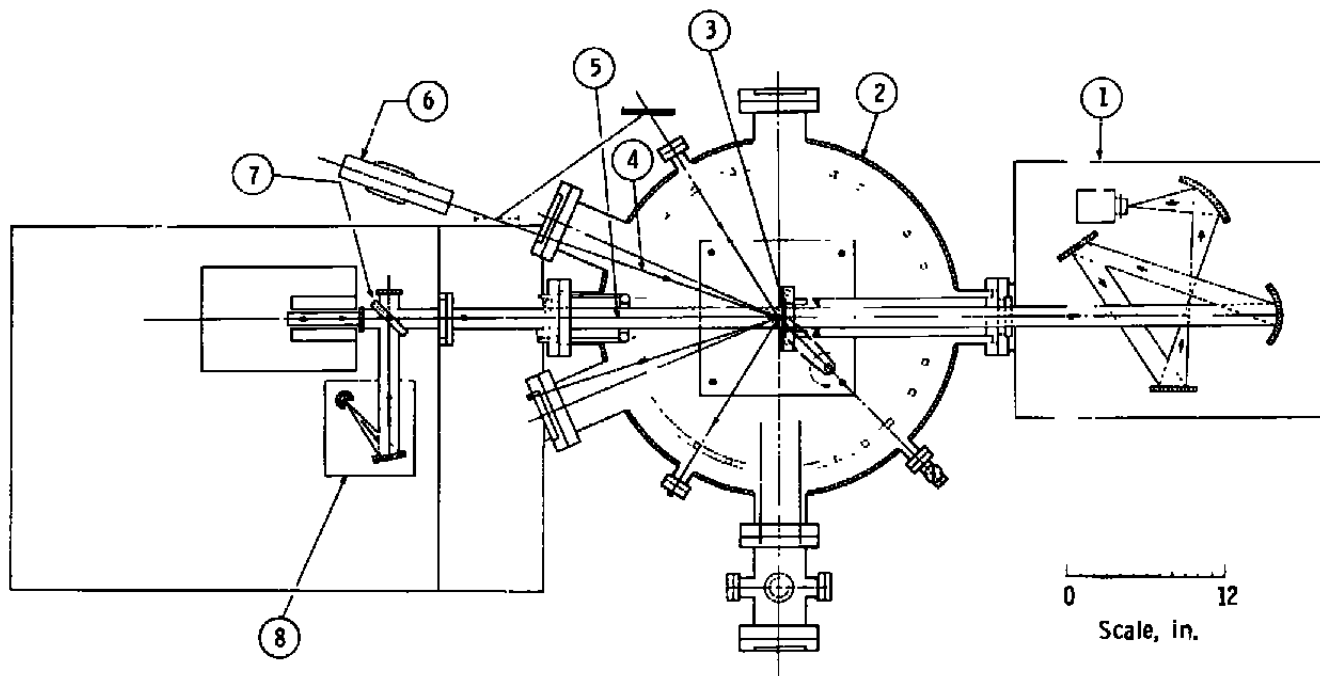


Figure 1. Schematic of the Infrared Optical Transmission Chamber (IROTC) with FTS-14 interferometer spectrometer.

1. Infrared beam, 38-mm-diameter (1.5 in.).
2. Optical stop required to underfill cryocooled window with infrared beam. Also, this stop is supported by a 3-in. -ID pipe that prevents gas added to chamber from cryopumping on rear of window.
3. Aluminum holder with cryogenic passageways.
4. Germanium window heat sunk with an indium gasket to the aluminum holder.
5. Cover plate.
6. Gaseous helium or liquid nitrogen inlet.
7. Gaseous helium or liquid nitrogen outlet.
8. Crosshatched area illustrates area of window heat sunk to holder. Clear diameter is 50.7 mm (2 in.) while infrared beam diameter is 38 mm (1.5 in. I).
9. QCM heat sunk with indium gasket to aluminum holder.

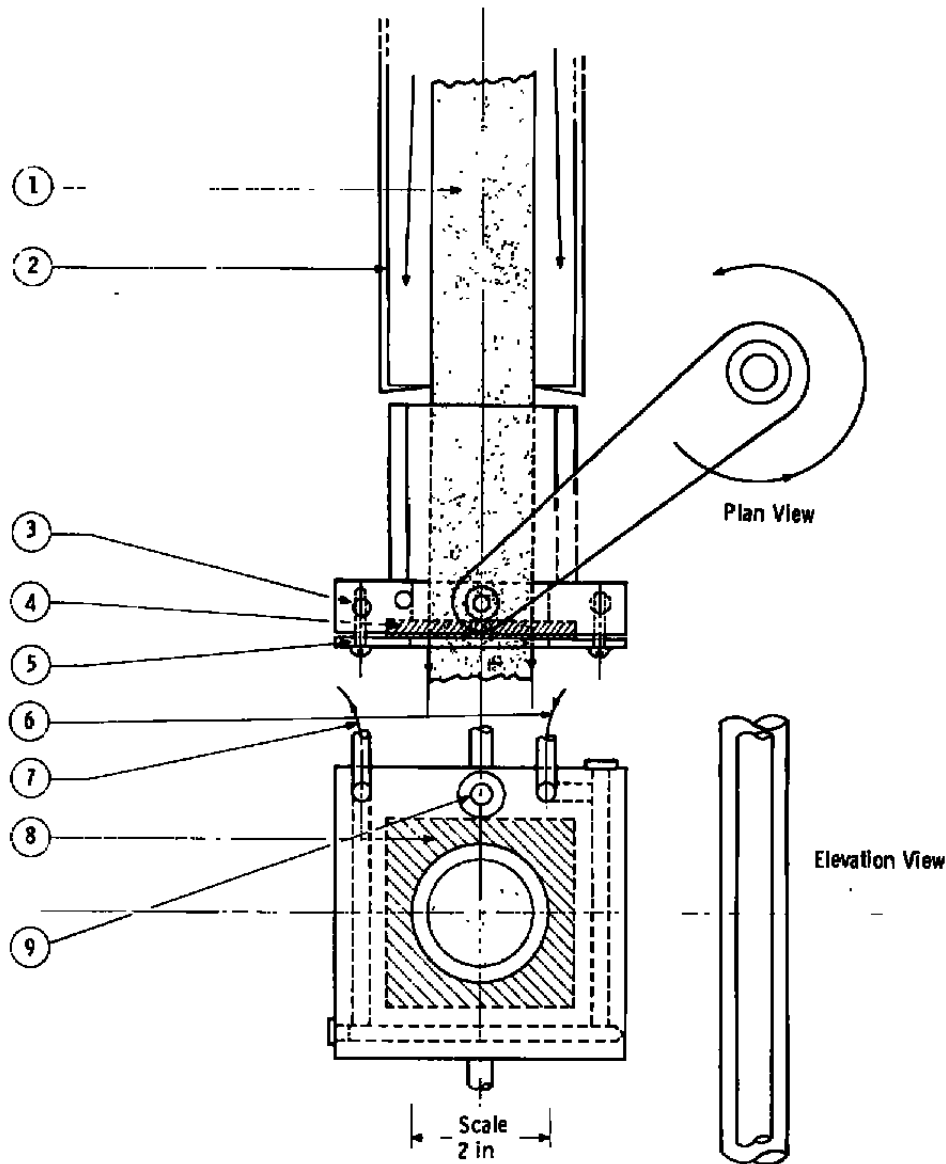


Figure 2. Plan and elevation views of cryogenically cooled window holder.

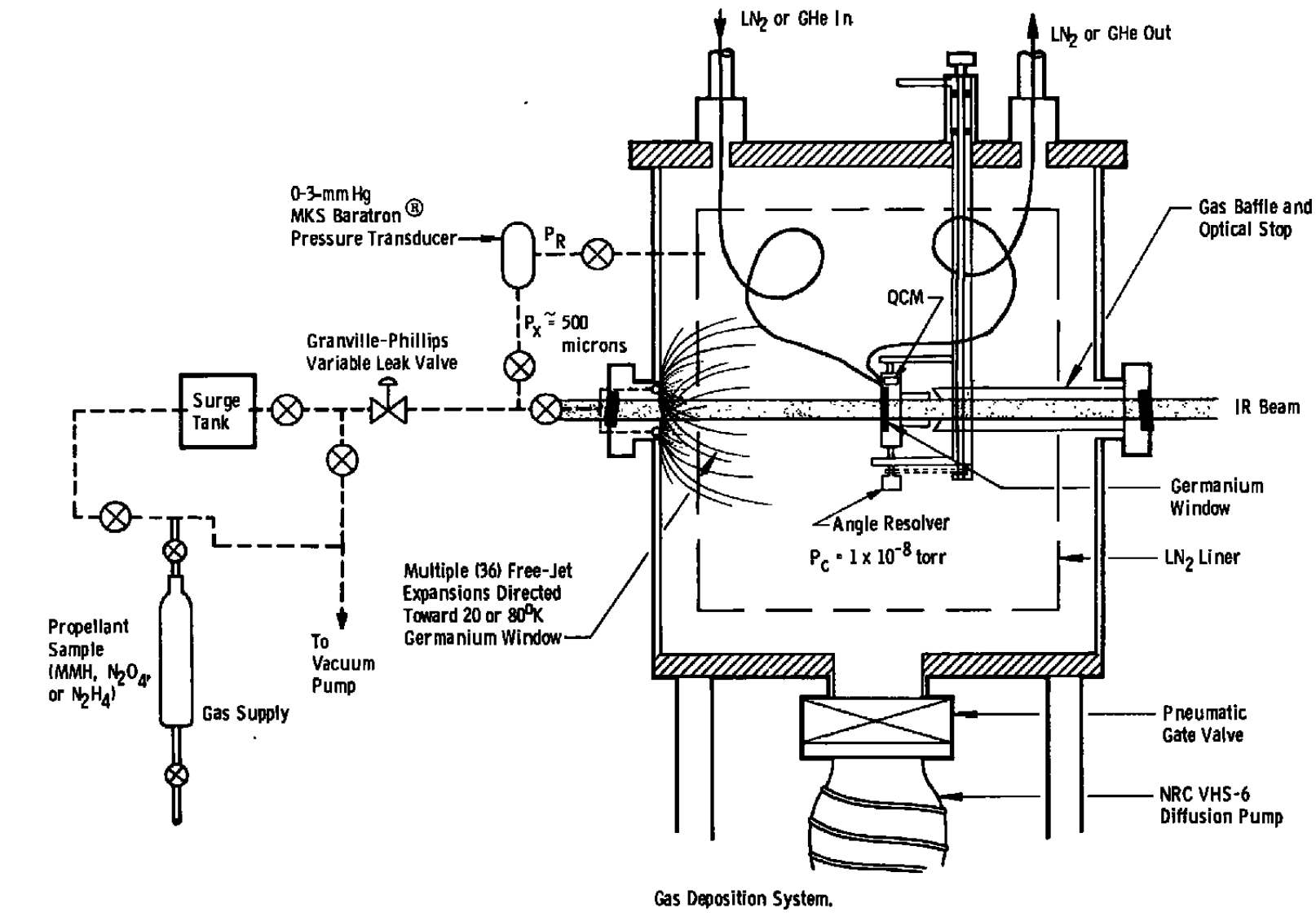


Figure 3. Gas deposition system.

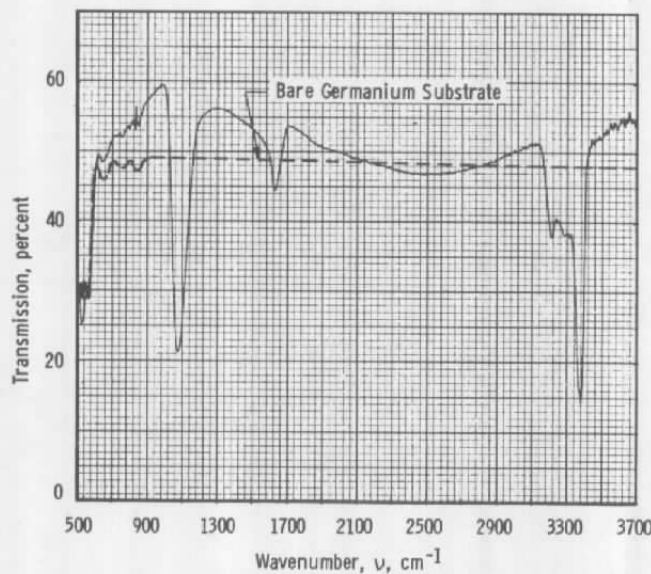


Figure 4. Transmittance of 1.43- μm -thick solid NH_3 on 20°K germanium.

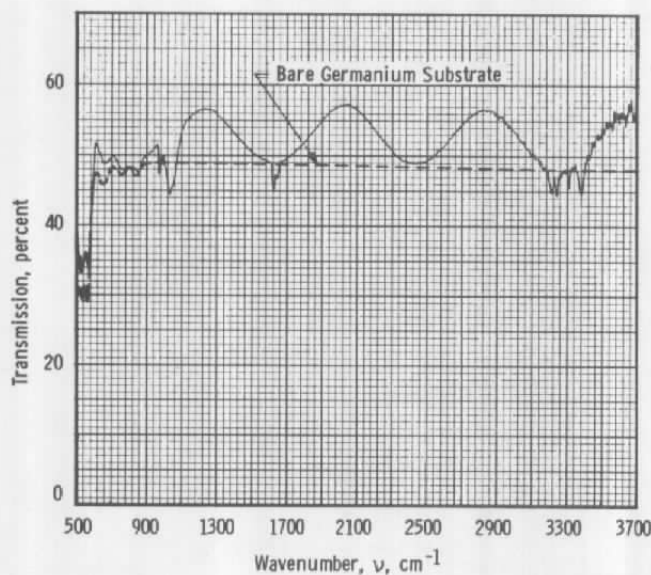


Figure 5. Transmittance of 4.97- μm -thick solid NH_3/N_2 mixture (20%/80%) on 20°K germanium.

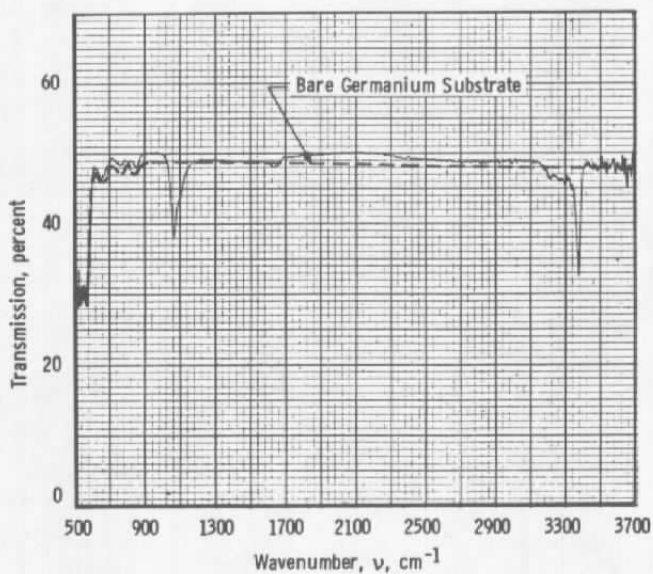


Figure 6. Transmittance of 4.97- μm -thick solid NH_3/N_2 mixture (20%/80%) after warmup from 20 to 59°K on germanium.

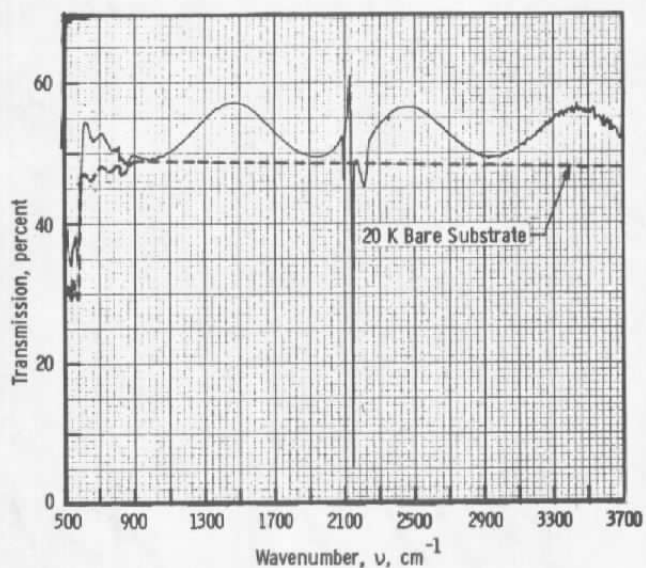


Figure 7. Transmittance of pure CO on 20°K germanium.

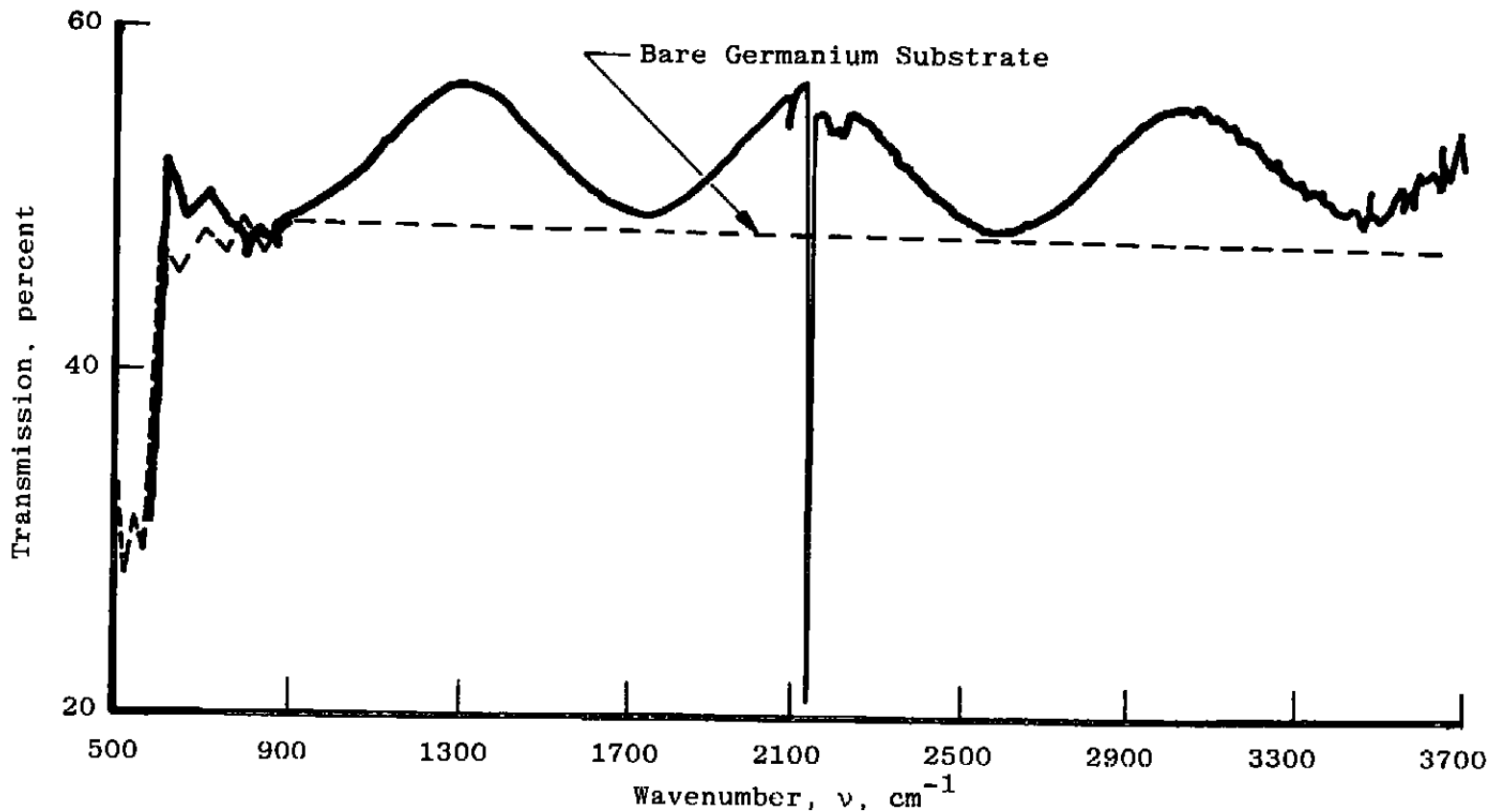


Figure 8. Transmittance of 4.765- μm -thick solid N_2/CO mixture (75%/20%) on 20°K germanium.

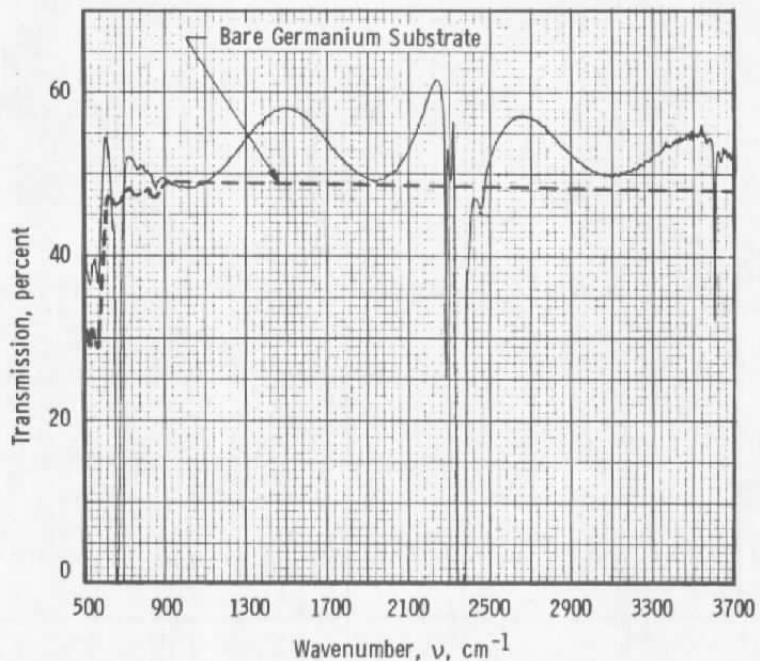


Figure 9. Transmittance of 3.88- μm -thick solid CO_2 on 20°K germanium.

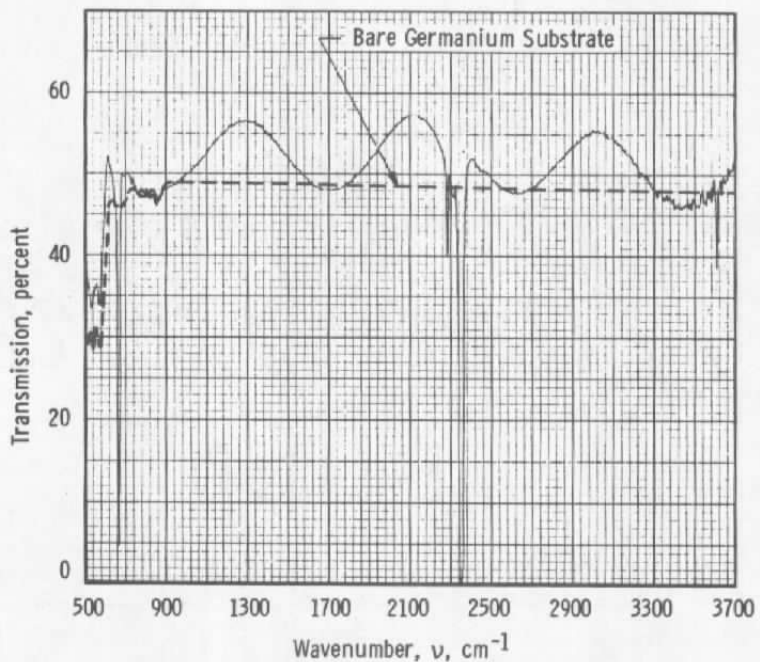


Figure 10. Transmittance of 4.74- μm -thick solid CO_2/N_2 mixture (20%/80%) on 20°K germanium.

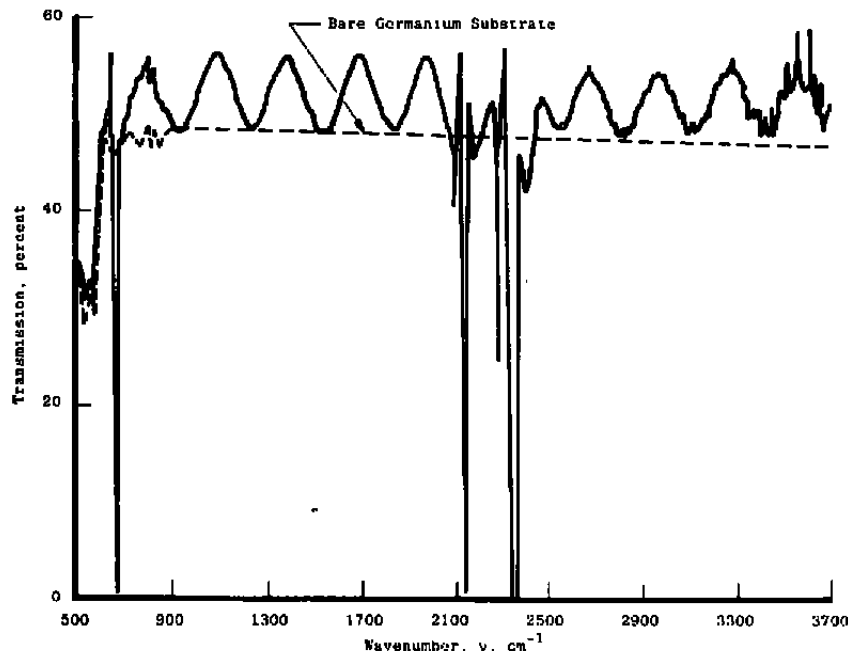


Figure 11. Transmittance of 13.16- μm -thick solid CO_2/CO mixture (50%/50%) on 20°K germanium.

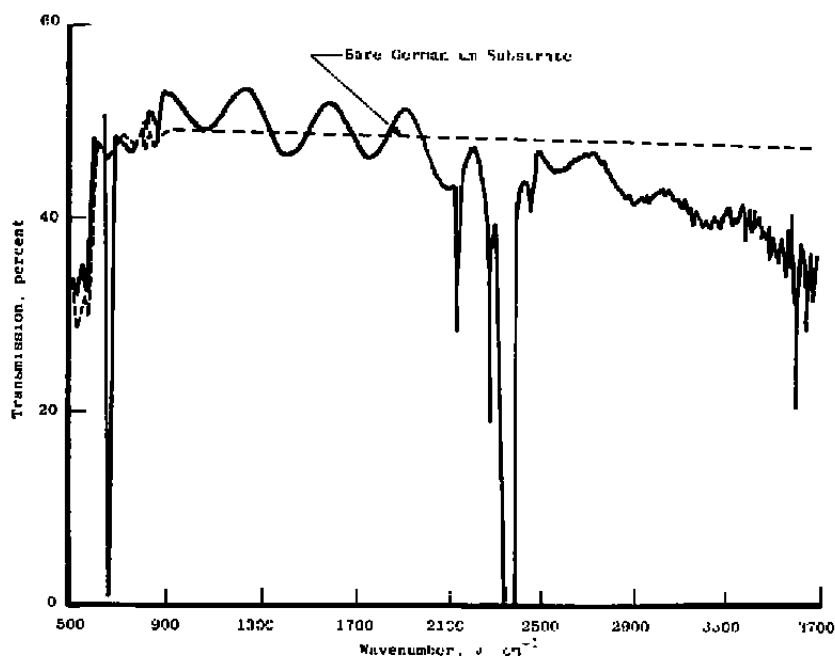


Figure 12. Transmittance of 13.16- μm -thick solid CO_2/CO mixture (50%/50%) after warmup from 20 to 50°K on germanium.

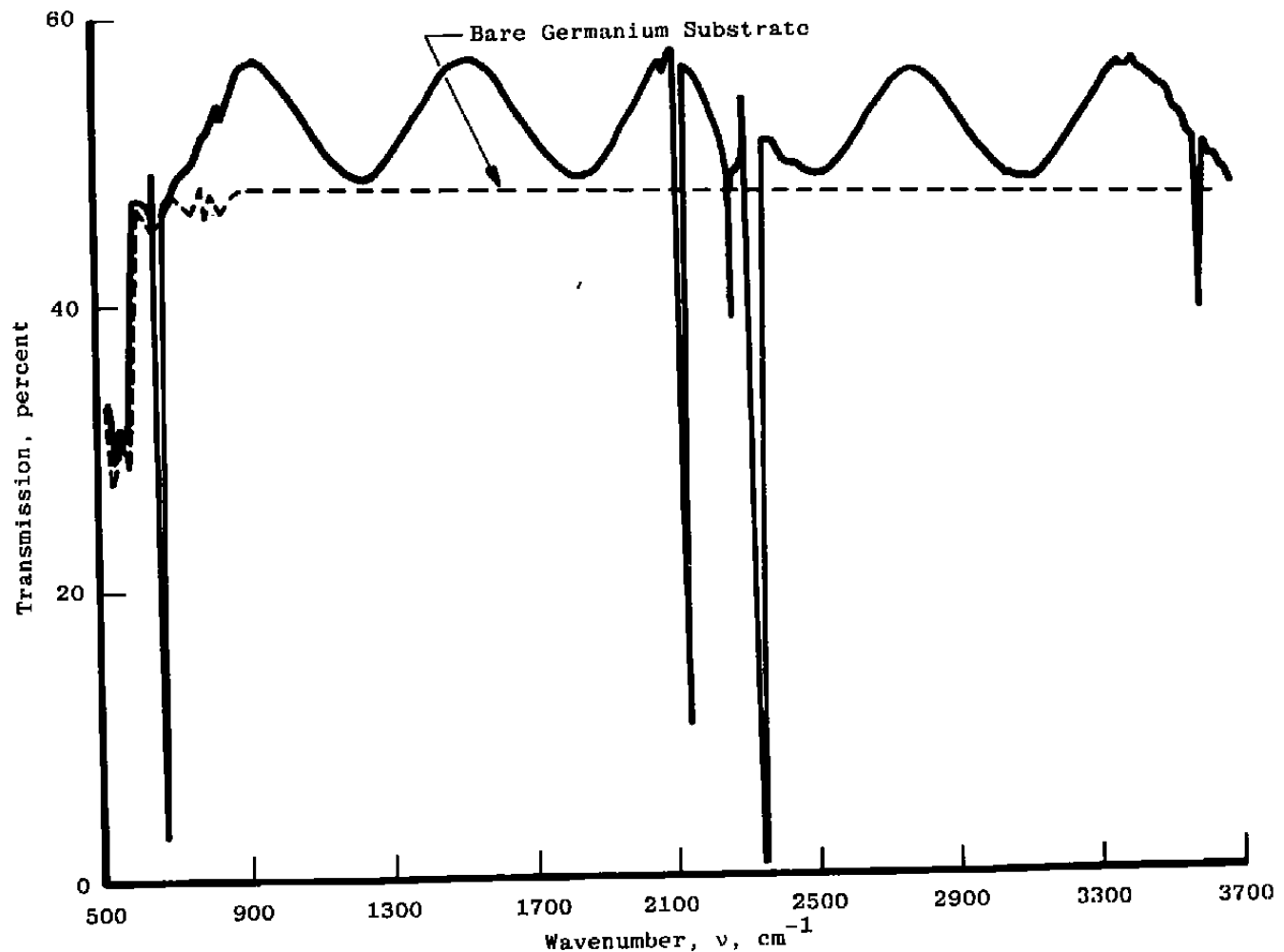


Figure 13. Transmittance of 6.602- μm -thick solid $\text{N}_2/\text{CO}/\text{CO}_2$ mixture
(64%/23%/13%) on 20°K germanium.

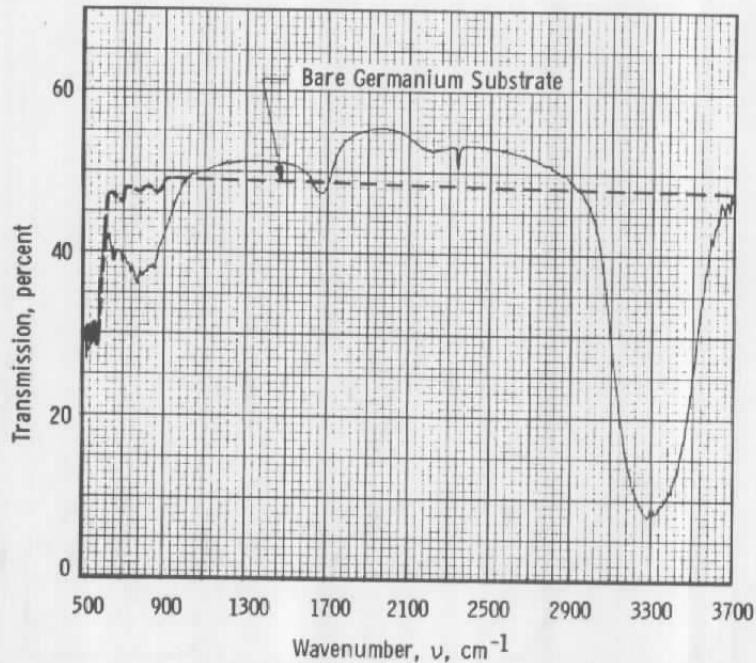


Figure 14. Transmittance of 1.00- μm -thick solid H_2O on 20°K germanium.

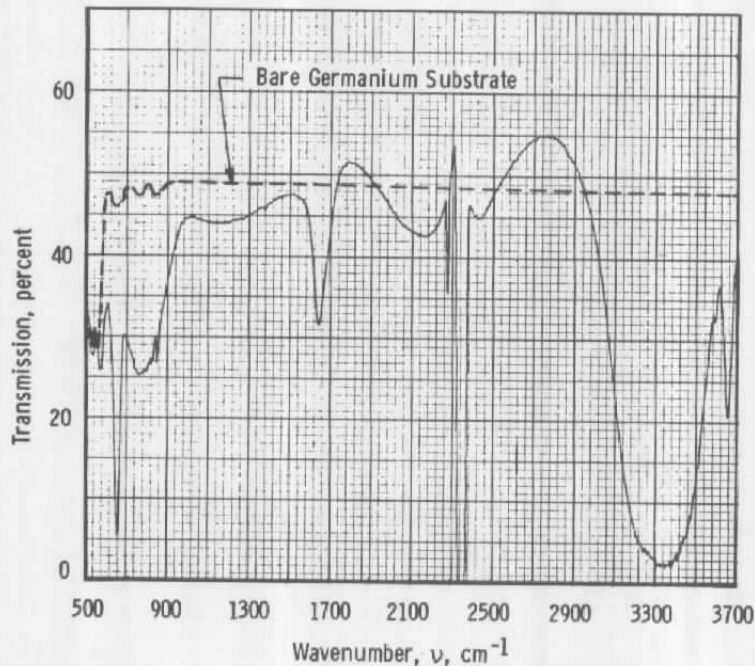


Figure 15. Transmittance of 3.49- μm -thick solid $\text{H}_2\text{O}/\text{CO}_2$ mixture (61%/36%) on 20°K germanium.

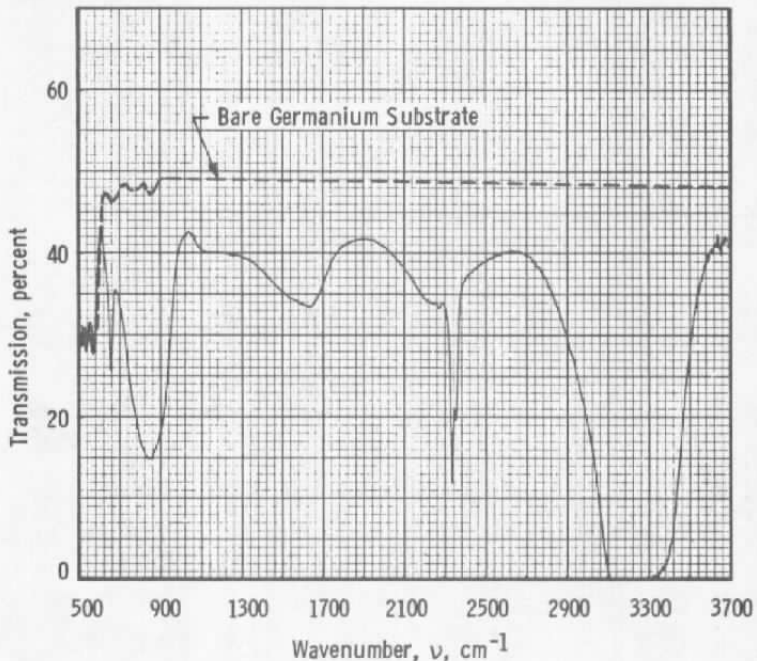


Figure 16. Transmittance of 3.49- μm -thick solid $\text{H}_2\text{O}/\text{CO}_2$ mixture (61%/36%) after warmup from 20 to 153°K on germanium.

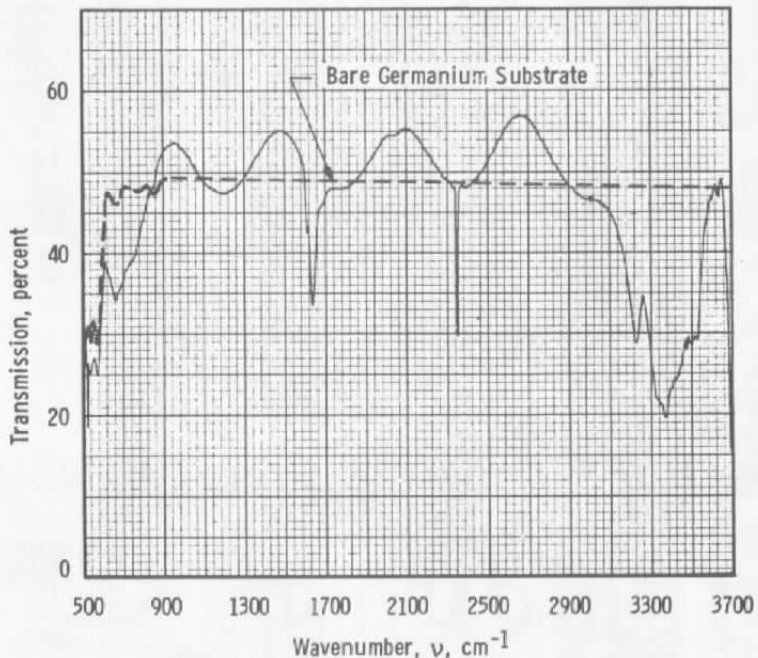


Figure 17. Transmittance of 6.78- μm -thick solid $\text{N}_2/\text{H}_2\text{O}/\text{CO}_2$ mixture (86%/13%/1%) on 20°K germanium.

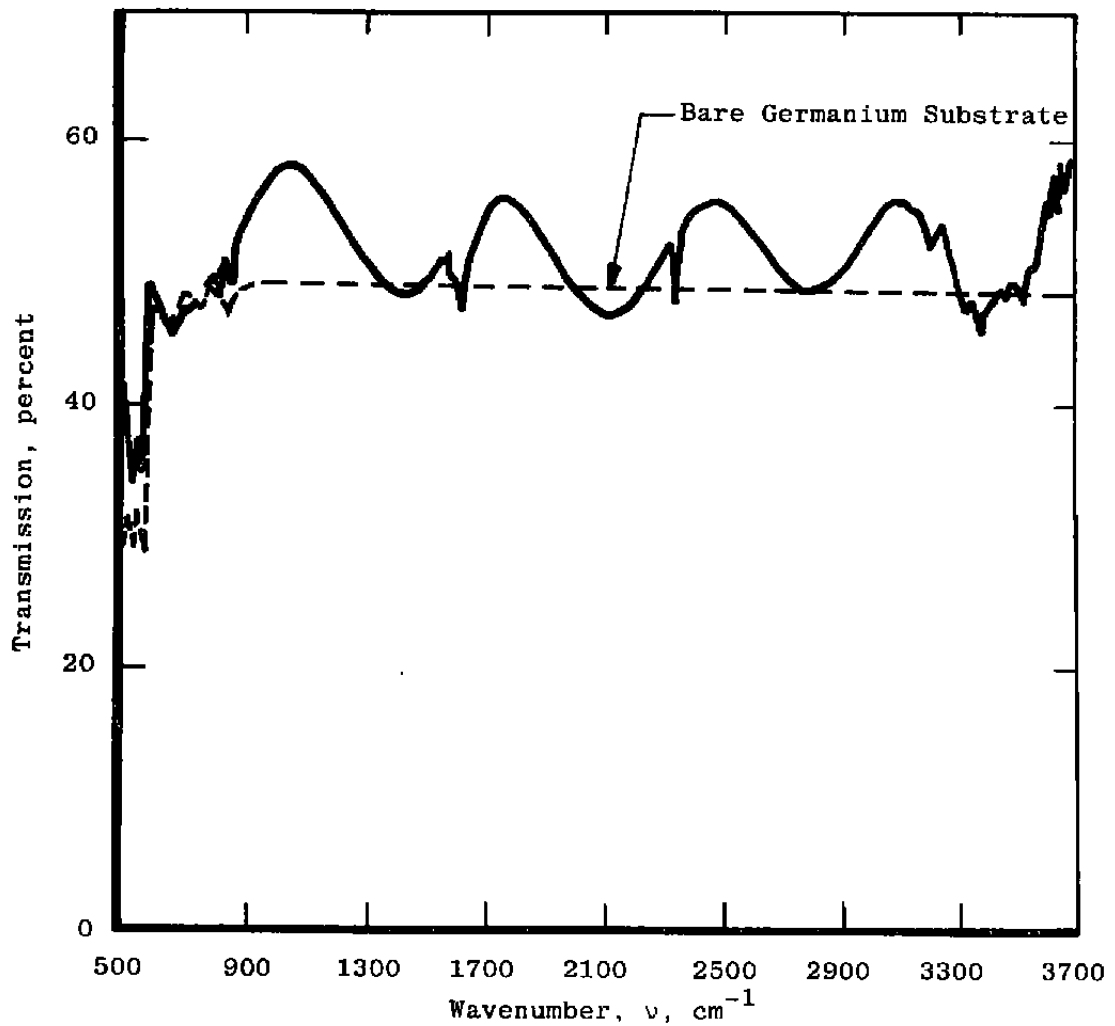


Figure 18. Transmittance of 5.75- μm -thick solid Ar/H₂O mixture (93%/6%) on 20°K germanium.

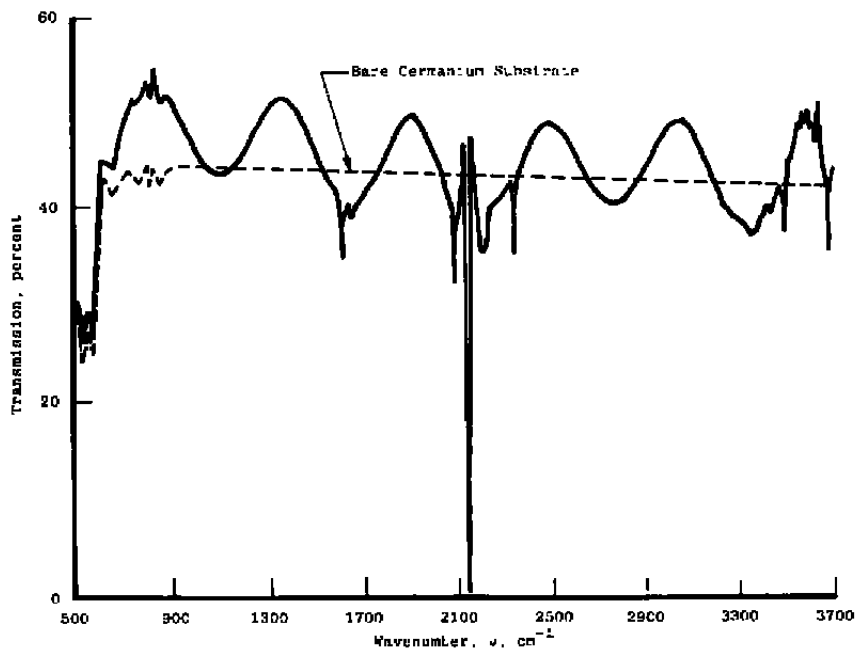


Figure 19. Transmittance of 6.54- μm -thick solid CO/H₂O mixture (91%/9%) on 20°K germanium.

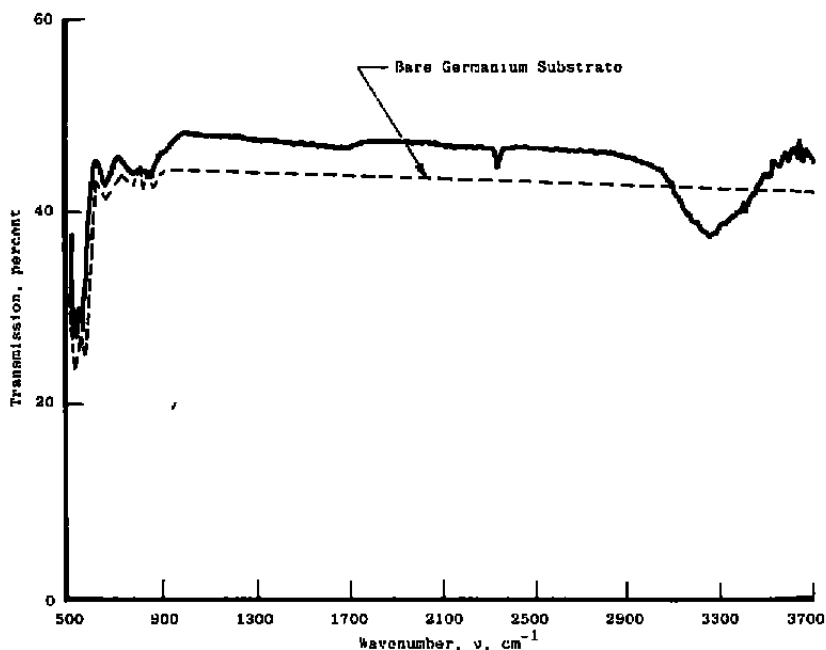


Figure 20. Transmittance of 6.54- μm -thick solid CO/H₂O mixture (91%/9%) after warmup from 20 to 105°K on germanium.

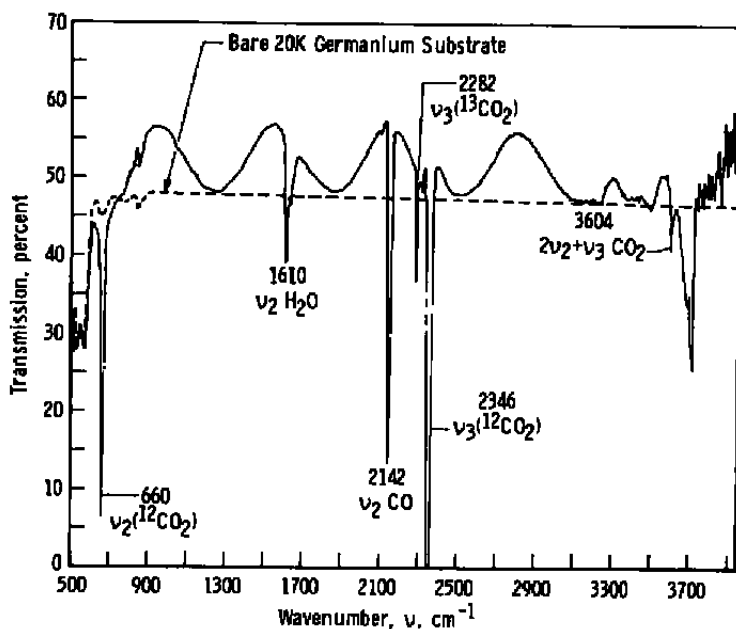


Figure 21. Transmittance of 6.72- μm -thick solid simulated plume mixture 1 on 20°K germanium.

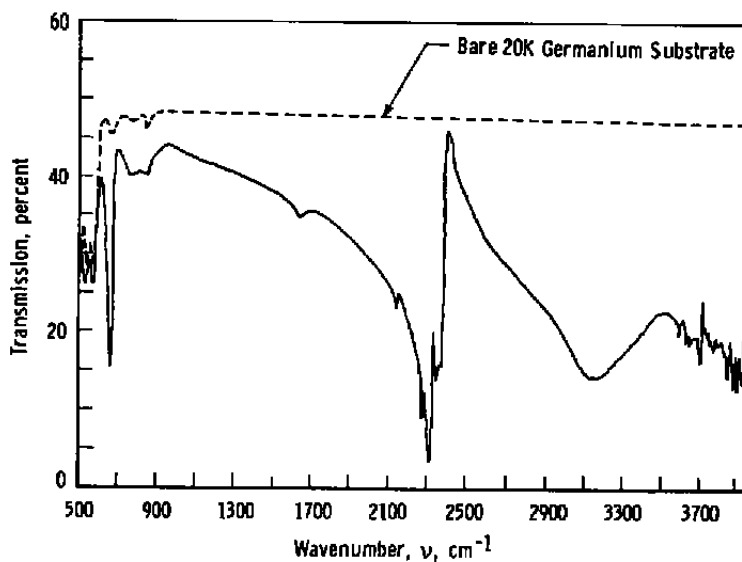


Figure 22. Transmittance of 6.72- μm -thick solid simulated plume mixture after warmup of germanium from 20 to 96°K.

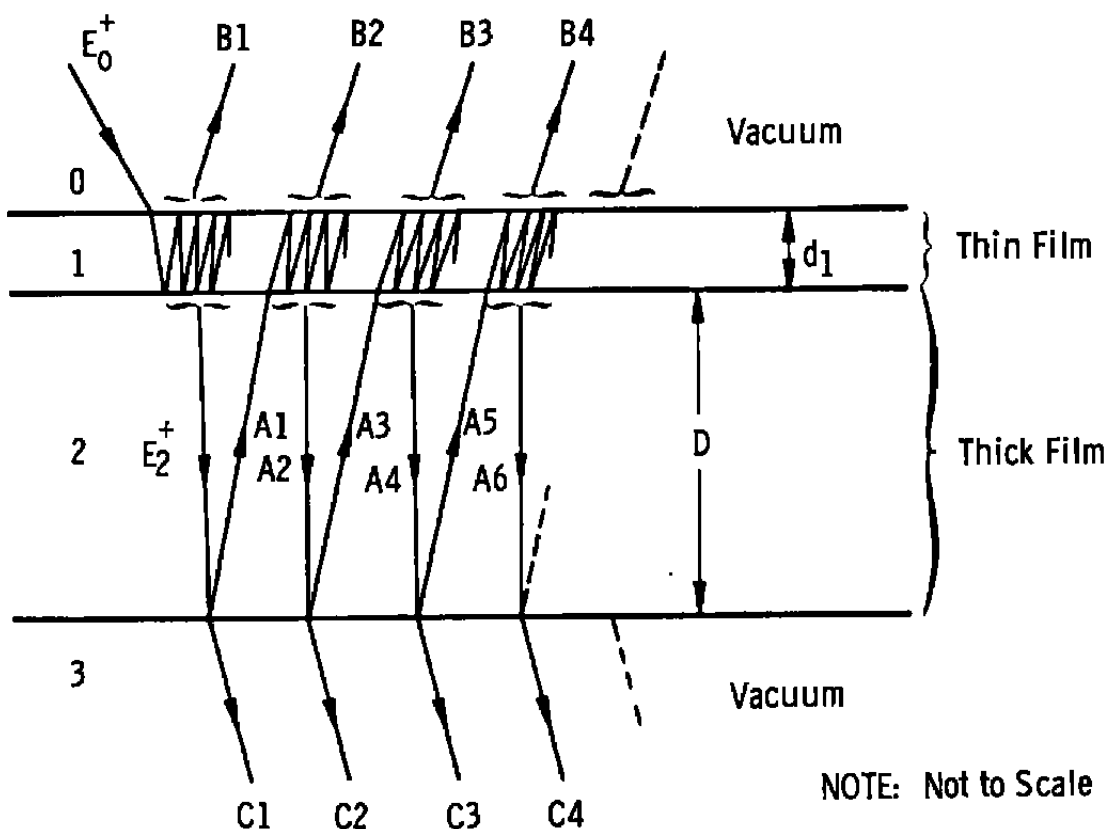


Figure 23. Geometry depicting analytical model for a thin film formed on a thick film.

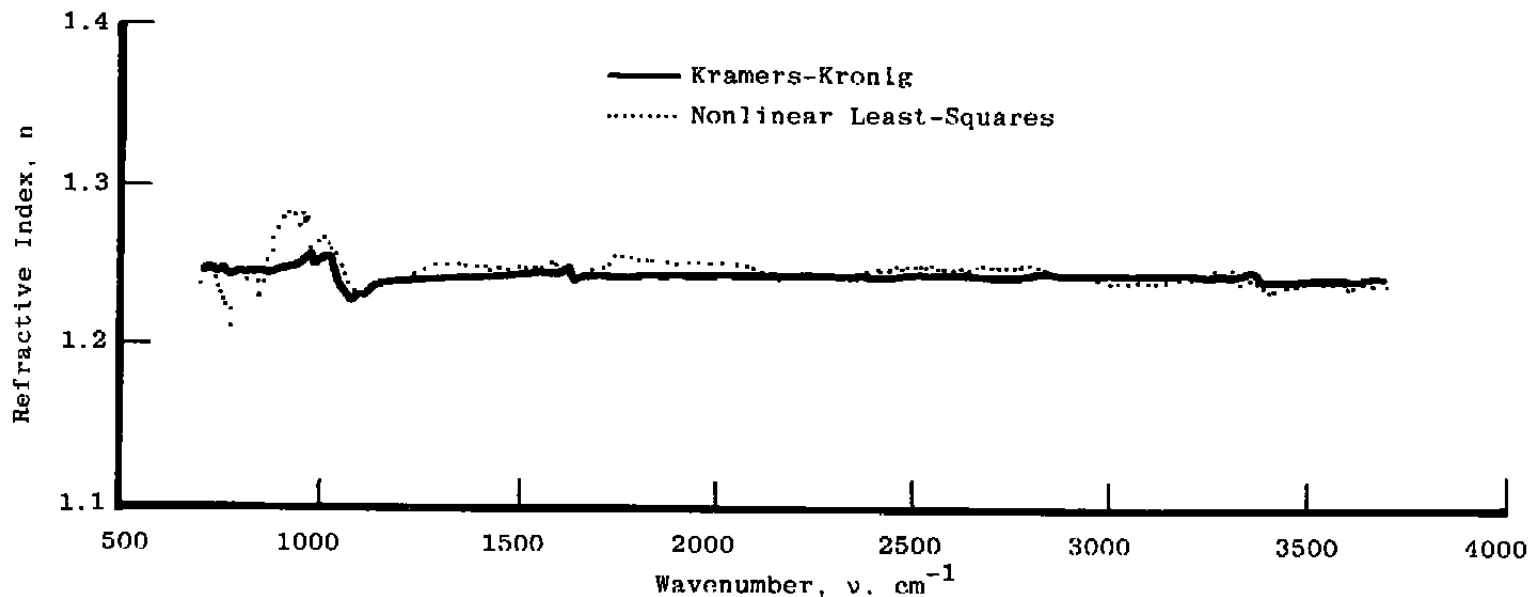


Figure 24. Refractive index of solid N_2/NH_3 mixture (85%/15%) on 20°K germanium.

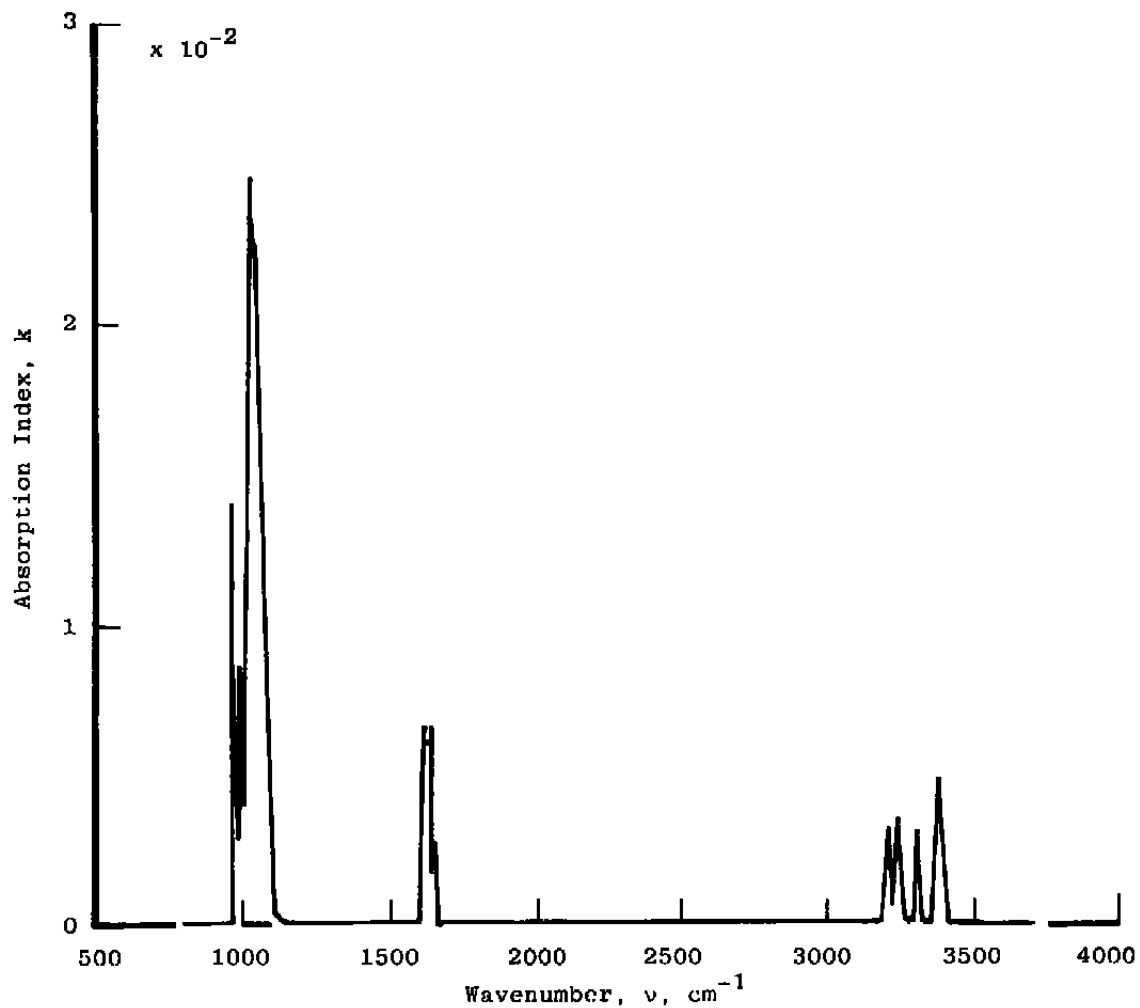


Figure 25. Absorption index of solid N_2/NH_3 mixture (85%/15%) on 20°K germanium.

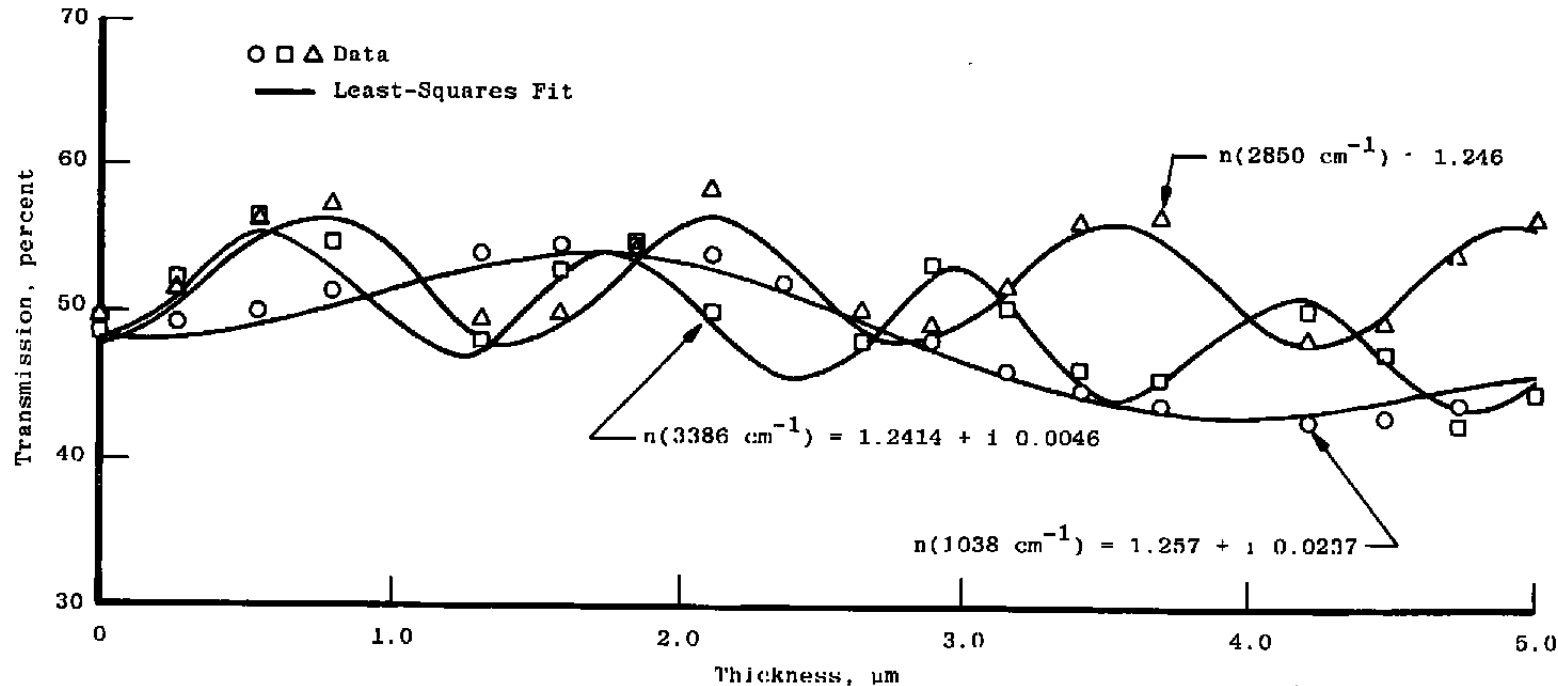


Figure 26. Comparison of the data with the nonlinear least-squares fit for N_2/NH_3 films (85%/15%) at 1038 , 2850 , and 3386 cm^{-1} .

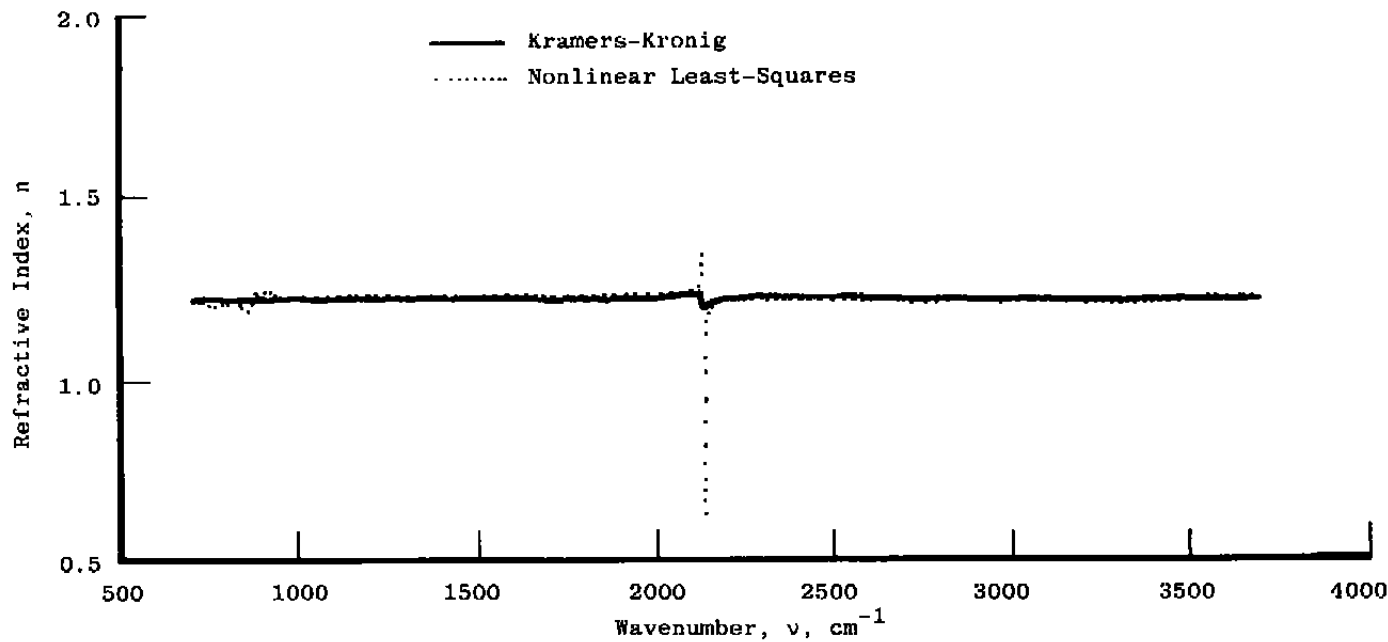


Figure 27. Refractive index of solid N_2/CO mixture (79%/20%) on 20°K germanium.

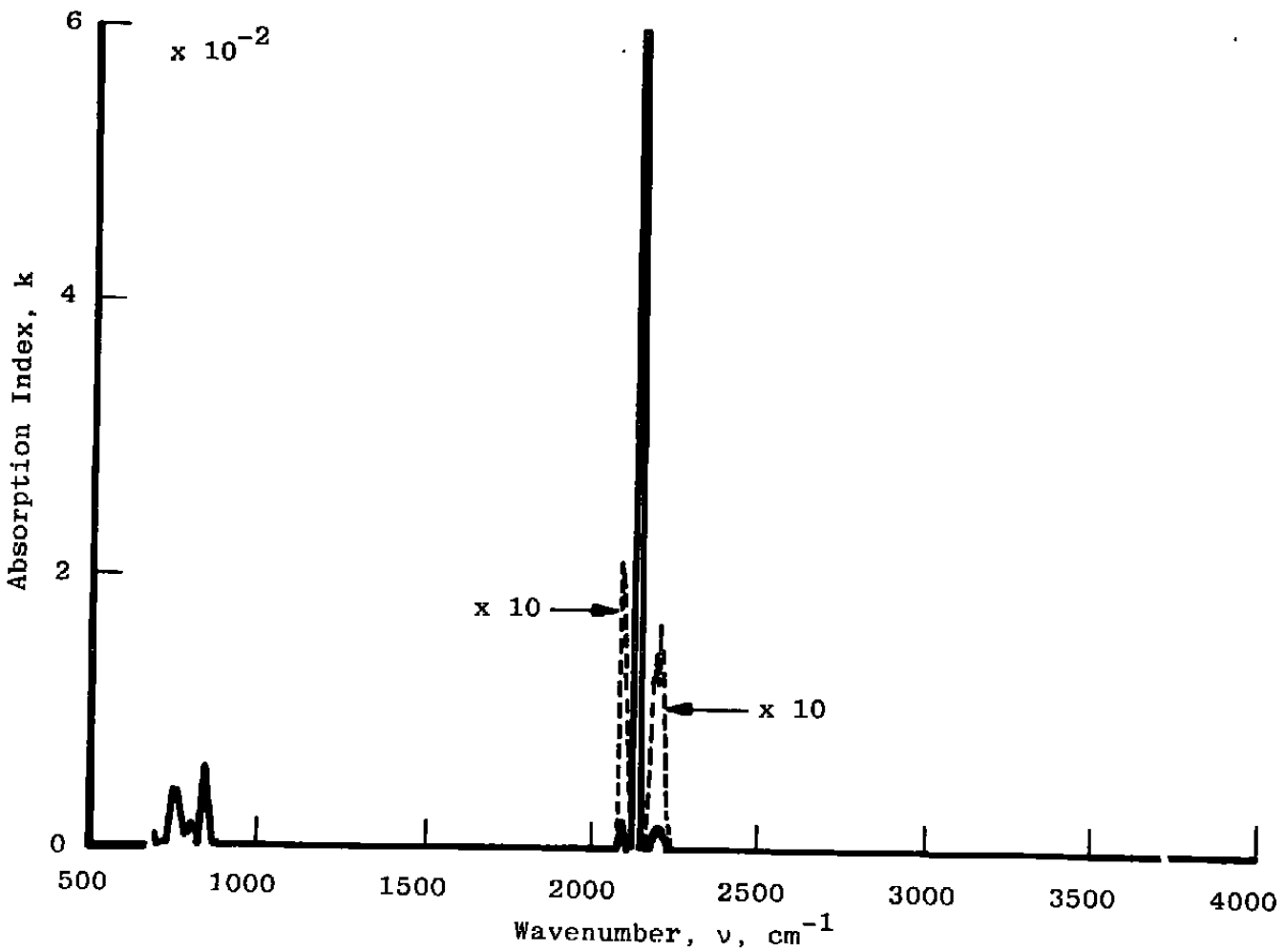


Figure 28. Absorption index of solid N_2/CO mixture (79%/20%) on 20°K germanium.

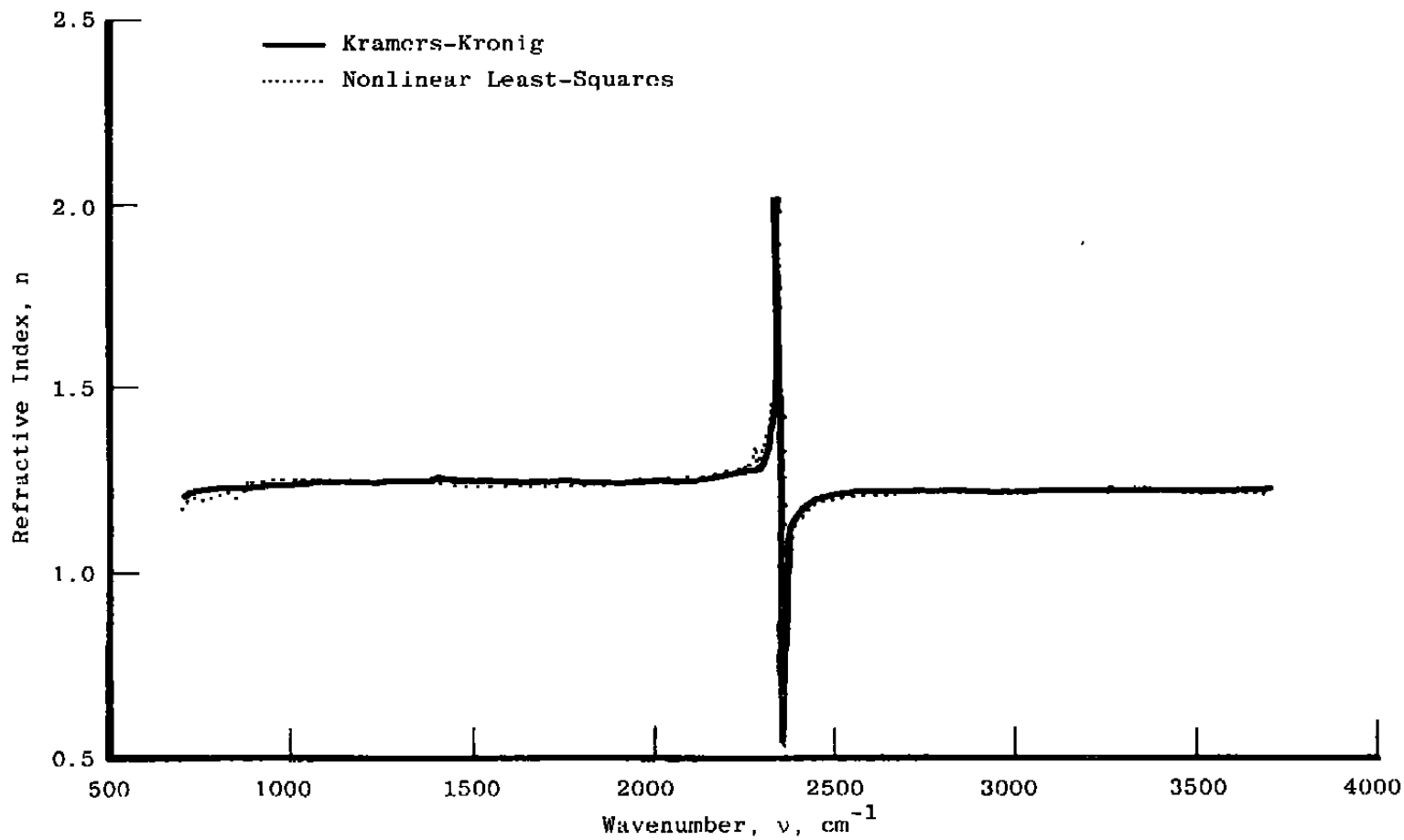


Figure 29. Refractive index of solid N_2/CO_2 mixture (75%/25%) on 20°K germanium.

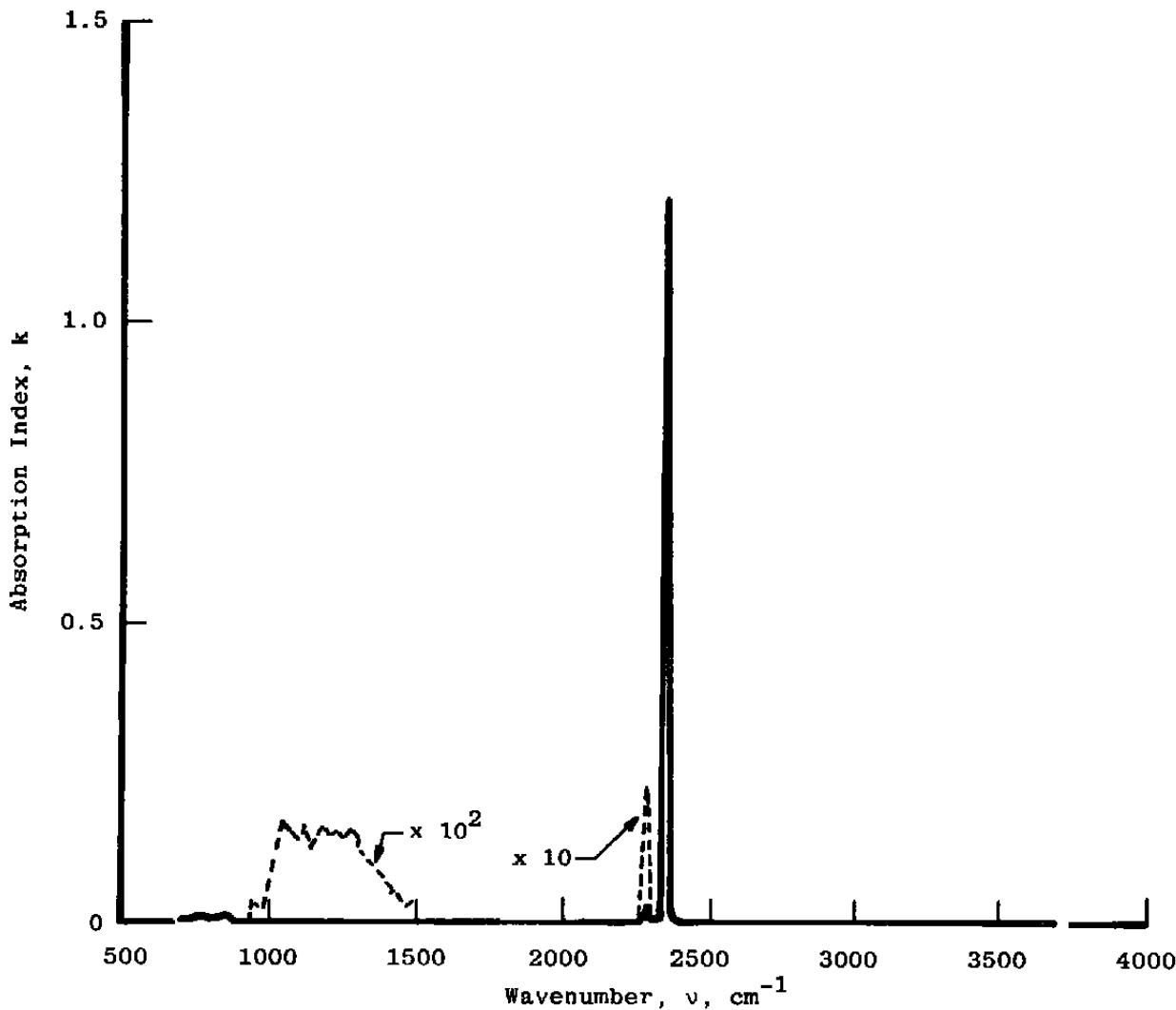


Figure 30. Absorption index of solid N_2/CO_2 mixture (75%/25%) on 20°K germanium.

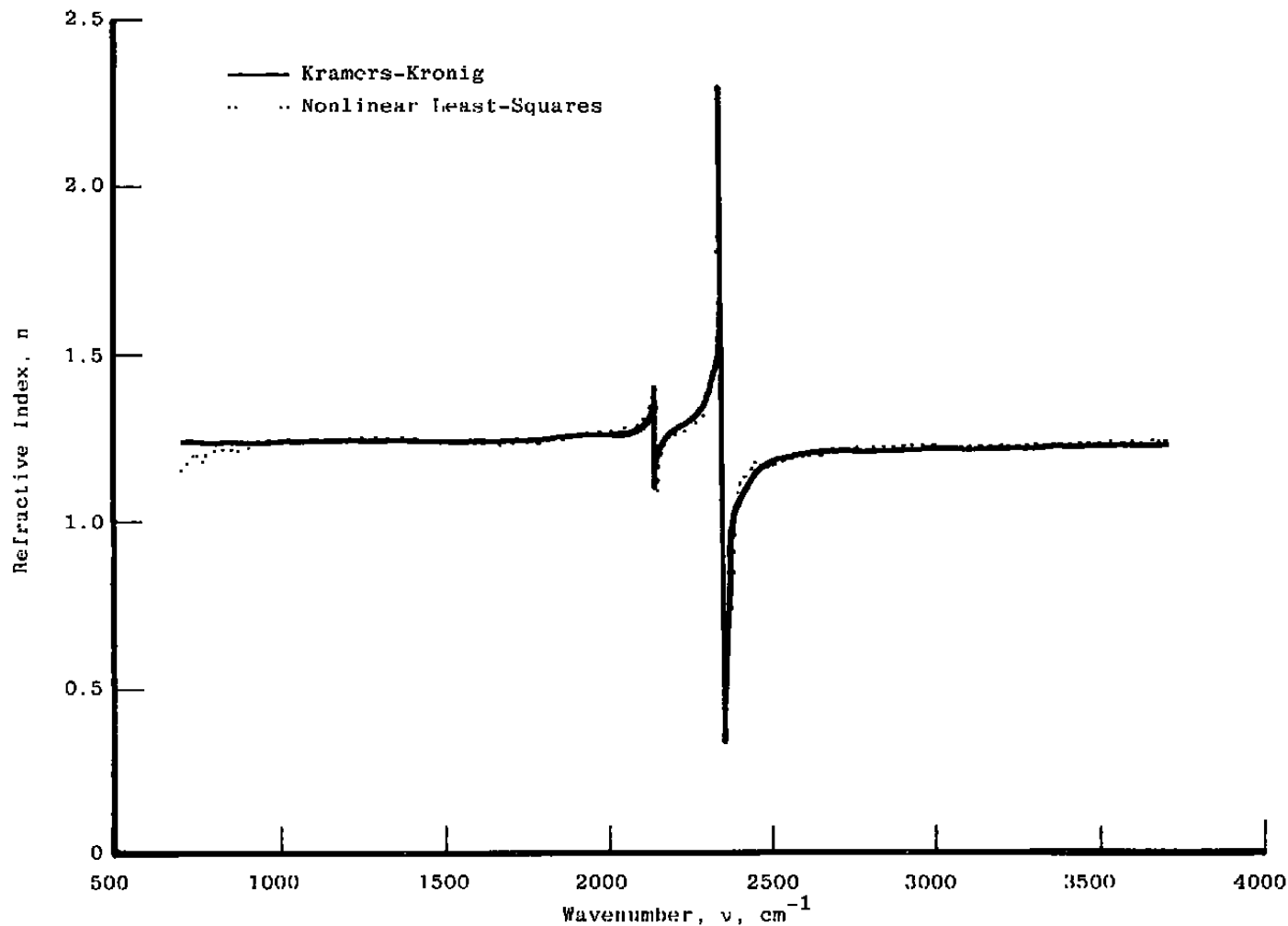


Figure 31. Refractive index of solid CO/CO₂ mixture (50%/50%) on 20°K germanium.

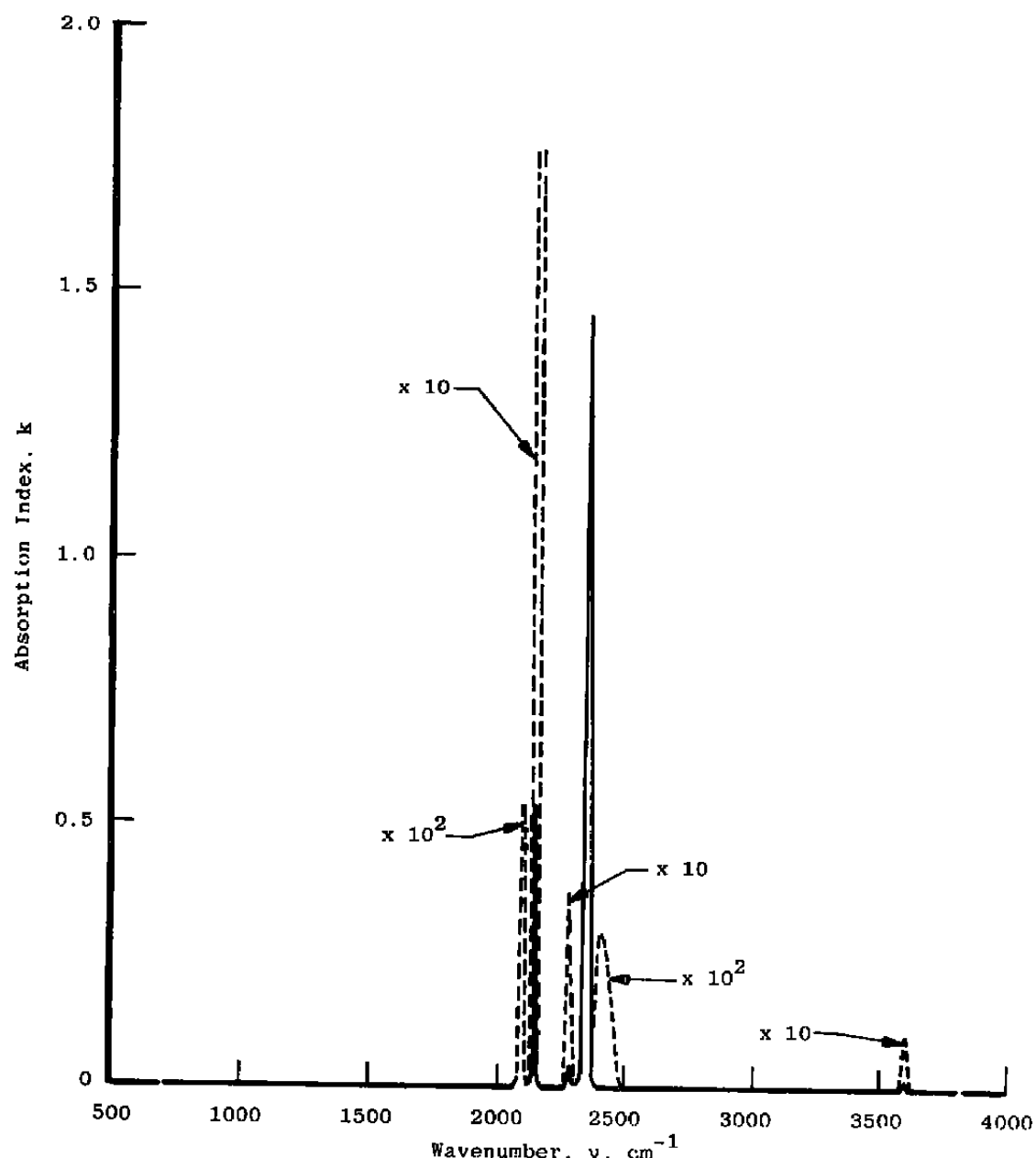


Figure 32. Absorption index of solid CO/CO_2 mixture (50%/50%) on 20°K germanium.

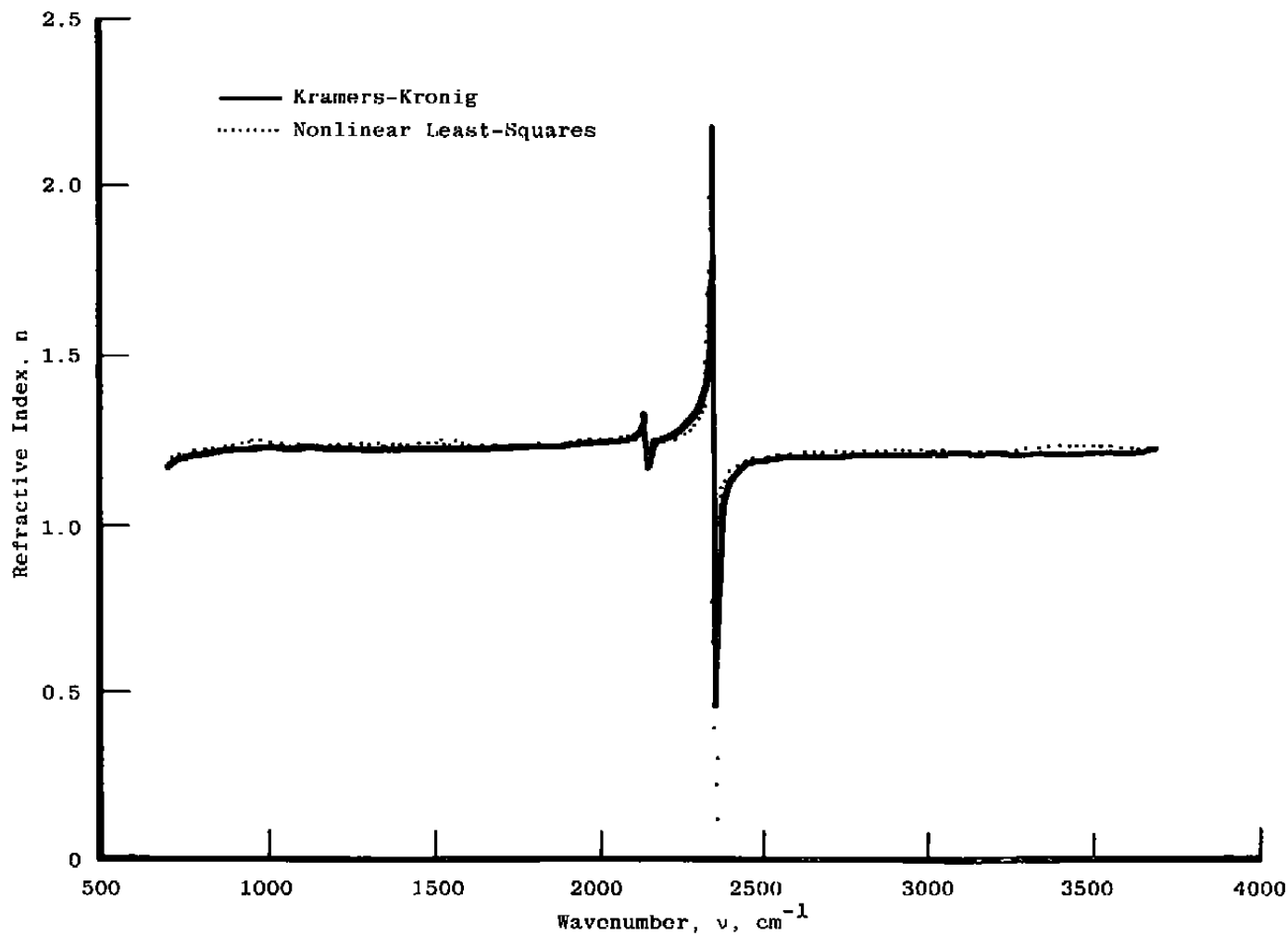


Figure 33. Refractive index of solid $\text{N}_2/\text{CO}/\text{CO}_2$ mixture (64%/23%/13%) on 20°K germanium.

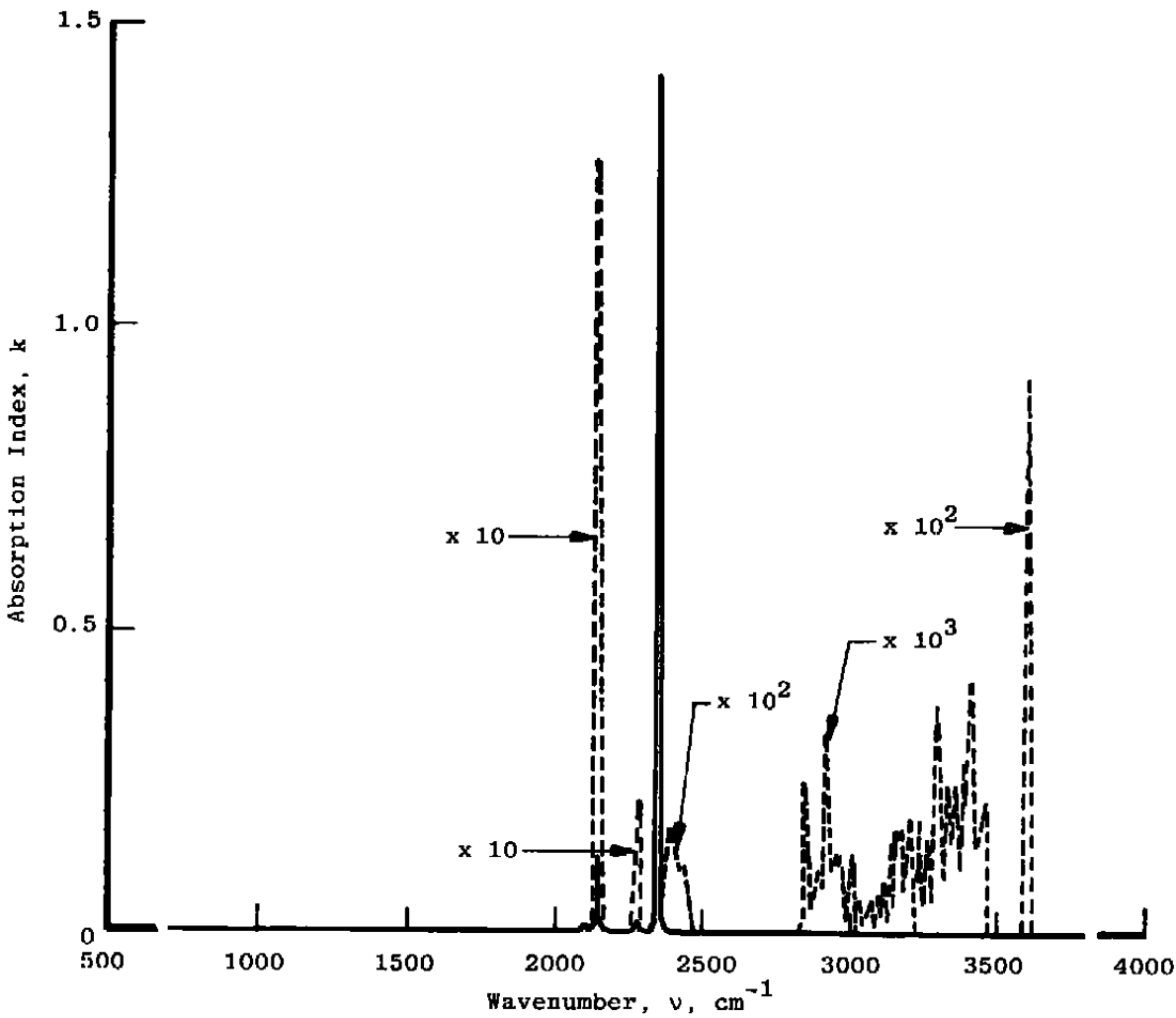


Figure 34. Absorption index of solid $\text{N}_2/\text{CO}/\text{CO}_2$ mixture (64%/23%/13%) on 20°K germanium.

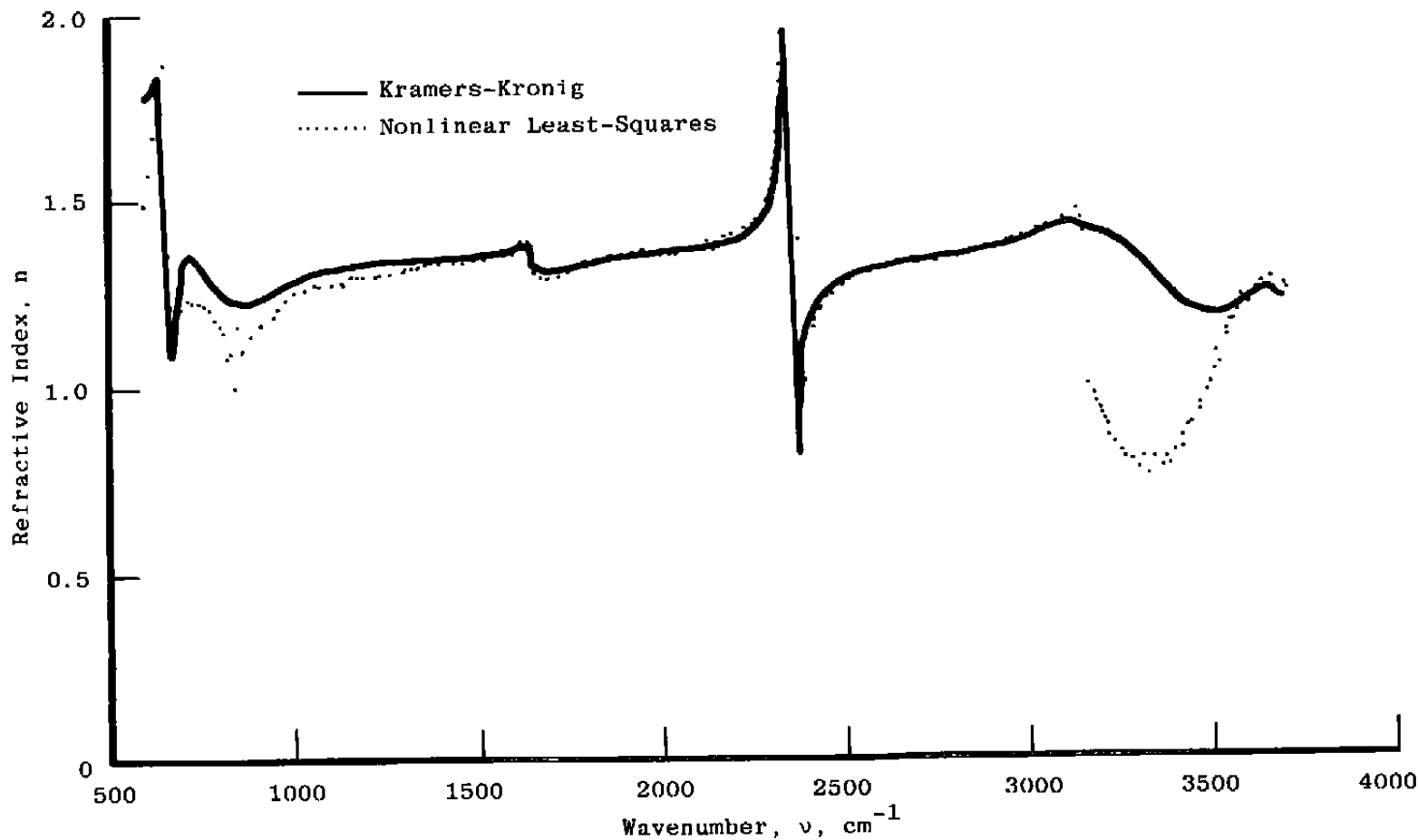


Figure 35. Refractive index of solid $\text{H}_2\text{O}/\text{CO}_2$ mixture (61%/36%) on 20°K germanium.

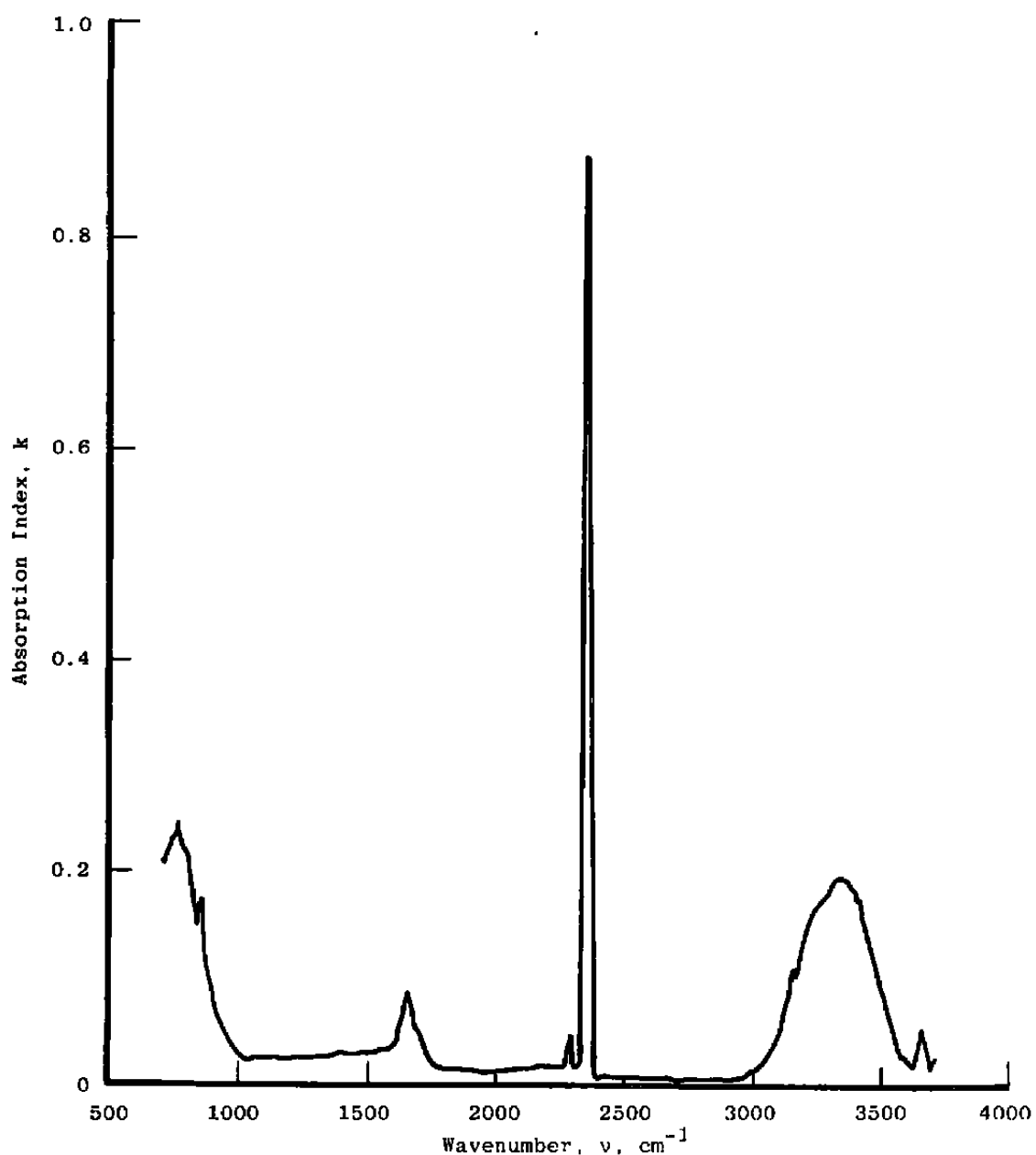


Figure 36. Absorption index of solid $\text{H}_2\text{O}/\text{CO}_2$ mixture (61%/36%) on 20°K germanium.

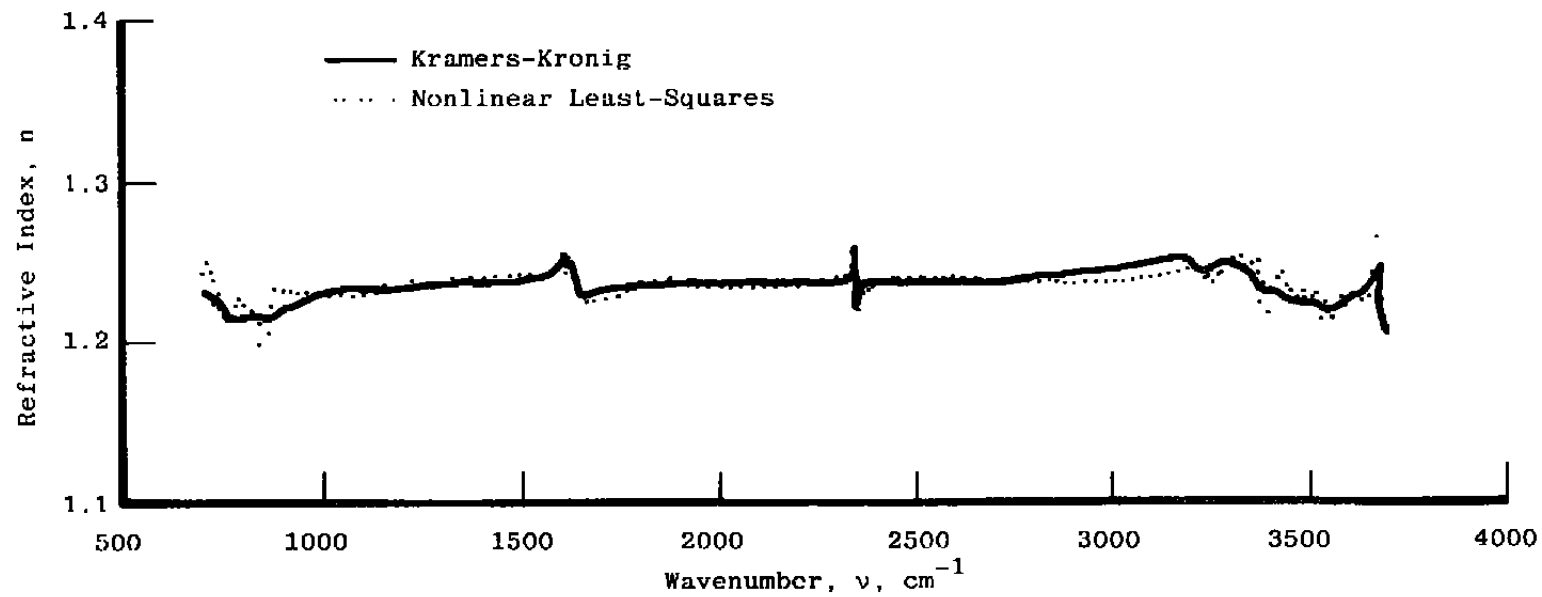


Figure 37. Refractive index of solid $\text{N}_2/\text{H}_2\text{O}$ mixture (87%/12%) on 20°K germanium.

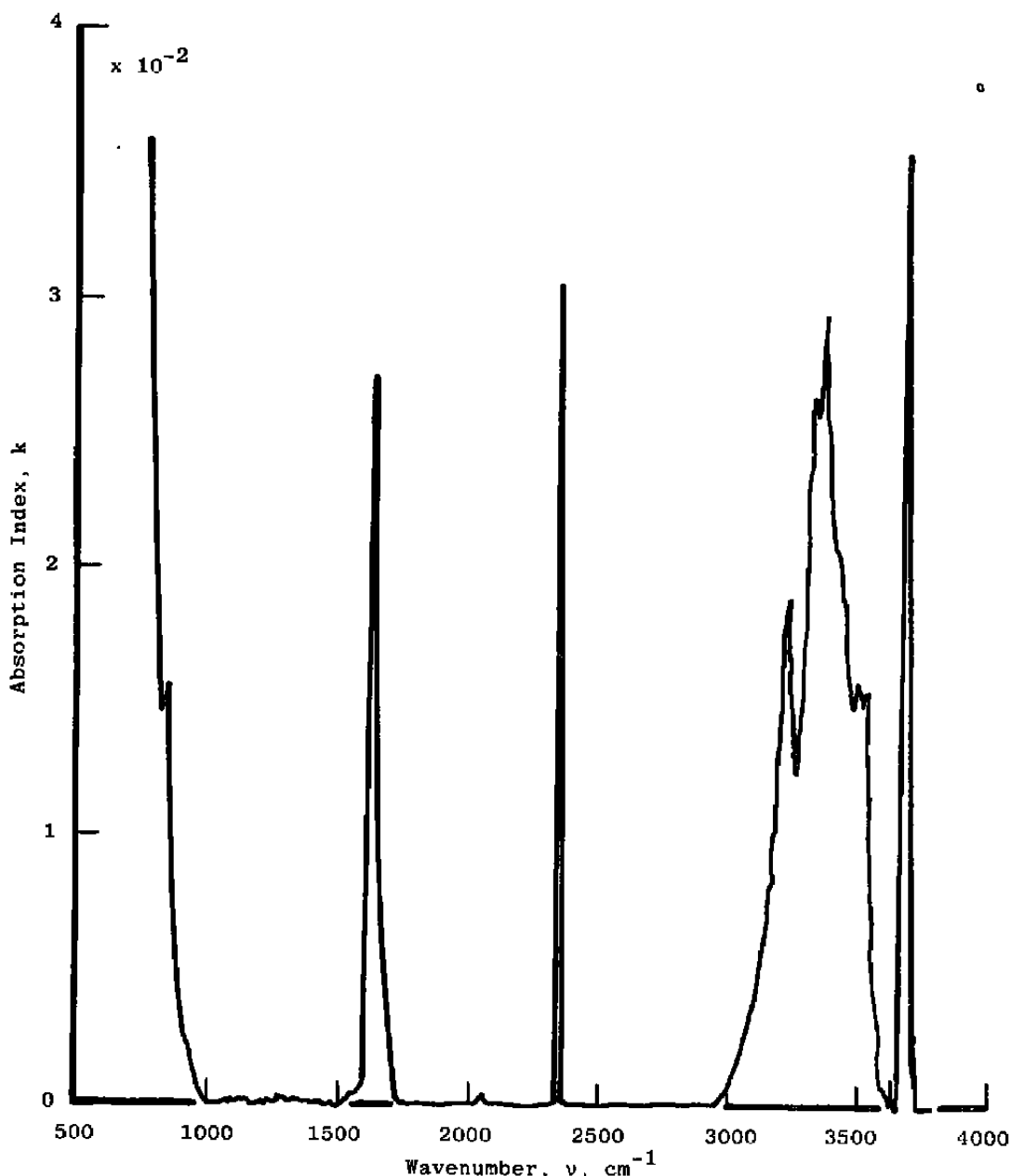


Figure 38. Absorption index of solid $\text{N}_2/\text{H}_2\text{O}$ mixture (87%/12%) on 20°K germanium.

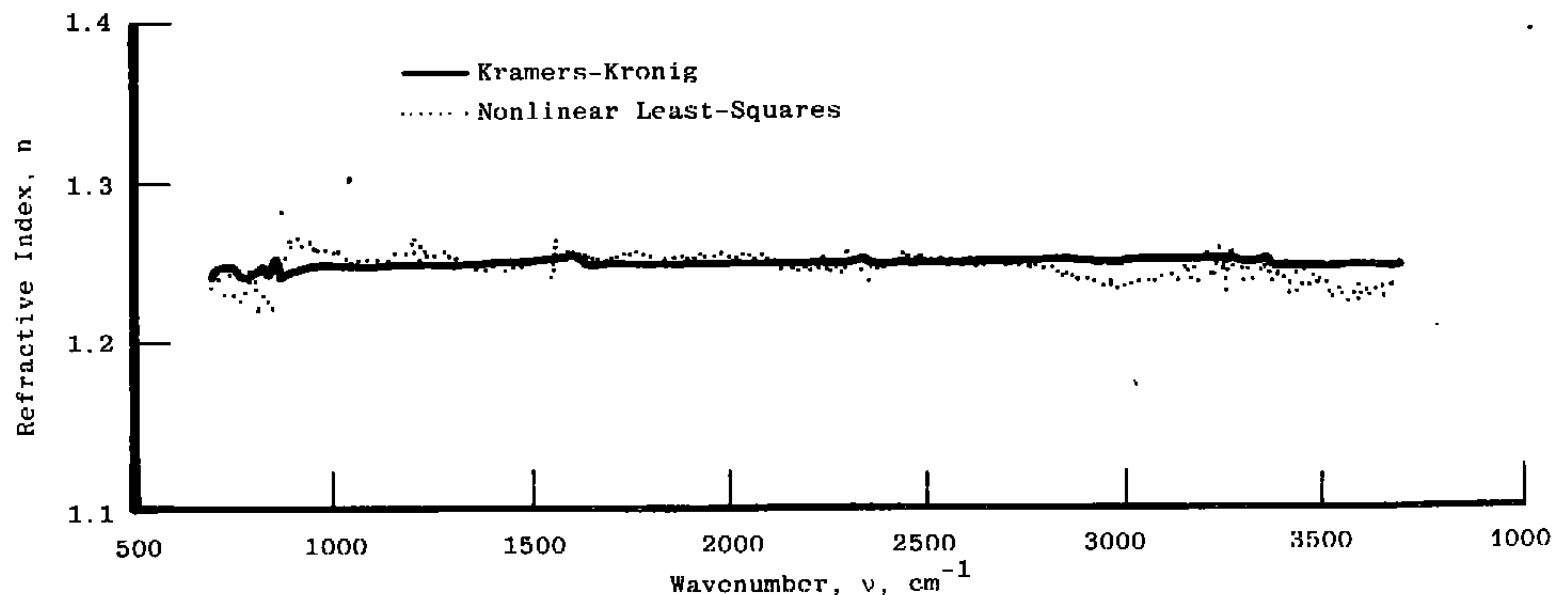


Figure 39. Refractive index of solid Ar/H₂O mixture (93%/6%) on 20°K germanium.

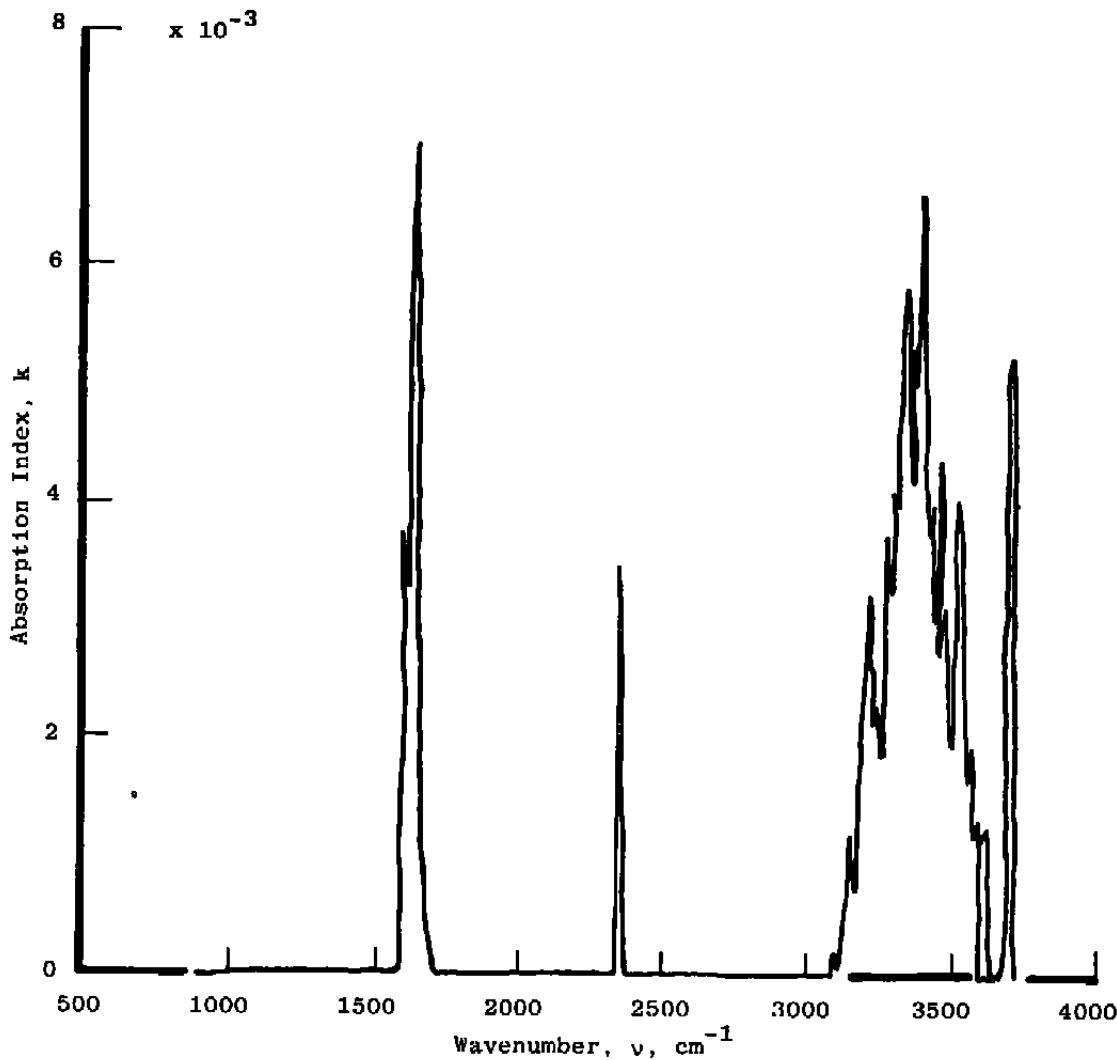


Figure 40. Absorption index of solid Ar/H₂O mixture (93%/6%) on 20°K germanium.

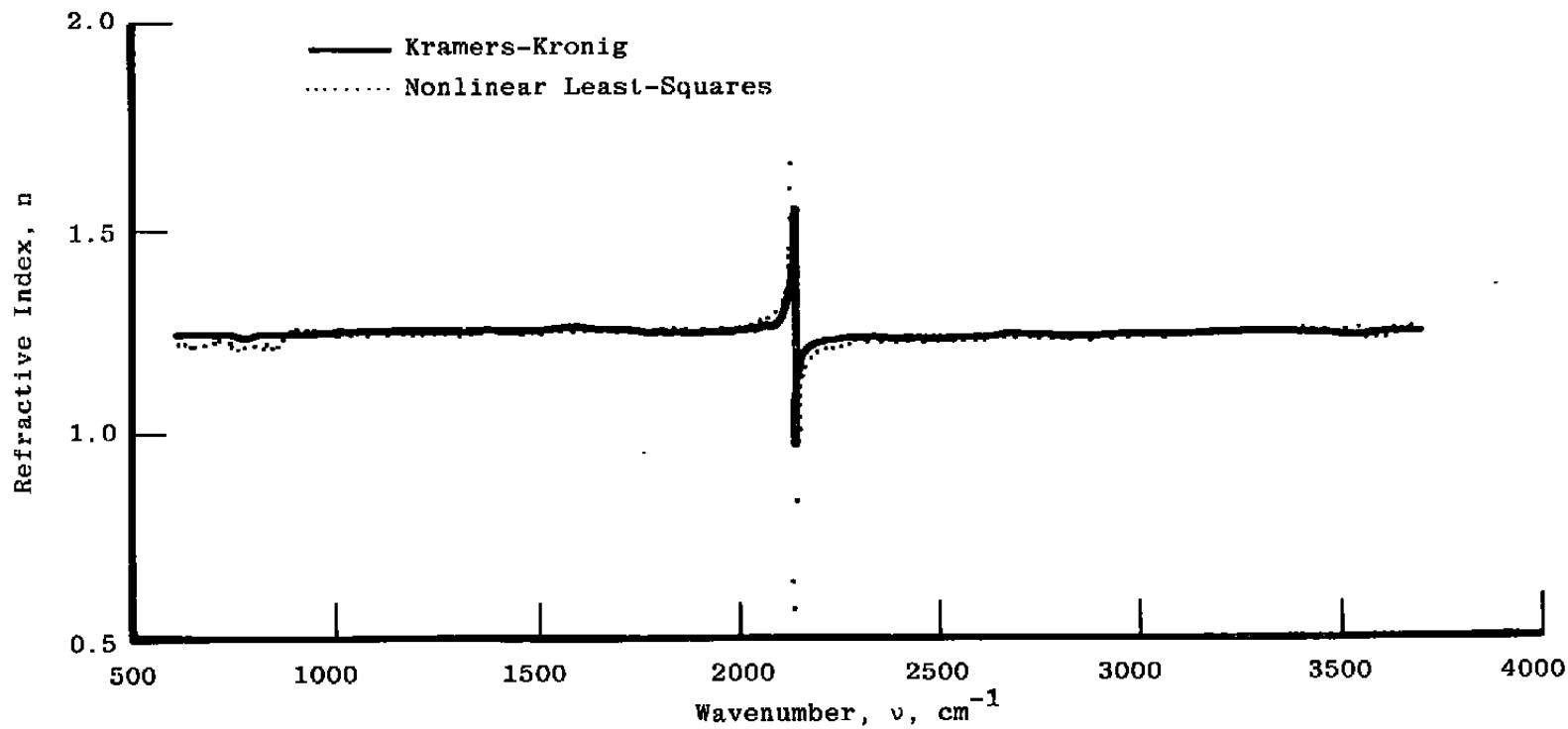


Figure 41. Refractive index of solid CO/H₂O mixture (91%/9%) on 20°K germanium.

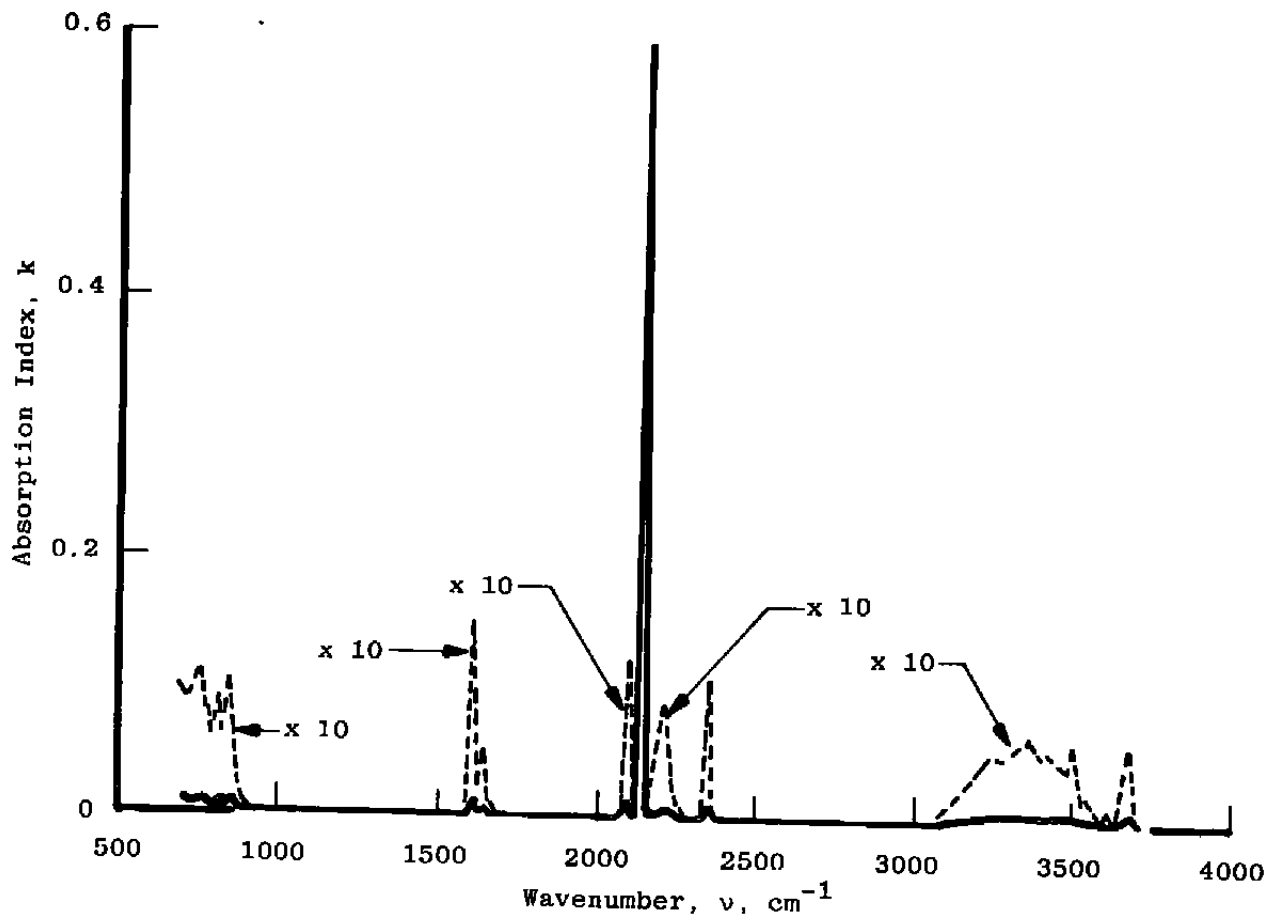


Figure 42. Absorption index of solid CO/H₂O mixture (91%/9%) on 20°K germanium.

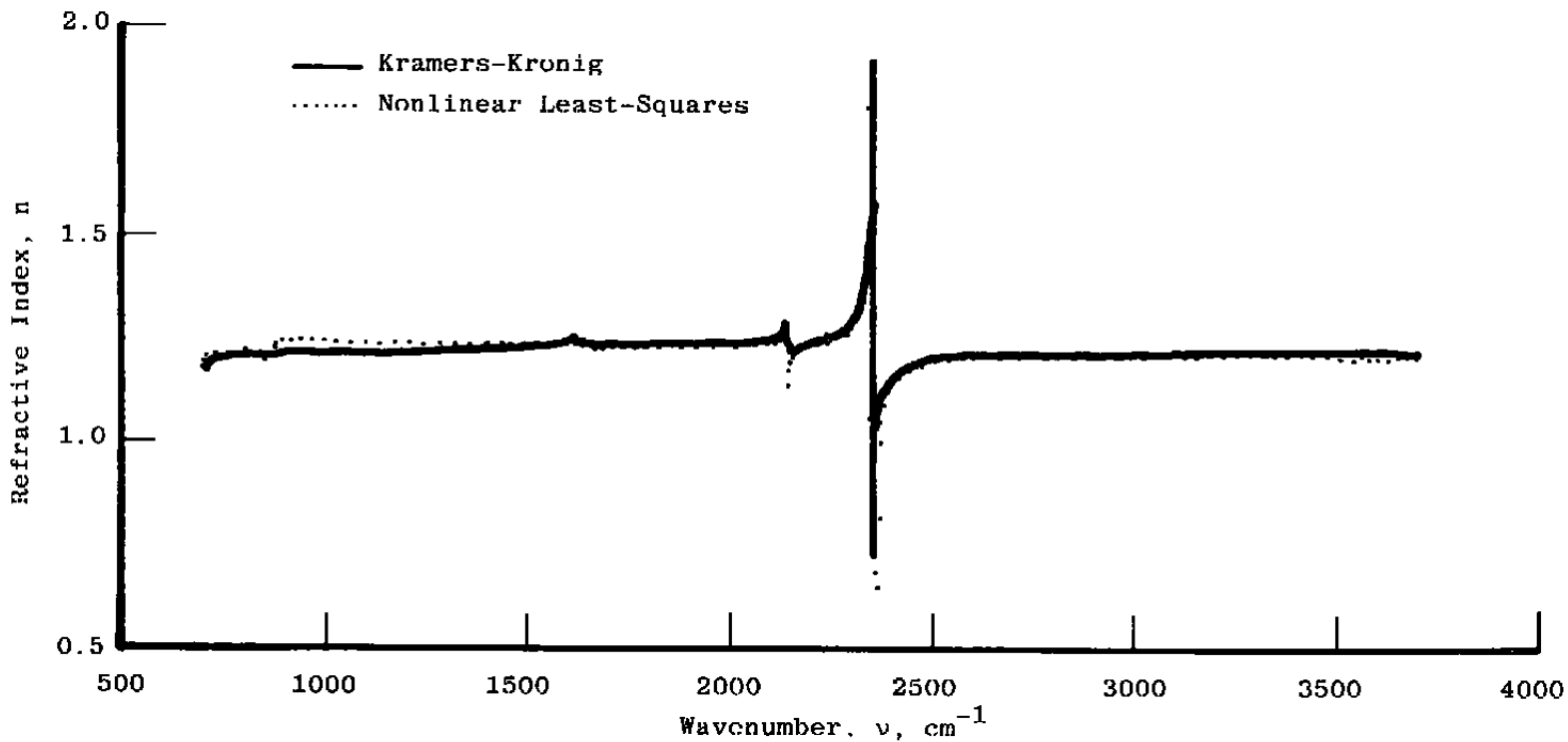


Figure 43. Refractive index of solid simulated plume mixture $\text{N}_2/\text{H}_2\text{O}/\text{CO}_2/\text{CO}$ (50%/23%/17%/10%) on 20°K germanium.

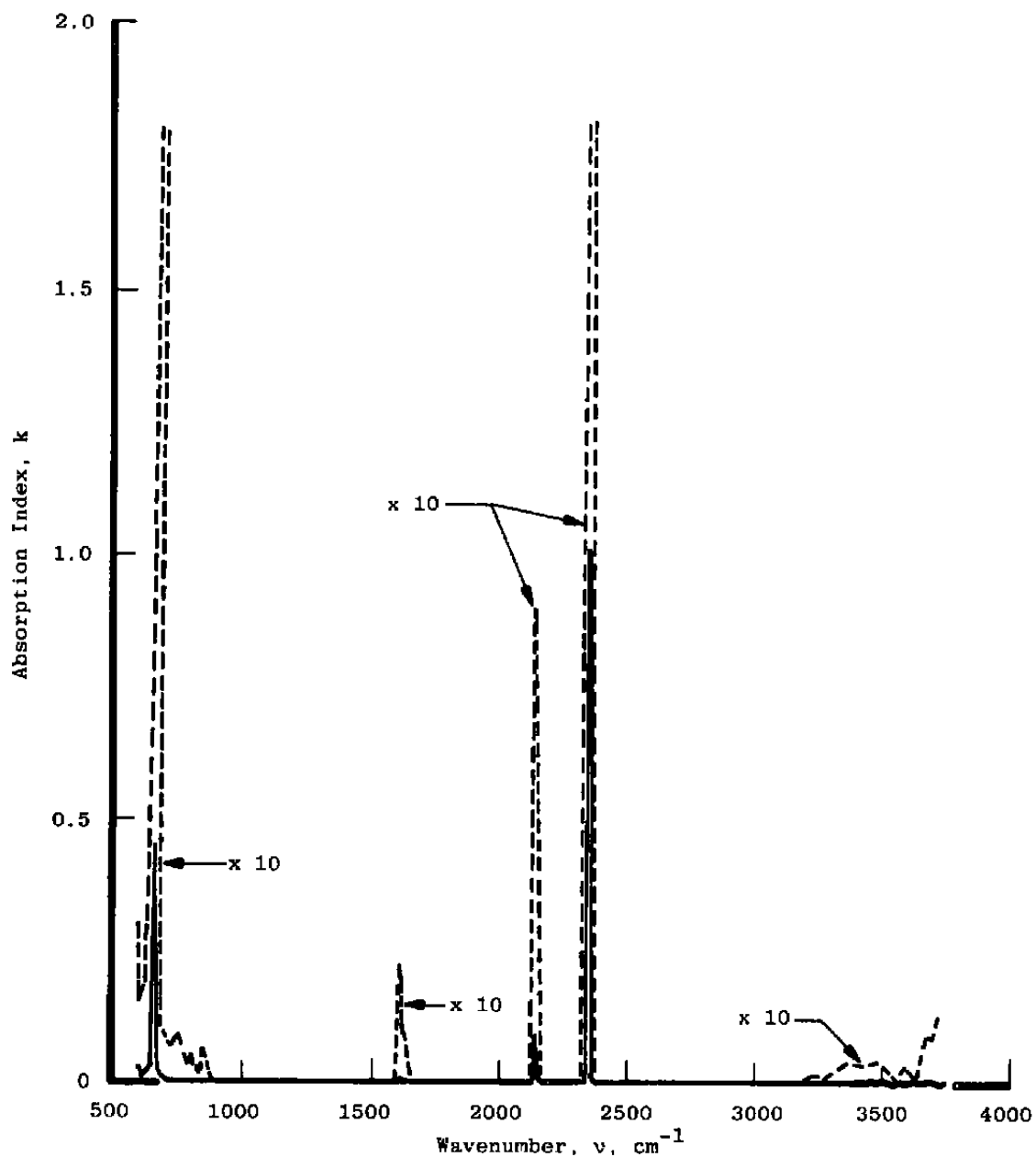


Figure 44. Absorption index of solid simulated plume mixture $\text{N}_2/\text{H}_2\text{O}/\text{CO}_2/\text{CO}$ (50%/23%/17%/10%) on 20°K germanium.

Table 1. Physical Properties of 20°K Cryofilms

Film	Percent Mole Fraction	Real Index at 0.6328 μm	Mass Density from QCM, (g/cm ³)*	Maximum Film Thickness in Calculation, μm	Number of Film Thicknesses in Calculation
N ₂ /NH ₃	85/15	1.25	---	5.00	18
N ₂ /CO/(O ₂)	79/20/(<0.5)	1.24	---	4.76	16
N ₂ /CO ₂	75/25	1.25	(0.54)	4.48	17
CO ₂ /CO	50/50	1.245	(0.95)	6.68	26
N ₂ /CO/CO ₂	64/23/13	1.24	0.941	6.60	26
N ₂ /H ₂ O/(CO ₂)	87/12/(1)	1.24	0.84	5.54	21
Ar/H ₂ O/(CO ₂)	93/6/(<0.5)	1.25	1.44	4.97	8
H ₂ O/CO ₂ /(N ₂)	61/36/(2)	1.31	0.86	3.36	14
CO/H ₂ O	91/9	1.255	1.08	5.23	18
N ₂ /H ₂ O/CO ₂ /CO (Simulated Plume Mixture)	50/23/17/10	1.26	0.77	5.38	21

*Values within parentheses are inexact because of difficulties with the QCM.

**Table 2. Locations of Absorption Bands of Molecular Species in
20°K Cryofilms (cm⁻¹)**

Molecular Species	Band Identification	Vapor (a)	Pure Solid (b)	N ₂ /NH ₃	N ₂ /CO	N ₂ /CO ₂	CO ₂ /CO ₂	N ₂ /CO/CO ₂	N ₂ /H ₂ O	Ar/H ₂ O	H ₂ O/CO ₂	CO/H ₂ O	Simulated Plume Mixture
NH ₃	Lattice	---	525	---									
	v ₂	932, 968	1075	988, 1050									
	v ₄	1628	1627	1624, 1630									
	2v ₄	3219	3210	3213									
	v ₁	3337	3295	3310									
	v ₃	3414	3376	3381									
¹³ CO	1-0	2096	2092		2090		2094	2094				2092	2096
¹² CO	1-0	2143	2140		2140		2142	2142				2141	2142
	1-0 + Lattice	---	2180 to 2230		2200		2225	2210				2200	---
¹³ CO ₂	v ₂	648	630			642	---						---
	v ₃	2285	2284			2282	2282	2282			2281	(2280) ⁽²⁾	2281
	v ₃ + Lattice	---	2316			---	---	---					---
¹² CO ₂	v ₂	667	660		665	665	663	(665)	(660)	667	(660)	663	
	2v ₂	1286	1285										---
	2v ₂ + Lattice ?	---	1450 to 1750		1450								---
	v ₃	2349	2346	(2350)	2350	2346	2346	(2347)	(2346)	2345	(2347)	2346	
	v ₃ + Lattice	---	2370, 2458		2430	2412	2390 to 2434						2380 to 2436
Fermi Resonance	v ₂ - v ₃	3609	3602		3606	3605	3605				(3598)	3604	
	2v ₂ - v ₃ + Lattice ?	---	3630										---
	v ₁ - v ₃	3716	3710		3710	3710	3710	(3714)	(3710)	3703	(3706)	3708	

Table 2. Concluded.

Molecular Species	Band Identification	Vapor (a)	Pure Solid (b)	N ₂ /NH ₃	N ₂ /CO	N ₂ /CO ₂	CO ₂ /CO	N ₂ /CO/CO ₂	N ₂ /H ₂ O	Ar/H ₂ O	H ₂ O/CO ₂	CO/H ₂ O	Simulated Plume Mixture
N ₂ O	v _L (Liberation)	—	770						665	----	660	655	655
	v ₂	1595	1660						1608	1625	1643	1604	1609
	v _x	—	2210						1633	—	—	1638	1631
	2v ₂	3151							3226	3220	—	3236	3239
	v ₁	3652		3300						3340	—	—	3690
	v ₃	3756							3730	—	—	3734	
	2v ₂ + v _T ?	—							JJ35	3338	—	3362	
	Multimer ^(d)								3367	J374	—	—	
	Dimer								3517	3518	—	3492	3488
									3687	3698	—	3674	
									3714	3717	—	3706	

(a) From Ref. 10.

(b) All pure species absorption locations are from the data presented in Ref. 1,
except those attributable to pure CO, which are from Ref. 11.

(c) Due to molecular species present in amounts less than 1 percent mole fraction.

(d) The dimer and higher multimer assignments are made by Huong and Cornut (Ref. 21).

Table 3. Optical Constants of 20°K N₂/NH₃

<u>v, cm⁻¹</u>	<u>n</u>	<u>k</u>	<u>v, cm⁻¹</u>	<u>n</u>	<u>k</u>
3680	1.242212	0.0	3370	1.244486	0.002235
3670	1.242204	0.0	3368	1.244309	0.002008
3640	1.242176	0.0	3366	1.244234	0.001867
3630	1.242165	0.0	3364	1.244271	0.001685
3620	1.242154	0.0	3362	1.244303	0.001507
3610	1.242142	0.0	3360	1.244287	0.001193
3600	1.242128	0.0	3358	1.244296	0.001103
3590	1.242114	0.0	3356	1.244269	0.000715
3580	1.242098	0.0	3354	1.244141	0.000483
3570	1.242081	0.0	3352	1.243989	0.000300
3560	1.242063	0.0	3350	1.243764	0.0
3550	1.242042	0.0	3348	1.243473	0.0
3540	1.242020	0.0	3346	1.243297	0.0
3530	1.241994	0.0	3344	1.243162	0.0
3520	1.241966	0.0	3342	1.243047	0.0
3510	1.241934	0.0	3340	1.242940	0.0
3500	1.241896	0.0	3338	1.242846	0.0
3490	1.241853	0.0	3336	1.242751	0.0
3480	1.241802	0.0	3334	1.242665	0.0
3470	1.241740	0.0	3332	1.242571	0.0
3460	1.241663	0.0	3330	1.242484	0.0
3450	1.241565	0.0	3328	1.242378	0.0
3440	1.241435	0.0	3326	1.242276	0.0
3430	1.241245	0.0	3324	1.242138	0.0
3420	1.240943	0.0	3322	1.241991	0.0
3410	1.240262	0.0	3320	1.241746	0.0
3408	1.239905	0.0	3318	1.241279	0.0
3406	1.239559	0.000398	3316	1.240711	0.000569
3404	1.239345	0.000729	3314	1.240564	0.001603
3402	1.239316	0.001283	3312	1.241275	0.002794
3400	1.239422	0.001598	3310	1.242585	0.003089
3398	1.239531	0.001839	3308	1.243584	0.002386
3396	1.239530	0.002034	3306	1.243888	0.001585
3394	1.239468	0.002301	3304	1.243867	0.001110
3392	1.239359	0.002729	3302	1.243773	0.000678
3390	1.239455	0.003418	3300	1.243604	0.000383
3388	1.239839	0.004100	3298	1.243368	0.000135
3386	1.240551	0.004639	3296	1.243145	0.000076
3384	1.241282	0.004785	3294	1.242974	0.000029
3382	1.241951	0.004806	3292	1.242823	0.0
3380	1.242685	0.004920	3290	1.242691	0.000027
3378	1.243481	0.004536	3288	1.242620	0.000066
3376	1.244057	0.004063	3286	1.242524	0.000024
3374	1.244412	0.003405	3284	1.242460	0.000112
3372	1.244571	0.002872	3282	1.242474	0.000139

Table 3. Continued

<u>v, cm⁻¹</u>	<u>n</u>	<u>k</u>	<u>v, cm⁻¹</u>	<u>n</u>	<u>k</u>
3280	1.242432	0.0	3190	1.244339	0.0
3278	1.242312	0.0	3188	1.244151	0.0
3276	1.242213	0.0	3186	1.244018	0.0
3274	1.242129	0.0	3184	1.243920	0.0
3272	1.242019	0.0	3182	1.243832	0.0
3270	1.241886	0.0	3180	1.243762	0.0
3268	1.241801	0.000127	3178	1.243696	0.0
3266	1.241692	0.000067	3176	1.243643	0.0
3264	1.241566	0.000185	3174	1.243591	0.0
3262	1.241477	0.000259	3160	1.243350	0.0
3260	1.241354	0.000243	3150	1.243237	0.0
3258	1.241156	0.000359	3140	1.243154	0.0
3256	1.240944	0.000453	3130	1.243087	0.0
3254	1.240677	0.000681	3120	1.243033	0.0
3252	1.240444	0.001036	3110	1.242987	0.0
3250	1.240267	0.001529	3100	1.242949	0.0
3248	1.240208	0.002159	3090	1.242915	0.0
3246	1.240620	0.003136	3080	1.242886	0.0
3244	1.241502	0.003594	3070	1.242859	0.0
3242	1.242387	0.003484	3060	1.242837	0.0
3240	1.242992	0.003171	3050	1.242815	0.0
3238	1.243461	0.002778	3040	1.242796	0.0
3236	1.243739	0.002257	3030	1.242778	0.0
3234	1.243770	0.001620	3020	1.242762	0.0
3232	1.243599	0.001241	3010	1.242747	0.0
3230	1.243233	0.000732	3000	1.242733	0.0
3228	1.242695	0.000663	2990	1.242720	0.0
3226	1.242156	0.000767	2980	1.242708	0.0
3224	1.241790	0.001213	2970	1.242697	0.0
3222	1.241629	0.001713	2960	1.242686	0.0
3220	1.241671	0.002223	2950	1.242676	0.0
3218	1.241924	0.002809	2940	1.242666	0.0
3216	1.242400	0.003166	2930	1.242657	0.0
3214	1.242933	0.003376	2920	1.242648	0.0
3212	1.243546	0.003445	2910	1.242640	0.0
3210	1.244210	0.003314	2900	1.242632	0.0
3208	1.244623	0.002750	2890	1.242624	0.0
3206	1.244801	0.002435	2880	1.242617	0.0
3204	1.245045	0.002229	2870	1.242610	0.0
3202	1.245248	0.001688	2860	1.242603	0.0
3200	1.245264	0.001293	2850	1.242596	0.0
3198	1.245189	0.000873	2840	1.242590	0.0
3196	1.245038	0.000541	2830	1.242584	0.0
3194	1.244824	0.000275	2820	1.242578	0.0
3192	1.244586	0.000091	2810	1.242572	0.0

Table 3. Continued

$\nu, \text{ cm}^{-1}$	<u>n</u>	<u>k</u>	$\nu, \text{ cm}^{-1}$	<u>n</u>	<u>k</u>
2800	1.242566	0.0	2350	1.242363	0.0
2790	1.242561	0.0	2340	1.242359	0.0
2780	1.242555	0.0	2330	1.242354	0.0
2770	1.242550	0.0	2320	1.242349	0.0
2760	1.242545	0.0	2310	1.242344	0.0
2750	1.242540	0.0	2300	1.242339	0.0
2740	1.242535	0.0	2290	1.242335	0.0
2730	1.242530	0.0	2280	1.242330	0.0
2720	1.242525	0.0	2270	1.242324	0.0
2710	1.242520	0.0	2260	1.242319	0.0
2700	1.242515	0.0	2250	1.242314	0.0
2690	1.242511	0.0	2240	1.242309	0.0
2680	1.242506	0.0	2230	1.242303	0.0
2670	1.242502	0.0	2220	1.242298	0.0
2660	1.242497	0.0	2210	1.242292	0.0
2650	1.242493	0.0	2200	1.242287	0.0
2640	1.242488	0.0	2180	1.242275	0.0
2630	1.242484	0.0	2160	1.242263	0.0
2620	1.242480	0.0	2150	1.242257	0.0
2610	1.242475	0.0	2140	1.242251	0.0
2600	1.242471	0.0	2130	1.242244	0.0
2590	1.242467	0.0	2120	1.242238	0.0
2580	1.242463	0.0	2110	1.242231	0.0
2570	1.242458	0.0	2100	1.242224	0.0
2560	1.242454	0.0	2090	1.242217	0.0
2550	1.242450	0.0	2080	1.242210	0.0
2540	1.242446	0.0	2070	1.242203	0.0
2530	1.242442	0.0	2060	1.242195	0.0
2520	1.242437	0.0	2050	1.242187	0.0
2510	1.242433	0.0	2040	1.242179	0.0
2500	1.242429	0.0	2030	1.242171	0.0
2490	1.242425	0.0	2020	1.242163	0.0
2480	1.242420	0.0	2010	1.242154	0.0
2470	1.242416	0.0	2000	1.242145	0.0
2460	1.242412	0.0	1990	1.242136	0.0
2450	1.242408	0.0	1980	1.242127	0.0
2440	1.242403	0.0	1970	1.242117	0.0
2430	1.242399	0.0	1960	1.242107	0.0
2420	1.242395	0.0	1950	1.242097	0.0
2410	1.242390	0.0	1940	1.242086	0.0
2400	1.242386	0.0	1930	1.242075	0.0
2390	1.242381	0.0	1920	1.242063	0.0
2380	1.242377	0.0	1910	1.242051	0.0
2370	1.242372	0.0	1900	1.242038	0.0
2360	1.242368	0.0	1890	1.242025	0.0

Table 3. Continued

<u>v, cm⁻¹</u>	<u>n</u>	<u>k</u>	<u>v, cm⁻¹</u>	<u>n</u>	<u>k</u>
1880	1.242011	0.0	1614	1.244844	0.0
1870	1.241997	0.0	1612	1.244323	0.0
1860	1.241982	0.0	1610	1.244000	0.0
1850	1.241965	0.0	1600	1.243158	0.0
1840	1.241948	0.0	1590	1.242787	0.0
1830	1.241930	0.0	1580	1.242568	0.0
1820	1.241911	0.0	1570	1.242417	0.0
1810	1.241890	0.0	1560	1.242305	0.0
1800	1.241868	0.0	1550	1.242215	0.0
1790	1.241843	0.0	1540	1.242140	0.0
1780	1.241817	0.0	1530	1.242074	0.0
1770	1.241788	0.0	1520	1.242017	0.0
1760	1.241756	0.0	1510	1.241963	0.0
1750	1.241719	0.0	1500	1.241914	0.0
1740	1.241678	0.0	1490	1.241865	0.0
1730	1.241630	0.0	1480	1.241820	0.0
1720	1.241573	0.0	1470	1.241773	0.0
1710	1.241503	0.0	1460	1.241730	0.0
1700	1.241416	0.0	1450	1.241684	0.0
1690	1.241301	0.0	1440	1.241640	0.0
1680	1.241138	0.0	1430	1.241593	0.0
1670	1.240882	0.0	1420	1.241548	0.0
1660	1.240360	0.0	1410	1.241499	0.0
1658	1.240183	0.0	1400	1.241451	0.0
1656	1.239893	0.0	1390	1.241399	0.0
1654	1.239320	0.0	1380	1.241347	0.0
1652	1.238739	0.000738	1370	1.241290	0.0
1650	1.238702	0.001787	1360	1.241234	0.0
1648	1.239432	0.002719	1350	1.241171	0.0
1646	1.240319	0.002674	1340	1.241108	0.0
1644	1.240717	0.002157	1330	1.241038	0.0
1642	1.240698	0.001966	1320	1.240967	0.0
1640	1.240675	0.001776	1310	1.240887	0.0
1638	1.240387	0.001445	1300	1.240806	0.0
1636	1.239333	0.001116	1290	1.240715	0.0
1634	1.237992	0.002317	1280	1.240620	0.0
1632	1.238051	0.004941	1270	1.240514	0.0
1630	1.239926	0.006708	1260	1.240402	0.0
1628	1.241786	0.006409	1250	1.240275	0.0
1626	1.242864	0.006190	1240	1.240141	0.0
1624	1.244230	0.006490	1230	1.239987	0.0
1622	1.246062	0.005627	1220	1.239821	0.0
1620	1.247325	0.003777	1210	1.239629	0.0
1618	1.247196	0.001384	1200	1.239418	0.0
1616	1.245967	0.0	1190	1.239171	0.0

Table 3. Continued

$\nu, \text{ cm}^{-1}$	n	k	$\nu, \text{ cm}^{-1}$	n	k
1180	1.238892	0.0	1042	1.239937	0.022408
1170	1.238559	0.0	1040	1.240639	0.022792
1160	1.238170	0.0	1038	1.241582	0.023732
1150	1.237690	0.0	1036	1.243382	0.024891
1140	1.237097	0.0	1034	1.245853	0.024999
1130	1.236318	0.0	1032	1.247927	0.024093
1120	1.235231	0.0	1030	1.249341	0.023121
1118	1.234947	0.0	1028	1.250818	0.022702
1116	1.234634	0.0	1026	1.252529	0.021544
1114	1.234263	0.0	1024	1.253862	0.019890
1112	1.233807	0.000019	1022	1.254433	0.017998
1110	1.233253	0.000133	1020	1.254464	0.016625
1108	1.232744	0.000473	1018	1.254384	0.015749
1106	1.232317	0.000791	1016	1.254739	0.015319
1104	1.231971	0.001170	1014	1.255514	0.014498
1102	1.231627	0.001460	1012	1.255971	0.012878
1100	1.231236	0.001734	1010	1.255394	0.011287
1098	1.230747	0.002093	1008	1.254726	0.011203
1096	1.230314	0.002577	1006	1.255324	0.011654
1094	1.229895	0.003081	1004	1.256960	0.010741
1092	1.229433	0.003539	1002	1.257547	0.007794
1090	1.229010	0.004332	1000	1.256323	0.005267
1088	1.228650	0.004949	998	1.254185	0.004136
1086	1.228356	0.005833	996	1.252245	0.004059
1084	1.228258	0.006698	994	1.250650	0.004743
1082	1.228122	0.007268	992	1.249768	0.006011
1080	1.227819	0.008054	990	1.250123	0.007859
1078	1.227609	0.009078	988	1.252004	0.008663
1076	1.227534	0.010085	986	1.253741	0.007192
1074	1.227591	0.011214	984	1.253644	0.004497
1072	1.227804	0.012319	982	1.251643	0.003052
1070	1.228046	0.013293	980	1.249028	0.003204
1068	1.228360	0.014479	978	1.247005	0.005504
1066	1.228844	0.015610	976	1.246868	0.009015
1064	1.229520	0.016744	974	1.249785	0.012860
1062	1.230308	0.017743	972	1.255835	0.013973
1060	1.231154	0.018618	970	1.260661	0.008826
1058	1.232148	0.019600	968	1.260000	0.001731
1056	1.233302	0.020254	966	1.256483	0.0
1054	1.234396	0.020719	964	1.254249	0.0
1052	1.235461	0.021176	962	1.253195	0.0
1050	1.236544	0.021491	960	1.252382	0.0
1048	1.237550	0.021654	958	1.251786	0.0
1046	1.238408	0.021806	956	1.251262	0.0
1044	1.239170	0.022017	954	1.250845	0.0

Table 3. Concluded

<u>v, cm⁻¹</u>	<u>n</u>	<u>k</u>	<u>v, cm⁻¹</u>	<u>n</u>	<u>k</u>
952	1.250460	0.0	830	1.247144	0.000925
950	1.250137	0.0	820	1.245994	0.000384
940	1.248878	0.0	810	1.245497	0.000975
930	1.248002	0.0	800	1.245616	0.000969
920	1.247311	0.0	790	1.244955	0.000159
910	1.246731	0.0	780	1.243845	0.000997
900	1.246189	0.0	770	1.244232	0.003132
890	1.245672	0.0	760	1.246076	0.003433
880	1.244971	0.0	750	1.247518	0.002356
870	1.243437	0.0	740	1.247401	0.000314
860	1.243036	0.002842	730	1.246503	0.0
850	1.245312	0.004891	720	1.245939	0.0
840	1.247454	0.002661	710	1.245735	0.0

Table 4. Optical Constants of 20°K N₂/CO

<u>v, cm⁻¹</u>	<u>n</u>	<u>k</u>	<u>v, cm⁻¹</u>	<u>n</u>	<u>k</u>
3690	1.219797	0.0	3240	1.219761	0.0
3680	1.219796	0.0	3230	1.219759	0.0
3670	1.219796	0.0	3220	1.219758	0.0
3660	1.219795	0.0	3210	1.219757	0.0
3650	1.219795	0.0	3200	1.219756	0.0
3640	1.219794	0.0	3190	1.219755	0.0
3630	1.219793	0.0	3180	1.219753	0.0
3620	1.219793	0.0	3170	1.219752	0.0
3610	1.219792	0.0	3160	1.219751	0.0
3600	1.219791	0.0	3150	1.219749	0.0
3590	1.219791	0.0	3140	1.219748	0.0
3580	1.219790	0.0	3130	1.219747	0.0
3570	1.219790	0.0	3120	1.219745	0.0
3560	1.219789	0.0	3110	1.219744	0.0
3550	1.219788	0.0	3100	1.219742	0.0
3540	1.219787	0.0	3090	1.219741	0.0
3530	1.219787	0.0	3080	1.219739	0.0
3520	1.219786	0.0	3070	1.219738	0.0
3510	1.219785	0.0	3060	1.219736	0.0
3500	1.219785	0.0	3050	1.219734	0.0
3490	1.219784	0.0	3040	1.219733	0.0
3480	1.219783	0.0	3030	1.219731	0.0
3470	1.219782	0.0	3020	1.219729	0.0
3460	1.219781	0.0	3010	1.219728	0.0
3450	1.219781	0.0	3000	1.219726	0.0
3440	1.219780	0.0	2990	1.219724	0.0
3430	1.219779	0.0	2980	1.219722	0.0
3420	1.219778	0.0	2970	1.219720	0.0
3410	1.219777	0.0	2960	1.219718	0.0
3400	1.219777	0.0	2950	1.219716	0.0
3390	1.219776	0.0	2940	1.219714	0.0
3380	1.219775	0.0	2930	1.219712	0.0
3370	1.219774	0.0	2920	1.219709	0.0
3360	1.219773	0.0	2910	1.219707	0.0
3350	1.219772	0.0	2900	1.219705	0.0
3340	1.219771	0.0	2890	1.219702	0.0
3330	1.219770	0.0	2880	1.219700	0.0
3320	1.219769	0.0	2870	1.219697	0.0
3310	1.219768	0.0	2860	1.219695	0.0
3300	1.219767	0.0	2850	1.219692	0.0
3290	1.219766	0.0	2840	1.219689	0.0
3280	1.219765	0.0	2830	1.219686	0.0
3270	1.219764	0.0	2820	1.219683	0.0
3260	1.219763	0.0	2810	1.219680	0.0
3250	1.219762	0.0	2800	1.219677	0.0

Table 4. Continued

<u>ν, cm⁻¹</u>	<u>n</u>	<u>k</u>	<u>ν, cm⁻¹</u>	<u>n</u>	<u>k</u>
2790	1.219674	0.0	2340	1.219269	0.0
2780	1.219671	0.0	2330	1.219183	0.0
2770	1.219667	0.0	2320	1.219115	0.0
2760	1.219664	0.0	2300	1.219000	0.0
2750	1.219650	0.0	2280	1.218847	0.0
2740	1.219656	0.0	2270	1.218747	0.0
2730	1.219653	0.0	2260	1.218622	0.0
2720	1.219649	0.0	2250	1.218457	0.0
2710	1.219644	0.0	2240	1.218219	0.0
2700	1.219640	0.0	2230	1.217773	0.0
2690	1.219636	0.0	2228	1.217578	0.000001
2680	1.219631	0.0	2226	1.217357	0.000139
2670	1.219626	0.0	2224	1.217141	0.000313
2660	1.219621	0.0	2222	1.216995	0.000632
2650	1.219616	0.0	2220	1.216946	0.000981
2640	1.219611	0.0	2218	1.217034	0.001343
2630	1.219605	0.0	2216	1.217292	0.001712
2620	1.219599	0.0	2214	1.217625	0.001783
2610	1.219593	0.0	2212	1.217909	0.001808
2600	1.219587	0.0	2210	1.218153	0.001711
2590	1.219580	0.0	2208	1.218238	0.001474
2580	1.219573	0.0	2206	1.218192	0.001394
2570	1.219566	0.0	2204	1.218157	0.001413
2560	1.219558	0.0	2202	1.218209	0.001433
2550	1.219550	0.0	2200	1.218296	0.001413
2540	1.219541	0.0	2198	1.218282	0.001210
2530	1.219532	0.0	2196	1.218129	0.001192
2520	1.219523	0.0	2194	1.218036	0.001305
2510	1.219513	0.0	2192	1.218094	0.001458
2500	1.219502	0.0	2190	1.218247	0.001455
2490	1.219491	0.0	2188	1.218313	0.001300
2480	1.219479	0.0	2186	1.218260	0.001161
2470	1.219467	0.0	2184	1.218096	0.001098
2460	1.219453	0.0	2182	1.218027	0.001207
2450	1.219439	0.0	2180	1.218068	0.001285
2440	1.219423	0.0	2178	1.218214	0.001190
2430	1.219406	0.0	2176	1.218198	0.000962
2420	1.219388	0.0	2174	1.218152	0.000729
2410	1.219365	0.0	2172	1.217901	0.000487
2400	1.219347	0.0	2170	1.217699	0.000243
2390	1.219308	0.0	2160	1.215350	0.0
2380	1.219296	0.0	2150	1.208628	0.000001
2370	1.219229	0.0	2148	1.205946	0.000629
2360	1.219172	0.0	2146	1.198598	0.001687
2350	1.219213	0.000200	2144	1.188082	0.010207

Table 4. Continued

<u>v, cm⁻¹</u>	<u>n</u>	<u>k</u>	<u>v, cm⁻¹</u>	<u>n</u>	<u>k</u>
2142	1.189828	0.038419	1790	1.220192	0.0
2140	1.219022	0.059887	1780	1.220226	0.0
2138	1.250664	0.042618	1770	1.220172	0.0
2136	1.254516	0.008234	1760	1.220189	0.0
2134	1.241661	0.000983	1750	1.220153	0.0
2132	1.234045	0.000001	1740	1.220146	0.0
2130	1.231036	0.0	1730	1.220136	0.0
2120	1.225216	0.0	1720	1.220136	0.0
2110	1.223404	0.0	1710	1.220120	0.0
2100	1.222284	0.0	1700	1.220119	0.0
2098	1.221870	0.000001	1690	1.220105	0.0
2096	1.221121	0.000104	1680	1.220105	0.0
2094	1.221419	0.002033	1670	1.220092	0.0
2092	1.222953	0.002066	1660	1.220092	0.0
2090	1.223451	0.000431	1650	1.220079	0.0
2088	1.223021	0.000001	1640	1.220079	0.0
2080	1.222007	0.0	1630	1.220066	0.0
2070	1.221580	0.0	1620	1.220067	0.0
2060	1.221402	0.0	1610	1.220055	0.0
2050	1.221194	0.0	1600	1.220056	0.0
2040	1.221087	0.0	1590	1.220043	0.0
2030	1.220952	0.0	1580	1.220044	0.0
2020	1.220882	0.0	1570	1.220033	0.0
2010	1.220785	0.0	1560	1.220032	0.0
2000	1.220736	0.0	1550	1.220022	0.0
1990	1.220663	0.0	1540	1.220023	0.0
1980	1.220627	0.0	1530	1.220012	0.0
1970	1.220568	0.0	1520	1.220014	0.0
1960	1.220542	0.0	1510	1.220002	0.0
1950	1.220493	0.0	1500	1.220001	0.0
1940	1.220473	0.0	1490	1.219992	0.0
1930	1.220432	0.0	1480	1.219991	0.0
1920	1.220422	0.0	1470	1.219983	0.0
1910	1.220381	0.0	1460	1.219982	0.0
1900	1.220373	0.0	1450	1.219973	0.0
1890	1.220338	0.0	1440	1.219972	0.0
1880	1.220347	0.0	1430	1.219964	0.0
1870	1.220301	0.0	1420	1.219963	0.0
1860	1.220311	0.0	1410	1.219954	0.0
1850	1.220269	0.0	1400	1.219954	0.0
1840	1.220288	0.0	1390	1.219944	0.0
1830	1.220240	0.0	1380	1.219944	0.0
1820	1.220241	0.0	1370	1.219934	0.0
1810	1.220215	0.0	1360	1.219934	0.0
1800	1.220210	0.0	1350	1.219924	0.0

Table 4. Concluded

<u>v, cm⁻¹</u>	<u>n</u>	<u>k</u>	<u>v, cm⁻¹</u>	<u>n</u>	<u>k</u>
1340	1.219925	0.0	1020	1.219617	0.0
1330	1.219914	0.0	1010	1.219566	0.0
1320	1.219914	0.0	1000	1.219567	0.0
1310	1.219903	0.0	990	1.219506	0.0
1300	1.219904	0.0	980	1.219505	0.0
1290	1.219892	0.0	970	1.219430	0.0
1280	1.219893	0.0	960	1.219425	0.0
1270	1.219880	0.0	950	1.219329	0.0
1260	1.219881	0.0	940	1.219318	0.0
1250	1.219867	0.0	930	1.219188	0.0
1240	1.219869	0.0	920	1.219164	0.0
1230	1.219854	0.0	910	1.218971	0.0
1220	1.219855	0.0	900	1.218916	0.0
1210	1.219839	0.0	890	1.218585	0.0
1200	1.219841	0.0	880	1.218408	0.0
1190	1.219824	0.0	870	1.217272	0.0
1180	1.219826	0.0	860	1.216072	0.001100
1170	1.219807	0.0	850	1.217905	0.005800
1160	1.219809	0.0	840	1.221078	0.003400
1150	1.219789	0.0	830	1.221526	0.001500
1140	1.219791	0.0	820	1.219965	0.000100
1130	1.219768	0.0	810	1.219471	0.001600
1120	1.219771	0.0	800	1.219630	0.001500
1110	1.219745	0.0	790	1.219273	0.000900
1100	1.219748	0.0	780	1.218434	0.002300
1090	1.219719	0.0	770	1.219370	0.003800
1080	1.219722	0.0	760	1.220988	0.004300
1070	1.219690	0.0	750	1.222663	0.003300
1060	1.219692	0.0	740	1.223369	0.002100
1050	1.219655	0.0	730	1.222986	0.0
1040	1.219658	0.0	720	1.221860	0.0
1030	1.219615	0.0	710	1.221190	0.0

Table 5. Optical Constants of 20°K N₂/CO₂

<u>v, cm⁻¹</u>	<u>n</u>	<u>k</u>	<u>v, cm⁻¹</u>	<u>n</u>	<u>k</u>
3700	1.244295	0.000198	3370	1.236119	0.000847
3690	1.240496	0.000755	3360	1.235787	0.001017
3680	1.237715	0.000757	3350	1.235824	0.001246
3670	1.238681	0.000588	3340	1.235802	0.001264
3660	1.237091	0.0	3330	1.235933	0.001352
3650	1.237336	0.000575	3320	1.236046	0.001442
3640	1.236345	0.000297	3310	1.235970	0.000892
3630	1.236712	0.000894	3300	1.235677	0.001312
3620	1.235179	0.000197	3290	1.235793	0.001377
3618	1.235502	0.000327	3280	1.235820	0.001366
3616	1.234304	0.000473	3270	1.235920	0.001385
3614	1.234295	0.000685	3260	1.235832	0.001202
3612	1.232393	0.001078	3250	1.235632	0.001124
3610	1.231062	0.002671	3240	1.235605	0.001585
3608	1.230867	0.007810	3230	1.235692	0.001297
3606	1.236208	0.011537	3220	1.235588	0.001468
3604	1.241001	0.009198	3210	1.235659	0.001579
3602	1.243194	0.004750	3200	1.235724	0.001479
3600	1.241779	0.002439	3190	1.235718	0.001479
3598	1.241212	0.001400	3180	1.235680	0.001425
3596	1.239923	0.000916	3170	1.235606	0.001431
3594	1.240038	0.000794	3160	1.235655	0.001590
3592	1.239185	0.000351	3150	1.235861	0.001564
3590	1.239350	0.000043	3140	1.235779	0.001108
3580	1.237574	0.000474	3130	1.235624	0.001284
3570	1.237729	0.000538	3120	1.235506	0.001133
3560	1.237314	0.000325	3110	1.235465	0.001253
3550	1.237209	0.000105	3100	1.235414	0.001233
3540	1.236714	0.000437	3090	1.235393	0.001161
3530	1.236829	0.000337	3080	1.235357	0.001249
3520	1.236449	0.000468	3070	1.235363	0.001069
3510	1.236618	0.000667	3060	1.235177	0.000966
3500	1.236297	0.000506	3050	1.235024	0.001067
3490	1.236614	0.001000	3040	1.235028	0.001152
3480	1.236532	0.000590	3030	1.235096	0.001107
3470	1.236408	0.000311	3020	1.234892	0.000748
3460	1.235996	0.000869	3010	1.234728	0.001062
3450	1.236306	0.000753	3000	1.234628	0.000894
3440	1.236079	0.000828	2990	1.234596	0.001060
3430	1.236053	0.000664	2980	1.234491	0.000946
3420	1.235908	0.001215	2970	1.234478	0.000990
3410	1.236154	0.000909	2960	1.234366	0.000930
3400	1.235971	0.001099	2950	1.234204	0.000765
3390	1.236022	0.000985	2940	1.234102	0.001052
3380	1.236049	0.001328	2930	1.234115	0.000831

Table 5. Continued

<u>v, cm⁻¹</u>	<u>n</u>	<u>k</u>	<u>v, cm⁻¹</u>	<u>n</u>	<u>k</u>
2920	1.233892	0.000750	2470	1.205231	0.0
2910	1.233782	0.000940	2460	1.202096	0.000132
2900	1.233695	0.000736	2450	1.197963	0.000673
2890	1.233692	0.000847	2440	1.193917	0.001028
2880	1.233482	0.000777	2430	1.188215	0.001168
2870	1.233464	0.000700	2420	1.181419	0.001105
2860	1.233180	0.000659	2410	1.171146	0.000976
2850	1.233162	0.000707	2400	1.157887	0.001584
2840	1.232891	0.000468	2390	1.137362	0.001922
2830	1.232842	0.000624	2380	1.103449	0.001620
2820	1.232570	0.000423	2378	1.092716	0.001498
2810	1.232427	0.000385	2376	1.080996	0.001519
2800	1.232102	0.000341	2374	1.066047	0.002059
2790	1.232231	0.000295	2372	1.049534	0.003459
2780	1.231621	0.000239	2370	1.029211	0.005208
2770	1.231443	0.000212	2368	1.004716	0.007049
2760	1.231112	0.000209	2366	0.972069	0.009740
2750	1.230619	0.000091	2364	0.927068	0.015711
2740	1.230508	0.000131	2362	0.867181	0.031303
2730	1.230047	0.000037	2360	0.781386	0.064835
2720	1.229640	0.000105	2358	0.641253	0.127321
2710	1.229359	0.000060	2356	0.544338	0.376726
2700	1.229160	0.000024	2354	0.586549	0.661239
2690	1.228591	0.0	2352	0.756847	0.897010
2680	1.228355	0.000064	2350	1.009606	1.087069
2670	1.227771	0.000003	2348	1.436680	1.213311
2660	1.227492	0.0	2346	1.887094	0.998804
2650	1.226831	0.0	2344	2.014740	0.439824
2640	1.226503	0.0	2342	1.867005	0.236580
2630	1.225781	0.0	2340	1.744519	0.138239
2620	1.225388	0.0	2338	1.669851	0.074652
2610	1.224577	0.0	2336	1.593944	0.035194
2600	1.224107	0.0	2334	1.538180	0.021563
2590	1.223191	0.0	2332	1.494968	0.020825
2580	1.222613	0.0	2330	1.472947	0.020632
2570	1.221565	0.0	2328	1.453244	0.013959
2560	1.220843	0.0	2326	1.436097	0.005704
2550	1.219613	0.0	2324	1.415783	0.002166
2540	1.218706	0.0	2322	1.401383	0.001415
2530	1.217236	0.0	2320	1.387766	0.001104
2520	1.216071	0.0	2318	1.378308	0.000927
2510	1.214267	0.0	2316	1.368403	0.000816
2500	1.212731	0.0	2314	1.361382	0.000688
2490	1.210440	0.0	2312	1.353705	0.000643
2480	1.208336	0.0	2310	1.348292	0.000528

Table 5. Continued

$\nu, \text{ cm}^{-1}$	<u>n</u>	<u>k</u>	$\nu, \text{ cm}^{-1}$	<u>n</u>	<u>k</u>
2308	1.342074	0.000297	2126	1.259305	0.0
2306	1.337526	0.000134	2124	1.259131	0.0
2304	1.332193	0.000017	2122	1.258965	0.0
2302	1.328326	0.0	2120	1.258796	0.0
2300	1.323769	0.0	2118	1.258637	0.0
2298	1.320435	0.0	2116	1.258473	0.0
2296	1.316363	0.0	2114	1.258320	0.0
2294	1.313231	0.0	2112	1.258161	0.0
2292	1.309207	0.0	2110	1.258013	0.0
2290	1.305400	0.0	2108	1.257859	0.0
2288	1.298792	0.000603	2106	1.257717	0.0
2286	1.292416	0.006348	2104	1.257567	0.0
2284	1.294504	0.020319	2102	1.257430	0.0
2282	1.296983	0.024157	2100	1.257284	0.0
2280	1.291454	0.012532	2098	1.257152	0.0
2278	1.2912074	0.003654	2096	1.257010	0.0
2276	1.296079	0.000315	2094	1.256882	0.0
2274	1.292071	0.0	2092	1.256744	0.0
2272	1.299017	0.0	2090	1.256621	0.0
2270	1.297140	0.0	2088	1.256487	0.0
2260	1.289270	0.0	2086	1.256368	0.0
2250	1.284060	0.0	2084	1.256237	0.0
2240	1.279710	0.0	2082	1.256122	0.0
2230	1.276387	0.0	2080	1.255994	0.0
2220	1.273429	0.0	2078	1.255884	0.0
2210	1.271062	0.0	2076	1.255758	0.0
2200	1.268904	0.0	2074	1.255652	0.0
2190	1.267117	0.0	2072	1.255529	0.0
2180	1.265473	0.0	2070	1.255426	0.0
2170	1.264067	0.0	2068	1.255306	0.0
2160	1.262775	0.0	2066	1.255207	0.0
2158	1.262546	0.0	2064	1.255090	0.0
2156	1.262303	0.0	2062	1.254994	0.0
2154	1.262081	0.0	2060	1.254879	0.0
2152	1.261850	0.0	2050	1.254389	0.0
2150	1.261635	0.0	2040	1.253906	0.0
2148	1.261416	0.0	2030	1.253478	0.0
2144	1.260998	0.0	2020	1.253047	0.0
2140	1.260596	0.0	2010	1.252672	0.0
2138	1.260401	0.0	2000	1.252283	0.0
2136	1.260209	0.0	1990	1.251953	0.0
2134	1.260022	0.0	1980	1.251598	0.0
2132	1.259837	0.0	1970	1.251306	0.0
2130	1.259657	0.0	1960	1.250980	0.0
2128	1.259477	0.0	1950	1.250721	0.0

Table 5. Continued

$\nu, \text{ cm}^{-1}$	n	k	$\nu, \text{ cm}^{-1}$	n	k
1940	1.250419	0.0	1490	1.243657	0.0
1930	1.250188	0.0	1480	1.243343	0.000193
1920	1.249906	0.0	1470	1.243399	0.000090
1910	1.249700	0.0	1460	1.243102	0.000337
1900	1.249435	0.0	1450	1.243183	0.000213
1890	1.249251	0.0	1440	1.242789	0.000369
1880	1.249000	0.0	1430	1.242862	0.000510
1870	1.248836	0.0	1420	1.242775	0.000815
1860	1.248596	0.0	1410	1.242885	0.000425
1850	1.248451	0.0	1400	1.242503	0.000760
1840	1.248220	0.0	1390	1.242667	0.000802
1830	1.248091	0.0	1380	1.242440	0.000860
1820	1.247867	0.0	1370	1.242572	0.000936
1810	1.247754	0.0	1360	1.242380	0.001045
1800	1.247536	0.0	1350	1.242605	0.000991
1790	1.247437	0.0	1340	1.242288	0.000942
1780	1.247223	0.0	1330	1.242308	0.000905
1770	1.247137	0.0	1320	1.241931	0.001180
1760	1.246926	0.0	1310	1.242225	0.001300
1750	1.246852	0.0	1300	1.241983	0.001322
1740	1.246643	0.0	1290	1.242130	0.001260
1730	1.246581	0.0	1280	1.241884	0.001628
1720	1.246372	0.0	1270	1.242225	0.001415
1710	1.246321	0.0	1260	1.241949	0.001573
1700	1.246112	0.0	1250	1.242183	0.001405
1690	1.246071	0.0	1240	1.241870	0.001539
1680	1.245860	0.0	1230	1.242116	0.001444
1670	1.245829	0.0	1220	1.241738	0.001462
1660	1.245616	0.0	1210	1.242058	0.001580
1650	1.245595	0.0	1200	1.241668	0.001371
1640	1.245377	0.0	1190	1.241854	0.001472
1630	1.245365	0.0	1180	1.241582	0.001684
1620	1.245142	0.0	1170	1.241994	0.001357
1610	1.245140	0.0	1160	1.241460	0.001312
1600	1.244910	0.0	1150	1.241626	0.001217
1590	1.244916	0.0	1140	1.240963	0.001279
1580	1.244678	0.0	1130	1.241337	0.001617
1570	1.244691	0.0	1120	1.241061	0.001605
1560	1.244442	0.0	1110	1.241424	0.001298
1550	1.244462	0.0	1100	1.240720	0.001373
1540	1.244199	0.0	1090	1.241087	0.001454
1530	1.244219	0.0	1080	1.240489	0.001448
1520	1.243918	0.0	1070	1.240889	0.001538
1510	1.243985	0.000075	1060	1.240398	0.001704
1500	1.243685	0.0	1050	1.241109	0.001630

Table 5. Concluded

<u>v, cm⁻¹</u>	<u>n</u>	<u>k</u>	<u>v, cm⁻¹</u>	<u>n</u>	<u>k</u>
1040	1.240490	0.001284	860	1.228867	0.008681
1030	1.241057	0.001269	850	1.234294	0.009026
1020	1.240278	0.000804	840	1.234700	0.006652
1010	1.240572	0.000512	830	1.235538	0.004427
1000	1.239506	0.000520	820	1.232061	0.004329
990	1.239897	0.000237	810	1.233566	0.005159
980	1.238629	0.000152	800	1.231005	0.004200
970	1.238957	0.000199	790	1.231148	0.002892
960	1.237678	0.000189	780	1.226010	0.004836
950	1.238242	0.000343	770	1.228460	0.006908
940	1.236882	0.000057	760	1.225563	0.007182
930	1.237245	0.0	750	1.228269	0.005644
920	1.235477	0.0	740	1.221615	0.005097
910	1.235833	0.0	730	1.224209	0.004625
900	1.233734	0.000069	720	1.212443	0.001083
890	1.233681	0.0	710	1.211320	0.001267
880	1.230054	0.000474	700	1.189649	0.002841
870	1.229098	0.002938			

Table 6. Optical Constants of 20°K CO/CO₂

<u>v, cm⁻¹</u>	<u>n</u>	<u>k</u>	<u>v, cm⁻¹</u>	<u>n</u>	<u>k</u>
3690	1.217699	0.0	3320	1.215788	0.0
3680	1.217001	0.000100	3310	1.215721	0.0
3670	1.217129	0.001300	3300	1.215603	0.0
3660	1.217657	0.0	3290	1.215531	0.0
3650	1.216913	0.000100	3280	1.215413	0.0
3640	1.216437	0.0	3270	1.215335	0.0
3630	1.216340	0.001100	3260	1.215215	0.0
3620	1.216120	0.0	3250	1.215132	0.0
3610	1.212416	0.0	3240	1.215010	0.0
3608	1.210357	0.000351	3230	1.214921	0.0
3606	1.207231	0.004261	3220	1.214796	0.0
3604	1.209679	0.011466	3210	1.214701	0.0
3602	1.215903	0.014952	3200	1.214573	0.0
3600	1.222865	0.010514	3190	1.214472	0.0
3598	1.221904	0.005384	3180	1.214340	0.0
3596	1.217623	0.002149	3170	1.214233	0.0
3594	1.222807	0.016895	3160	1.214096	0.0
3592	1.222805	0.0	3150	1.213982	0.0
3590	1.224181	0.0	3140	1.213841	0.0
3580	1.219447	0.0	3130	1.213720	0.0
3570	1.219031	0.0	3120	1.213573	0.0
3560	1.218309	0.0	3110	1.213444	0.0
3550	1.218237	0.0	3100	1.213291	0.0
3540	1.217860	0.0	3090	1.213154	0.0
3530	1.217835	0.0	3080	1.212994	0.0
3520	1.217575	0.0	3070	1.212848	0.0
3510	1.217557	0.0	3060	1.212681	0.0
3500	1.217353	0.0	3050	1.212526	0.0
3490	1.217333	0.0	3040	1.212350	0.0
3480	1.217160	0.0	3030	1.212185	0.0
3470	1.217135	0.0	3020	1.212000	0.0
3460	1.216982	0.0	3010	1.211824	0.0
3450	1.216952	0.0	3000	1.211628	0.0
3440	1.216812	0.0	2990	1.211440	0.0
3430	1.216777	0.0	2980	1.211234	0.0
3420	1.216645	0.0	2970	1.211033	0.0
3410	1.216604	0.0	2960	1.210813	0.0
3400	1.216479	0.0	2950	1.210598	0.0
3390	1.216432	0.0	2940	1.210365	0.0
3380	1.216311	0.0	2930	1.210135	0.0
3370	1.216260	0.0	2920	1.209886	0.0
3360	1.216141	0.0	2910	1.209638	0.0
3350	1.216084	0.0	2900	1.209372	0.0
3340	1.215967	0.0	2890	1.209106	0.0
3330	1.215905	0.0	2880	1.208821	0.0

Table 6. Continued

<u>v, cm⁻¹</u>	<u>n</u>	<u>k</u>	<u>v, cm⁻¹</u>	<u>n</u>	<u>k</u>
2870	1.208533	0.0	2470	1.157376	0.000464
2860	1.208226	0.0	2468	1.156215	0.000501
2850	1.207914	0.0	2466	1.154978	0.000595
2840	1.207584	0.0	2464	1.153786	0.000861
2830	1.207245	0.0	2462	1.152663	0.000977
2820	1.206887	0.0	2460	1.151392	0.001003
2810	1.206519	0.0	2458	1.150089	0.001223
2800	1.206129	0.0	2456	1.148825	0.001404
2790	1.205727	0.0	2454	1.147571	0.001484
2780	1.205302	0.0	2452	1.146184	0.001536
2770	1.204861	0.0	2450	1.144750	0.001587
2760	1.204395	0.0	2448	1.143177	0.001645
2750	1.203910	0.0	2446	1.141599	0.001758
2740	1.203397	0.0	2444	1.139916	0.001876
2730	1.202860	0.0	2442	1.138244	0.001981
2720	1.202291	0.0	2440	1.136460	0.002132
2710	1.201694	0.0	2438	1.134649	0.002157
2700	1.201061	0.0	2436	1.132658	0.002309
2690	1.200393	0.0	2434	1.130763	0.002457
2680	1.199684	0.0	2432	1.128636	0.002408
2670	1.198932	0.0	2430	1.126406	0.002441
2660	1.198131	0.0	2428	1.123975	0.002594
2650	1.197278	0.0	2426	1.121625	0.002661
2640	1.196366	0.0	2424	1.118989	0.002717
2630	1.195391	0.0	2422	1.116358	0.002724
2620	1.194343	0.0	2420	1.113346	0.002715
2600	1.192000	0.0	2418	1.110322	0.002726
2580	1.189253	0.0	2416	1.106925	0.002808
2570	1.187697	0.0	2414	1.103576	0.002795
2560	1.185985	0.0	2412	1.099669	0.002773
2550	1.184113	0.0	2410	1.095815	0.002854
2540	1.182030	0.0	2408	1.091437	0.002891
2530	1.179729	0.0	2406	1.087026	0.002764
2520	1.177139	0.0	2404	1.081800	0.002780
2510	1.174233	0.0	2402	1.076670	0.002837
2500	1.170909	0.0	2400	1.070680	0.002827
2490	1.167079	0.0	2398	1.064687	0.002747
2486	1.165326	0.000000	2396	1.057530	0.002670
2484	1.164395	0.000034	2394	1.050322	0.002482
2482	1.163481	0.000148	2392	1.041532	0.002266
2480	1.162601	0.000184	2390	1.032625	0.002104
2476	1.161622	0.000129	2388	1.021585	0.001771
2476	1.160536	0.000166	2386	1.010247	0.001702
2474	1.159472	0.000315	2384	0.996220	0.001643
2472	1.158438	0.000403	2382	0.981569	0.001397

Table 6. Continued

<u>v, cm⁻¹</u>	<u>n</u>	<u>k</u>	<u>v, cm⁻¹</u>	<u>n</u>	<u>k</u>
2380	0.962458	0.001299	2290	1.336625	0.001009
2378	0.941821	0.001971	2288	1.327751	0.002014
2376	0.915321	0.004159	2286	1.316724	0.008722
2374	0.887550	0.007704	2284	1.317346	0.027735
2372	0.850641	0.012042	2282	1.333223	0.037525
2370	0.807165	0.018030	2280	1.345637	0.020889
2368	0.744652	0.033118	2278	1.341869	0.007735
2366	0.689562	0.069407	2276	1.333770	0.002875
2364	0.597046	0.091000	2274	1.326928	0.001195
2362	0.427416	0.135000	2272	1.322075	0.000970
2360	0.335497	0.454470	2270	1.317759	0.000964
2358	0.387938	0.657580	2268	1.314609	0.001072
2356	0.478794	0.837310	2266	1.311260	0.001296
2354	0.581781	1.016800	2264	1.308899	0.001392
2352	0.762620	1.198600	2262	1.305991	0.001513
2350	0.981322	1.313500	2260	1.304023	0.001678
2348	1.233482	1.384300	2258	1.301416	0.001774
2346	1.556456	1.456500	2256	1.299702	0.001905
2344	2.011403	1.366800	2254	1.297319	0.002157
2342	2.340407	0.923200	2252	1.296025	0.002328
2340	2.299513	0.355050	2250	1.293893	0.002345
2338	2.062829	0.185520	2248	1.292689	0.002370
2336	1.902079	0.103150	2246	1.290592	0.002461
2334	1.800936	0.064947	2244	1.289552	0.002477
2332	1.720262	0.038423	2242	1.287513	0.002534
2330	1.662245	0.025002	2240	1.286637	0.002653
2328	1.613116	0.013569	2238	1.284756	0.002671
2326	1.573806	0.005790	2236	1.283969	0.002629
2324	1.538542	0.002570	2234	1.282053	0.002711
2322	1.511187	0.001308	2232	1.281420	0.002749
2320	1.487527	0.000864	2230	1.279577	0.002739
2318	1.468385	0.000723	2228	1.278980	0.002752
2316	1.451395	0.000712	2226	1.277164	0.002827
2314	1.437024	0.000748	2224	1.276766	0.002850
2312	1.424146	0.000830	2222	1.274990	0.002841
2310	1.412908	0.000882	2220	1.274668	0.002767
2308	1.402786	0.000791	2218	1.272782	0.002719
2306	1.393472	0.000644	2216	1.272532	0.002721
2304	1.385015	0.000559	2214	1.270658	0.002698
2302	1.377046	0.000569	2212	1.270185	0.002590
2300	1.369930	0.000526	2210	1.268490	0.002490
2298	1.352921	0.000513	2208	1.267857	0.002474
2296	1.356579	0.000460	2206	1.266291	0.002514
2294	1.349973	0.000539	2204	1.265896	0.002470
2292	1.343807	0.000641	2202	1.264248	0.002321

Table 6. Continued

<u>v, cm⁻¹</u>	<u>n</u>	<u>k</u>	<u>v, cm⁻¹</u>	<u>n</u>	<u>k</u>
2200	1.263781	0.002166	2108	1.279390	0.000743
2198	1.261849	0.002059	2106	1.275509	0.000688
2196	1.261364	0.002079	2104	1.275856	0.000756
2194	1.259391	0.002147	2102	1.272119	0.000986
2192	1.259018	0.002143	2100	1.272283	0.001712
2190	1.256998	0.002143	2098	1.269348	0.003099
2188	1.255744	0.002132	2096	1.271071	0.004652
2186	1.254475	0.002061	2094	1.270433	0.005286
2184	1.254208	0.001991	2092	1.273025	0.004420
2182	1.251656	0.001982	2090	1.271504	0.002740
2180	1.251613	0.001861	2088	1.272015	0.001388
2178	1.248500	0.001751	2086	1.269280	0.000698
2176	1.247956	0.001599	2084	1.269436	0.000384
2174	1.244692	0.001572	2082	1.267044	0.000314
2172	1.244265	0.001440	2080	1.267485	0.000329
2170	1.240184	0.001224	2078	1.265459	0.000288
2168	1.239807	0.000979	2076	1.265975	0.000306
2166	1.234119	0.000801	2074	1.264125	0.000329
2164	1.233099	0.000598	2072	1.264707	0.000357
2162	1.225686	0.000388	2070	1.263019	0.000373
2160	1.2223452	0.000278	2068	1.263597	0.000366
2158	1.212668	0.000315	2066	1.262025	0.000426
2156	1.207378	0.000672	2064	1.262681	0.000432
2154	1.188616	0.002033	2062	1.261209	0.000327
2152	1.173687	0.007602	2060	1.261732	0.000290
2150	1.138461	0.024778	2058	1.260254	0.000301
2148	1.117504	0.063415	2056	1.260827	0.000338
2146	1.093541	0.136690	2054	1.259491	0.000340
2144	1.139083	0.226610	2052	1.260024	0.000244
2142	1.293371	0.352430	2050	1.258654	0.000288
2140	1.400428	0.149340	2048	1.259190	0.000399
2138	1.403729	0.140570	2046	1.258009	0.000405
2136	1.400526	0.065458	2044	1.258561	0.000423
2134	1.386590	0.022367	2042	1.257401	0.000433
2132	1.347834	0.006100	2040	1.257985	0.000459
2130	1.334810	0.001396	2038	1.256928	0.000415
2128	1.315463	0.000065	2036	1.257453	0.000291
2126	1.311499	0.000000	2034	1.256251	0.000205
2122	1.295420	0.000000	2032	1.256688	0.000315
2120	1.294767	0.000000	2030	1.255722	0.000406
2118	1.287886	0.000166	2028	1.256287	0.000268
2116	1.287967	0.000396	2026	1.255220	0.000187
2114	1.282670	0.000529	2024	1.255656	0.000218
2112	1.283115	0.000659	2020	1.254396	0.000100
2110	1.278790	0.000786	2010	1.253718	0.000200

Table 6. Continued

<u>v, cm⁻¹</u>	<u>n</u>	<u>k</u>	<u>v, cm⁻¹</u>	<u>n</u>	<u>k</u>
2000	1.252027	0.000400	1550	1.235892	0.0
1990	1.251813	0.000300	1540	1.235485	0.0
1980	1.250281	0.000200	1530	1.235577	0.0
1970	1.249960	0.000200	1520	1.235128	0.0
1960	1.248646	0.000300	1510	1.235331	0.000200
1950	1.248479	0.000200	1500	1.234970	0.0
1940	1.247303	0.000300	1490	1.235091	0.000100
1930	1.247186	0.000200	1480	1.234707	0.000100
1920	1.246169	0.000300	1470	1.234798	0.0
1910	1.246058	0.000100	1460	1.234446	0.000300
1900	1.245045	0.000200	1450	1.234678	0.000100
1890	1.245031	0.000200	1440	1.234295	0.000200
1880	1.244166	0.000100	1430	1.234483	0.000200
1870	1.244010	0.0	1420	1.234190	0.000200
1860	1.243174	0.000200	1410	1.234320	0.000100
1850	1.243208	0.000100	1400	1.233976	0.000200
1840	1.242435	0.000100	1390	1.234103	0.000100
1830	1.242426	0.000100	1380	1.233851	0.000300
1820	1.241749	0.000100	1370	1.234058	0.000100
1810	1.241749	0.0	1360	1.233726	0.000100
1800	1.241020	0.0	1350	1.233867	0.000100
1790	1.240993	0.0	1340	1.233564	0.0
1780	1.240393	0.000100	1330	1.233646	0.0
1770	1.240445	0.0	1320	1.233322	0.0
1760	1.239795	0.0	1310	1.233447	0.0
1750	1.239865	0.000100	1300	1.233137	0.0
1740	1.239328	0.0	1290	1.233270	0.0
1730	1.239360	0.0	1280	1.232967	0.0
1720	1.238791	0.0	1270	1.233103	0.0
1710	1.238861	0.0	1260	1.232805	0.0
1700	1.238322	0.0	1250	1.232945	0.0
1690	1.238402	0.0	1240	1.232651	0.0
1680	1.237884	0.0	1230	1.232792	0.0
1670	1.237973	0.0	1220	1.232502	0.0
1660	1.237466	0.0	1210	1.232645	0.0
1650	1.237540	0.0	1200	1.232358	0.0
1640	1.237107	0.000100	1190	1.232501	0.0
1630	1.237248	0.0	1180	1.232218	0.0
1620	1.236771	0.0	1170	1.232362	0.0
1610	1.236859	0.0	1160	1.232081	0.0
1600	1.236420	0.0	1150	1.232225	0.0
1590	1.236522	0.0	1140	1.231946	0.0
1580	1.236094	0.0	1130	1.232090	0.0
1570	1.236201	0.0	1120	1.231813	0.0
1560	1.235784	0.0	1110	1.231956	0.0

Table 6. Concluded

<u>v, cm⁻¹</u>	<u>n</u>	<u>k</u>	<u>v, cm⁻¹</u>	<u>n</u>	<u>k</u>
1100	1.231681	0.0	900	1.229670	0.0
1090	1.231822	0.0	890	1.229501	0.0
1080	1.231548	0.0	880	1.228695	0.0
1070	1.231687	0.0	870	1.227585	0.000400
1060	1.231414	0.0	860	1.226904	0.002700
1050	1.231550	0.0	850	1.229298	0.005600
1040	1.231276	0.0	840	1.231255	0.003400
1030	1.231408	0.0	830	1.231706	0.002500
1020	1.231133	0.0	820	1.230792	0.001800
1010	1.231258	0.0	810	1.230507	0.001900
1000	1.230980	0.0	800	1.230899	0.003400
990	1.231097	0.0	790	1.231070	0.001100
980	1.230813	0.0	780	1.229542	0.002200
970	1.230918	0.0	770	1.229943	0.004300
960	1.230623	0.0	760	1.231888	0.005000
950	1.230709	0.0	750	1.233345	0.004000
940	1.230397	0.0	740	1.233877	0.002800
930	1.230450	0.0	730	1.234321	0.002700
920	1.230103	0.0	720	1.234158	0.000500
910	1.230093	0.0	710	1.233345	0.000800

Table 7. Optical Constants of 20°K N₂/CO/CO₂

<u>v, cm⁻¹</u>	<u>n</u>	<u>k</u>	<u>v, cm⁻¹</u>	<u>n</u>	<u>k</u>
3700	1.231448	0.000412	3490	1.223684	0.0
3690	1.227982	0.0	3480	1.223447	0.0
3680	1.224922	0.0	3470	1.223420	0.0
3670	1.225516	0.0	3460	1.223260	0.000216
3660	1.224264	0.0	3450	1.223403	0.000189
3650	1.224603	0.0	3440	1.223276	0.000162
3640	1.223718	0.0	3430	1.223276	0.000148
3630	1.224089	0.000162	3420	1.223051	0.000167
3628	1.223446	0.000004	3410	1.223143	0.000417
3626	1.223791	0.000032	3400	1.223197	0.000411
3624	1.223183	0.0	3390	1.223285	0.000235
3622	1.223477	0.0	3380	1.223181	0.000289
3620	1.222648	0.0	3370	1.223173	0.000109
3618	1.223038	0.0	3360	1.222974	0.000146
3616	1.222316	0.0	3350	1.222990	0.000254
3614	1.222250	0.0	3340	1.222899	0.000154
3612	1.220908	0.0	3330	1.222901	0.000258
3610	1.219562	0.000756	3320	1.222868	0.000222
3608	1.218084	0.003843	3310	1.222803	0.000099
3606	1.220794	0.008515	3300	1.222638	0.000212
3604	1.225468	0.009261	3290	1.222775	0.000383
3602	1.229134	0.005634	3280	1.222720	0.000057
3600	1.228984	0.002570	3270	1.222620	0.000152
3598	1.228249	0.000881	3260	1.222534	0.000163
3596	1.226881	0.000242	3250	1.222481	0.000053
3594	1.226494	0.000127	3240	1.222362	0.000192
3592	1.225762	0.0	3230	1.222420	0.000172
3590	1.225736	0.0	3220	1.222279	0.0
3588	1.225217	0.0	3210	1.222144	0.000110
3586	1.225342	0.0	3200	1.222104	0.000199
3584	1.224922	0.0	3190	1.222112	0.000130
3582	1.225091	0.0	3180	1.221979	0.000078
3580	1.224721	0.0	3170	1.221911	0.000179
3578	1.224910	0.0	3160	1.221874	0.000158
3576	1.224574	0.000002	3150	1.221862	0.000170
3574	1.224772	0.0	3140	1.221755	0.000042
3572	1.224458	0.0	3130	1.221692	0.000144
3570	1.224658	0.0	3120	1.221584	0.000004
3560	1.224212	0.0	3110	1.221495	0.000087
3550	1.224284	0.0	3100	1.221386	0.000034
3540	1.223945	0.0	3090	1.221324	0.000066
3530	1.224010	0.0	3080	1.221193	0.000014
3520	1.223780	0.000099	3070	1.221112	0.000059
3510	1.223898	0.0	3060	1.220999	0.000036
3500	1.223636	0.0	3050	1.220913	0.000037

Table 7. Continued

<u>v, cm⁻¹</u>	<u>n</u>	<u>k</u>	<u>v, cm⁻¹</u>	<u>n</u>	<u>k</u>
3040	1.220775	0.000025	2622	1.210469	0.0
3030	1.220695	0.000066	2620	1.210343	0.0
3020	1.220544	0.0	2618	1.210218	0.0
3010	1.220416	0.000083	2616	1.210088	0.0
3000	1.220343	0.000139	2614	1.209958	0.0
2990	1.220280	0.000076	2612	1.209825	0.0
2980	1.220097	0.000024	2610	1.209691	0.0
2970	1.219962	0.000128	2608	1.209554	0.0
2960	1.219857	0.000113	2606	1.209416	0.0
2950	1.219757	0.000138	2604	1.209275	0.0
2940	1.219617	0.000104	2600	1.208987	0.0
2930	1.219434	0.000112	2596	1.208690	0.0
2920	1.219294	0.000217	2594	1.208537	0.0
2910	1.219307	0.000338	2592	1.208383	0.0
2900	1.219220	0.000075	2590	1.208224	0.0
2890	1.219007	0.000106	2588	1.208066	0.0
2880	1.219819	0.000070	2586	1.207901	0.0
2870	1.218642	0.000081	2584	1.207739	0.0
2860	1.218404	0.000042	2582	1.207567	0.0
2850	1.218318	0.000251	2580	1.207400	0.0
2840	1.218195	0.000023	2578	1.207222	0.0
2830	1.217959	0.0	2576	1.207049	0.0
2820	1.217685	0.0	2574	1.206864	0.0
2810	1.217481	0.0	2572	1.206686	0.0
2800	1.217223	0.0	2570	1.206493	0.0
2790	1.216998	0.0	2560	1.205515	0.0
2780	1.216730	0.0	2550	1.204421	0.0
2770	1.216481	0.0	2540	1.203238	0.0
2760	1.216194	0.0	2530	1.201893	0.0
2750	1.215919	0.0	2520	1.200431	0.0
2740	1.215608	0.0	2510	1.198738	0.0
2730	1.215301	0.0	2500	1.196877	0.0
2720	1.214961	0.0	2498	1.196433	0.0
2710	1.214619	0.0	2496	1.196049	0.0
2700	1.214244	0.0	2494	1.195579	0.0
2690	1.213859	0.0	2492	1.195173	0.0
2680	1.213442	0.0	2490	1.194674	0.0
2670	1.213008	0.0	2488	1.194245	0.0
2660	1.212539	0.0	2486	1.193715	0.0
2650	1.212047	0.0	2484	1.193259	0.0
2640	1.211516	0.0	2482	1.192694	0.0
2630	1.210951	0.0	2480	1.192208	0.0
2628	1.210832	0.0	2478	1.191605	0.0
2626	1.210714	0.0	2476	1.191085	0.0
2624	1.210591	0.0	2474	1.190438	0.0

Table 7. Continued

<u>v, cm⁻¹</u>	<u>n</u>	<u>k</u>	<u>v, cm⁻¹</u>	<u>n</u>	<u>k</u>
2472	1.189878	0.0	2382	1.093525	0.001641
2470	1.189177	0.0	2380	1.089112	0.001569
2468	1.188561	0.0	2378	1.075149	0.001385
2466	1.187771	0.000004	2376	1.064962	0.001266
2464	1.187076	0.000070	2374	1.050287	0.001040
2462	1.186241	0.000162	2372	1.035849	0.000906
2460	1.185605	0.000328	2370	1.014538	0.001026
2458	1.184813	0.000353	2368	0.992714	0.001514
2456	1.184097	0.000403	2366	0.959162	0.002961
2454	1.183200	0.000530	2364	0.922211	0.006212
2452	1.182502	0.000626	2362	0.860093	0.014900
2450	1.181591	0.000688	2360	0.792361	0.040324
2448	1.180829	0.000757	2358	0.688837	0.095507
2446	1.179842	0.000824	2356	0.512007	0.156479
2444	1.179015	0.000869	2354	0.450591	0.561739
2442	1.177936	0.000944	2352	0.592549	0.815373
2440	1.177056	0.001021	2350	0.783567	0.987340
2438	1.175912	0.001044	2348	1.009576	1.192503
2436	1.174948	0.001104	2346	1.533884	1.415013
2434	1.173714	0.001160	2344	2.088927	1.067487
2432	1.172682	0.001130	2342	2.168048	0.328670
2430	1.171270	0.001118	2340	1.915074	0.160297
2428	1.170071	0.001114	2338	1.756139	0.065339
2426	1.168472	0.001095	2336	1.6555641	0.023500
2424	1.167136	0.001149	2334	1.570527	0.011215
2422	1.165377	0.001134	2332	1.521253	0.012340
2420	1.163884	0.001165	2330	1.485932	0.014506
2418	1.161921	0.001190	2328	1.464696	0.010268
2416	1.160257	0.001188	2326	1.441289	0.003973
2414	1.158015	0.001198	2324	1.421602	0.001150
2412	1.156106	0.001243	2322	1.403231	0.000686
2410	1.153589	0.001302	2320	1.389982	0.000553
2408	1.151456	0.001355	2318	1.377517	0.000502
2406	1.148608	0.001408	2316	1.367930	0.000475
2404	1.146167	0.001450	2314	1.358603	0.000418
2402	1.142897	0.001503	2312	1.351195	0.000400
2400	1.140061	0.001524	2310	1.343920	0.000359
2398	1.136204	0.001555	2308	1.337967	0.000245
2396	1.132894	0.001691	2306	1.332004	0.000165
2394	1.128440	0.001708	2304	1.327026	0.000121
2392	1.124511	0.001721	2302	1.322016	0.000012
2390	1.119116	0.001737	2300	1.317692	0.0
2388	1.114313	0.001723	2298	1.313351	0.0
2386	1.107739	0.001783	2296	1.309524	0.0
2384	1.101810	0.001692	2294	1.305570	0.0

Table 7. Continued

<u>v, cm⁻¹</u>	<u>n</u>	<u>k</u>	<u>v, cm⁻¹</u>	<u>n</u>	<u>k</u>
2292	1.301797	0.0	2122	1.261956	0.0
2290	1.297571	0.000144	2120	1.260239	0.0
2288	1.291896	0.000449	2118	1.259105	0.0
2286	1.284886	0.004520	2116	1.257825	0.0
2284	1.285276	0.016995	2114	1.256999	0.0
2282	1.295525	0.022556	2112	1.255981	0.0
2280	1.303117	0.012353	2110	1.255343	0.0
2278	1.300933	0.003953	2108	1.254491	0.0
2276	1.295588	0.000830	2106	1.253971	0.0
2274	1.291450	0.000084	2104	1.253220	0.0
2272	1.288410	0.000006	2102	1.252739	0.0
2270	1.286105	0.0	2100	1.251898	0.0
2268	1.284060	0.0	2098	1.251394	0.000388
2266	1.282301	0.000029	2096	1.251072	0.000984
2264	1.280647	0.000026	2094	1.251424	0.001140
2262	1.279153	0.0	2092	1.251441	0.000730
2260	1.277676	0.0	2090	1.251189	0.000122
2250	1.271608	0.000116	2088	1.250490	0.0
2240	1.266806	0.000290	2086	1.249844	0.0
2230	1.262865	0.000254	2084	1.249665	0.0
2220	1.259348	0.000369	2082	1.249025	0.0
2210	1.256332	0.000430	2080	1.249028	0.0
2200	1.253428	0.000400	2078	1.248499	0.0
2190	1.250533	0.000351	2076	1.248465	0.0
2180	1.247341	0.000377	2074	1.247991	0.0
2170	1.243174	0.000149	2072	1.247953	0.0
2160	1.235789	0.0	2070	1.247488	0.0
2158	1.233276	0.0	2068	1.247482	0.0
2156	1.230117	0.0	2066	1.246580	0.0
2154	1.225401	0.000086	2064	1.247044	0.0
2152	1.218546	0.001072	2062	1.246470	0.0
2150	1.207568	0.004499	2060	1.246634	0.0
2148	1.192671	0.015501	2050	1.245793	0.0
2146	1.179454	0.042715	2040	1.244896	0.0
2144	1.192380	0.090962	2030	1.244197	0.0
2142	1.247686	0.128249	2020	1.243518	0.0
2140	1.305817	0.095593	2010	1.242986	0.0
2138	1.322325	0.043890	2000	1.242375	0.0
2136	1.308288	0.014205	1990	1.241913	0.0
2134	1.291959	0.003311	1980	1.241402	0.0
2132	1.280271	0.000341	1970	1.241017	0.0
2130	1.273580	0.0	1960	1.240556	0.0
2128	1.269013	0.0	1950	1.240224	0.0
2126	1.266179	0.0	1940	1.239812	0.0
2124	1.263640	0.0	1930	1.239518	0.0

Table 7. Continued

<u>v, cm⁻¹</u>	<u>n</u>	<u>k</u>	<u>v, cm⁻¹</u>	<u>n</u>	<u>k</u>
1920	1.239148	0.0	1470	1.232322	0.0
1910	1.238892	0.0	1460	1.232115	0.0
1900	1.238552	0.0	1450	1.232141	0.0
1890	1.238329	0.0	1440	1.231937	0.0
1880	1.238011	0.0	1430	1.231969	0.0
1870	1.237813	0.0	1420	1.231762	0.0
1860	1.237519	0.0	1410	1.231802	0.0
1850	1.237343	0.0	1400	1.231588	0.0
1840	1.237067	0.0	1390	1.231633	0.0
1830	1.236911	0.0	1380	1.231414	0.0
1820	1.236650	0.0	1370	1.231467	0.0
1810	1.236512	0.0	1360	1.231241	0.0
1800	1.236264	0.0	1350	1.231300	0.0
1790	1.236142	0.0	1340	1.231067	0.0
1780	1.235905	0.0	1330	1.231132	0.0
1770	1.235797	0.0	1320	1.230891	0.0
1760	1.235570	0.0	1310	1.230963	0.0
1750	1.235475	0.0	1300	1.230713	0.0
1740	1.235256	0.0	1290	1.230792	0.0
1730	1.235172	0.0	1280	1.230532	0.0
1720	1.234960	0.0	1270	1.230619	0.0
1710	1.234888	0.0	1260	1.230347	0.0
1700	1.234680	0.0	1250	1.230441	0.0
1690	1.234618	0.0	1240	1.230158	0.0
1680	1.234416	0.0	1230	1.230258	0.0
1670	1.234363	0.0	1220	1.229962	0.0
1660	1.234164	0.0	1210	1.230070	0.0
1650	1.234120	0.0	1200	1.229758	0.0
1640	1.233924	0.0	1190	1.229875	0.0
1630	1.233889	0.0	1180	1.229546	0.0
1620	1.233695	0.0	1170	1.229671	0.0
1610	1.233667	0.0	1160	1.229323	0.0
1600	1.233475	0.0	1150	1.229457	0.0
1590	1.233455	0.0	1140	1.229088	0.0
1580	1.233263	0.0	1130	1.229230	0.0
1570	1.233250	0.0	1120	1.228838	0.0
1560	1.233058	0.0	1110	1.228989	0.0
1550	1.233053	0.0	1100	1.228570	0.0
1540	1.232860	0.0	1090	1.228731	0.0
1530	1.232861	0.0	1080	1.228282	0.0
1520	1.232667	0.0	1070	1.228452	0.0
1510	1.232674	0.0	1060	1.227968	0.0
1500	1.232479	0.0	1050	1.228148	0.0
1490	1.232496	0.0	1040	1.227624	0.0
1480	1.232295	0.0	1030	1.227813	0.0

Table 7. Concluded

<u>v, cm⁻¹</u>	<u>n</u>	<u>k</u>	<u>v, cm⁻¹</u>	<u>n</u>	<u>k</u>
1020	1.227244	0.0	850	1.221813	0.004757
1010	1.227440	0.0	840	1.222334	0.004405
1000	1.226817	0.0	830	1.222921	0.002137
990	1.227020	0.0	820	1.220486	0.002438
980	1.226332	0.0	810	1.220821	0.002766
970	1.226539	0.0	800	1.218978	0.002586
960	1.225771	0.0	790	1.218866	0.002370
950	1.225975	0.0	780	1.215732	0.003093
940	1.225107	0.0	770	1.216406	0.004651
930	1.225296	0.0	760	1.214657	0.005474
920	1.224287	0.0	750	1.216145	0.004376
910	1.224420	0.0	740	1.212003	0.003600
900	1.223199	0.0	730	1.211564	0.002196
890	1.223152	0.0	720	1.203074	0.001340
880	1.221078	0.0	710	1.200185	0.001631
870	1.220454	0.001285	700	1.184832	0.002801
860	1.219541	0.003732			

Table 8. Optical Constants of 20°K H₂O/CO₂

<u>v, cm⁻¹</u>	<u>n</u>	<u>k</u>	<u>v, cm⁻¹</u>	<u>n</u>	<u>k</u>
3700	1.241443	0.021113	3610	1.235598	0.018268
3698	1.241615	0.017845	3608	1.233903	0.018581
3696	1.239985	0.014709	3606	1.231697	0.018999
3694	1.237006	0.013497	3604	1.229968	0.019914
3692	1.234460	0.014011	3602	1.227794	0.020925
3690	1.232887	0.014942	3600	1.226752	0.022986
3688	1.231614	0.015105	3598	1.226117	0.024603
3686	1.229645	0.015202	3596	1.226511	0.025456
3684	1.226875	0.015951	3594	1.226117	0.025761
3682	1.224486	0.018507	3592	1.225737	0.025395
3680	1.223557	0.021547	3590	1.224586	0.026052
3678	1.222976	0.022990	3588	1.224250	0.026012
3676	1.221734	0.024934	3586	1.222817	0.025827
3674	1.220533	0.027693	3584	1.221778	0.026177
3672	1.220298	0.031093	3582	1.220412	0.026763
3670	1.220608	0.033908	3580	1.219664	0.026706
3668	1.221052	0.036511	3578	1.217805	0.026868
3666	1.221638	0.039796	3576	1.216333	0.027157
3664	1.223147	0.042863	3574	1.213879	0.028014
3662	1.224972	0.045746	3572	1.212763	0.029624
3660	1.227427	0.048302	3570	1.211081	0.030941
3658	1.230089	0.050724	3560	1.205796	0.035912
3656	1.233963	0.052990	3550	1.200293	0.043562
3654	1.238071	0.053767	3540	1.196074	0.050275
3652	1.242206	0.053494	3530	1.192548	0.060090
3650	1.246156	0.053265	3520	1.189003	0.067533
3648	1.250484	0.051253	3510	1.189433	0.079886
3646	1.253225	0.047978	3500	1.190314	0.086962
3644	1.255293	0.045234	3490	1.189815	0.095030
3642	1.256539	0.042159	3480	1.190871	0.107208
3640	1.257246	0.038791	3470	1.192852	0.114699
3638	1.257089	0.036304	3460	1.196906	0.127904
3636	1.257069	0.033734	3450	1.202141	0.135551
3634	1.256346	0.031269	3440	1.209152	0.144895
3632	1.256050	0.029573	3430	1.214162	0.151325
3630	1.255534	0.027066	3420	1.219942	0.158567
3628	1.254332	0.024022	3410	1.222909	0.172346
3626	1.252171	0.022228	3400	1.239271	0.171389
3624	1.250286	0.020532	3390	1.247234	0.181583
3622	1.247558	0.018948	3380	1.257358	0.183870
3620	1.245161	0.018777	3370	1.268832	0.189933
3618	1.243020	0.018748	3360	1.278871	0.189192
3616	1.241566	0.018517	3350	1.287710	0.191118
3614	1.239571	0.018260	3340	1.298475	0.195525
3612	1.237830	0.018037	3330	1.309667	0.192392

Table 8. Continued

<u>ν, cm^{-1}</u>	<u>n</u>	<u>k</u>	<u>ν, cm^{-1}</u>	<u>n</u>	<u>k</u>
3320	1.319857	0.193486	2870	1.356960	0.005489
3310	1.331119	0.191232	2860	1.355127	0.005153
3300	1.340865	0.185347	2850	1.353367	0.005146
3290	1.348412	0.182254	2840	1.351623	0.004977
3280	1.353849	0.175303	2830	1.350017	0.004927
3270	1.353949	0.175652	2820	1.348442	0.004881
3260	1.367368	0.173876	2810	1.346812	0.004549
3250	1.375163	0.168589	2800	1.345166	0.004736
3240	1.381163	0.164724	2790	1.343733	0.004679
3230	1.389360	0.163111	2780	1.342213	0.004530
3220	1.397666	0.155581	2770	1.340646	0.004579
3210	1.403893	0.149362	2750	1.337796	0.004521
3200	1.411359	0.144348	2730	1.334887	0.004806
3190	1.417608	0.133599	2720	1.333495	0.004638
3180	1.421568	0.124717	2710	1.332053	0.004752
3170	1.422942	0.115620	2700	1.330636	0.004768
3160	1.421098	0.105951	2690	1.329161	0.004719
3150	1.423814	0.109693	2680	1.327666	0.004857
3140	1.431275	0.099731	2670	1.326118	0.004814
3130	1.434926	0.089308	2660	1.324698	0.005107
3120	1.435116	0.079436	2650	1.323237	0.004952
3110	1.434919	0.070116	2640	1.321630	0.004876
3100	1.432879	0.061130	2630	1.319795	0.004876
3090	1.430617	0.053325	2620	1.318087	0.005038
3080	1.427291	0.045759	2610	1.316284	0.005089
3070	1.423606	0.038928	2600	1.314380	0.005014
3060	1.419222	0.033297	2590	1.312362	0.005292
3050	1.414893	0.027955	2580	1.310357	0.005228
3040	1.410025	0.023688	2570	1.307969	0.005230
3030	1.405491	0.020250	2560	1.305718	0.005688
3020	1.400869	0.017186	2550	1.303310	0.005553
3010	1.396766	0.015074	2540	1.300660	0.005581
3000	1.392540	0.012650	2530	1.297586	0.005598
2990	1.388512	0.011158	2520	1.294320	0.005582
2980	1.384741	0.010180	2510	1.290385	0.005707
2970	1.381424	0.008954	2500	1.286410	0.006206
2960	1.378152	0.008433	2490	1.281811	0.006514
2950	1.375253	0.007585	2480	1.277029	0.007099
2940	1.372366	0.007182	2470	1.271394	0.007589
2930	1.369789	0.006781	2460	1.265304	0.007891
2920	1.367405	0.006513	2450	1.257450	0.008099
2910	1.365107	0.006058	2440	1.248690	0.008482
2900	1.362832	0.005846	2430	1.237024	0.008342
2890	1.360753	0.005744	2420	1.222406	0.007859
2880	1.358787	0.005509	2410	1.201588	0.008008

Table 8. Continued

<u>ν, cm⁻¹</u>	<u>n</u>	<u>k</u>	<u>ν, cm⁻¹</u>	<u>n</u>	<u>k</u>
2400	1.173544	0.007275	2294	1.479689	0.015376
2390	1.124875	0.005627	2292	1.471768	0.015712
2380	1.023149	0.004197	2290	1.464077	0.016768
2378	0.985207	0.008426	2288	1.455741	0.019558
2376	0.933295	0.023790	2286	1.448816	0.024902
2374	0.875812	0.063722	2284	1.444838	0.033365
2372	0.832438	0.132628	2282	1.447523	0.042361
2370	0.814329	0.213977	2280	1.455217	0.046028
2368	0.822726	0.286159	2278	1.463457	0.041349
2366	0.833098	0.345523	2276	1.465718	0.031286
2364	0.837713	0.396608	2274	1.462035	0.022242
2362	0.871673	0.501282	2272	1.455191	0.017550
2360	0.921579	0.526280	2270	1.449122	0.015863
2358	0.954784	0.572562	2268	1.444133	0.015206
2356	0.981772	0.617860	2266	1.440067	0.015065
2354	1.025289	0.679953	2264	1.436607	0.014980
2352	1.081348	0.737672	2262	1.433494	0.014947
2350	1.156538	0.788387	2260	1.430689	0.014942
2348	1.239617	0.831659	2250	1.419342	0.015120
2346	1.346717	0.867225	2240	1.410793	0.015189
2344	1.470061	0.876688	2230	1.403731	0.015157
2342	1.594698	0.839593	2220	1.397988	0.015567
2340	1.700484	0.785995	2210	1.393266	0.015725
2338	1.795701	0.711925	2200	1.389217	0.015746
2336	1.875279	0.622301	2190	1.385857	0.016122
2334	1.932903	0.508715	2180	1.383032	0.015825
2332	1.957977	0.389344	2170	1.380329	0.015639
2330	1.952308	0.270506	2160	1.377806	0.015433
2328	1.910792	0.160570	2150	1.375568	0.015314
2326	1.843808	0.083628	2140	1.373535	0.015161
2324	1.773288	0.046161	2130	1.371616	0.014921
2322	1.717957	0.030610	2120	1.369804	0.014848
2320	1.675376	0.022923	2110	1.368152	0.014627
2318	1.642786	0.018861	2100	1.366682	0.014697
2316	1.615402	0.016790	2090	1.365382	0.014442
2314	1.593671	0.015766	2080	1.364042	0.014188
2312	1.574459	0.015268	2070	1.362845	0.014117
2310	1.558880	0.015091	2060	1.361714	0.013755
2308	1.544517	0.015141	2050	1.360596	0.013541
2306	1.532813	0.015215	2040	1.359532	0.013219
2304	1.521681	0.015238	2030	1.358523	0.012816
2302	1.512240	0.015362	2020	1.357296	0.012260
2300	1.503096	0.015335	2010	1.356151	0.012070
2298	1.495118	0.015243	2000	1.354953	0.011568
2296	1.487021	0.015289	1990	1.353704	0.011224

Table 8. Continued

$\nu, \text{ cm}^{-1}$	<u>n</u>	<u>k</u>	$\nu, \text{ cm}^{-1}$	<u>n</u>	<u>k</u>
1980	1.352323	0.010971	1706	1.304872	0.036500
1970	1.351152	0.010854	1704	1.304633	0.037616
1960	1.349848	0.010573	1702	1.304645	0.038949
1950	1.348503	0.010423	1700	1.304497	0.040165
1940	1.347237	0.010614	1698	1.304436	0.041276
1930	1.346081	0.010347	1696	1.304213	0.042903
1920	1.344710	0.010397	1694	1.304457	0.044331
1910	1.343490	0.010555	1692	1.304622	0.045850
1900	1.342256	0.010540	1690	1.305071	0.047156
1890	1.341074	0.010726	1688	1.305315	0.048476
1880	1.339755	0.010647	1686	1.305687	0.049676
1870	1.338458	0.010919	1684	1.305969	0.051166
1860	1.337141	0.011052	1682	1.306528	0.052345
1850	1.335864	0.011224	1680	1.306750	0.053513
1840	1.334317	0.011286	1678	1.307030	0.054829
1830	1.332829	0.011724	1676	1.307236	0.056424
1820	1.331207	0.011958	1674	1.307720	0.057933
1810	1.329594	0.012436	1672	1.308086	0.059624
1800	1.327679	0.012802	1670	1.308693	0.061336
1790	1.325770	0.013586	1668	1.309287	0.063240
1780	1.323636	0.014355	1666	1.310174	0.065135
1770	1.321523	0.015448	1664	1.310872	0.067054
1760	1.318935	0.016516	1662	1.312170	0.069676
1750	1.316269	0.018325	1660	1.313922	0.071917
1748	1.315545	0.018695	1658	1.315950	0.073672
1746	1.315114	0.019179	1656	1.317710	0.075610
1744	1.314327	0.019477	1654	1.320101	0.077824
1742	1.313765	0.020120	1652	1.322785	0.079713
1740	1.313087	0.020732	1650	1.326074	0.081334
1738	1.312697	0.021248	1648	1.329408	0.082545
1736	1.311922	0.021719	1646	1.333062	0.083183
1734	1.311282	0.022318	1644	1.336673	0.083801
1732	1.310499	0.023209	1642	1.340533	0.083500
1730	1.310057	0.023924	1640	1.344169	0.083232
1728	1.309347	0.024727	1638	1.348091	0.082308
1726	1.308832	0.025543	1636	1.351807	0.080881
1724	1.308192	0.026563	1634	1.355313	0.078678
1722	1.307831	0.027438	1632	1.358055	0.076124
1720	1.307218	0.028361	1630	1.360580	0.073644
1718	1.306758	0.029353	1628	1.362507	0.070681
1716	1.306210	0.030553	1626	1.364082	0.067815
1714	1.306023	0.031705	1624	1.365119	0.065064
1712	1.305584	0.032667	1622	1.365825	0.062082
1710	1.305254	0.033850	1620	1.365927	0.059754
1708	1.304865	0.035200	1618	1.366277	0.057747

Table 8. Continued

<u>v, cm⁻¹</u>	<u>n</u>	<u>k</u>	<u>v, cm⁻¹</u>	<u>n</u>	<u>k</u>
1616	1.366410	0.055583	1310	1.336119	0.024901
1614	1.366535	0.053614	1300	1.335425	0.024604
1612	1.366413	0.051791	1290	1.334865	0.024537
1610	1.366468	0.050002	1280	1.334048	0.024390
1608	1.366215	0.048194	1270	1.333539	0.024257
1606	1.365994	0.046441	1260	1.332780	0.024122
1604	1.365455	0.044833	1250	1.332207	0.023632
1602	1.365062	0.043322	1240	1.331029	0.023282
1600	1.364298	0.041786	1230	1.330134	0.023129
1598	1.363602	0.040529	1220	1.328806	0.022902
1596	1.362656	0.039436	1210	1.327858	0.022953
1594	1.361942	0.038506	1200	1.326655	0.022999
1592	1.360954	0.037694	1190	1.325712	0.022680
1590	1.360301	0.037158	1180	1.324289	0.022831
1588	1.359607	0.036717	1170	1.323279	0.022620
1586	1.359180	0.036025	1160	1.321731	0.022600
1584	1.358497	0.035610	1150	1.320451	0.022464
1582	1.358076	0.035010	1140	1.318785	0.022647
1580	1.357371	0.034581	1130	1.317399	0.022450
1570	1.354908	0.032953	1120	1.315554	0.022662
1560	1.352979	0.032352	1110	1.313996	0.022547
1550	1.351849	0.031536	1100	1.311862	0.022587
1540	1.350825	0.030914	1090	1.309998	0.022753
1530	1.349968	0.030029	1080	1.307610	0.022765
1520	1.348789	0.029308	1070	1.305526	0.023090
1510	1.347982	0.029184	1060	1.302731	0.022959
1500	1.347151	0.028566	1050	1.300082	0.023344
1490	1.346471	0.028355	1040	1.296782	0.023627
1480	1.345604	0.027994	1030	1.293622	0.023951
1470	1.345176	0.028026	1020	1.289523	0.024522
1460	1.344596	0.027611	1010	1.285457	0.025222
1450	1.344156	0.027289	1000	1.280339	0.026437
1440	1.343251	0.026925	990	1.275124	0.028088
1430	1.342969	0.027160	980	1.269243	0.030956
1420	1.342298	0.026524	970	1.263570	0.034038
1410	1.341848	0.026410	960	1.256975	0.038141
1400	1.340757	0.026188	950	1.251022	0.043921
1390	1.340151	0.026321	940	1.245319	0.050201
1380	1.340237	0.027672	930	1.239131	0.056335
1370	1.340621	0.025826	920	1.233801	0.066421
1360	1.339668	0.025663	910	1.230044	0.075376
1350	1.338981	0.025138	900	1.226771	0.084165
1340	1.338158	0.025076	890	1.221711	0.093980
1330	1.337447	0.024743	880	1.217818	0.105756
1320	1.336565	0.024826	870	1.211862	0.121508

Table 8. Concluded

<u>v, cm⁻¹</u>	<u>n</u>	<u>k</u>	<u>v, cm⁻¹</u>	<u>n</u>	<u>k</u>
860	1.212350	0.141021	770	1.296427	0.235431
850	1.232135	0.174981	760	1.309207	0.244025
840	1.240661	0.149262	750	1.330720	0.241737
830	1.238080	0.175116	740	1.337356	0.233837
820	1.238630	0.180702	730	1.346027	0.228081
810	1.248703	0.200495	720	1.341084	0.222335
800	1.257893	0.213795	710	1.341080	0.216352
790	1.275132	0.219927	700	1.315877	0.209359
780	1.281382	0.226851			

Table 9. Optical Constants of 20°K N₂/H₂O

<u>v, cm⁻¹</u>	<u>n</u>	<u>k</u>	<u>v, cm⁻¹</u>	<u>n</u>	<u>k</u>
3700	1.208666	0.007814	3610	1.226285	0.000190
3698	1.207110	0.011422	3608	1.225983	0.000456
3696	1.206148	0.016075	3606	1.225814	0.000576
3694	1.206639	0.022145	3604	1.225575	0.000538
3692	1.209778	0.028667	3602	1.225316	0.000683
3690	1.215447	0.033907	3600	1.225102	0.000678
3688	1.223355	0.037164	3598	1.224752	0.000610
3686	1.232386	0.037073	3596	1.224310	0.000708
3684	1.240070	0.032300	3594	1.223966	0.000992
3682	1.244510	0.026153	3592	1.223729	0.001132
3680	1.245696	0.019537	3590	1.223528	0.001340
3678	1.244692	0.014977	3588	1.223226	0.001295
3676	1.243064	0.012155	3586	1.222973	0.001606
3674	1.241772	0.010567	3584	1.222740	0.001606
3672	1.241123	0.009638	3582	1.222293	0.001569
3670	1.241029	0.008481	3580	1.221808	0.001988
3668	1.240774	0.006845	3578	1.221648	0.002397
3666	1.240173	0.005431	3576	1.221480	0.002472
3664	1.239358	0.004198	3574	1.221140	0.002597
3662	1.238501	0.003262	3572	1.220783	0.002934
3660	1.237717	0.002557	3570	1.220587	0.003259
3658	1.236971	0.001806	3568	1.220397	0.003446
3656	1.236046	0.001121	3566	1.220128	0.003589
3654	1.235187	0.000888	3564	1.219728	0.003769
3652	1.234551	0.000645	3562	1.219347	0.004118
3650	1.233882	0.000206	3560	1.218963	0.004454
3648	1.233078	0.0	3558	1.218582	0.004851
3646	1.232369	0.0	3556	1.218258	0.005430
3644	1.231797	0.0	3554	1.218054	0.005895
3642	1.231261	0.0	3552	1.217890	0.006412
3640	1.230751	0.000032	3550	1.217653	0.006721
3638	1.230258	0.000130	3548	1.217263	0.007203
3636	1.229766	0.000226	3546	1.216891	0.007908
3634	1.229419	0.000618	3544	1.216680	0.008739
3632	1.229301	0.000843	3542	1.216636	0.009609
3630	1.229345	0.001016	3540	1.216734	0.010431
3628	1.229448	0.000896	3538	1.216952	0.011237
3626	1.229369	0.000501	3536	1.217188	0.011890
3624	1.228926	0.000093	3534	1.217517	0.012671
3622	1.228419	0.000121	3532	1.218030	0.013360
3620	1.228077	0.000180	3530	1.218541	0.013702
3618	1.227805	0.000138	3528	1.218887	0.014110
3616	1.227448	0.000069	3526	1.219263	0.014621
3614	1.227080	0.000097	3524	1.219912	0.015237
3612	1.226697	0.000116	3522	1.220765	0.015442

Table 9. Continued

<u>v, cm⁻¹</u>	<u>n</u>	<u>k</u>	<u>v, cm⁻¹</u>	<u>n</u>	<u>k</u>
3520	1.221376	0.015192	3430	1.226223	0.020223
3518	1.221611	0.015036	3428	1.226484	0.020206
3516	1.221789	0.015164	3426	1.226644	0.020224
3514	1.221970	0.015215	3424	1.226780	0.020408
3512	1.222169	0.015450	3422	1.226975	0.020489
3510	1.222564	0.015769	3420	1.227156	0.020625
3508	1.223083	0.015769	3418	1.227349	0.020698
3506	1.223379	0.015565	3416	1.227441	0.020704
3504	1.223436	0.015492	3414	1.227493	0.020886
3502	1.223660	0.015810	3412	1.227609	0.021098
3500	1.224092	0.015803	3410	1.227854	0.021337
3498	1.224301	0.015490	3408	1.228111	0.021389
3496	1.224344	0.015543	3406	1.228304	0.021391
3494	1.224498	0.015602	3404	1.228354	0.021367
3492	1.224703	0.015596	3402	1.228373	0.021457
3490	1.224882	0.015580	3400	1.228400	0.021608
3488	1.225116	0.015561	3398	1.228425	0.021670
3486	1.225369	0.015412	3396	1.228361	0.021824
3484	1.225436	0.015034	3394	1.228248	0.021994
3482	1.225166	0.014770	3392	1.228108	0.022339
3480	1.224989	0.015017	3390	1.228069	0.022791
3478	1.225051	0.015134	3388	1.228006	0.023169
3476	1.225047	0.014967	3386	1.227970	0.023772
3474	1.224953	0.015105	3384	1.228085	0.024515
3472	1.224925	0.015078	3382	1.228361	0.025130
3470	1.224757	0.015043	3380	1.228653	0.025818
3468	1.224461	0.015148	3378	1.229011	0.026474
3466	1.224331	0.015611	3376	1.229494	0.027342
3464	1.224404	0.015859	3374	1.230247	0.028128
3462	1.224491	0.016019	3372	1.231258	0.028884
3460	1.224463	0.016103	3370	1.232429	0.029240
3458	1.224357	0.016258	3368	1.233602	0.029467
3456	1.224325	0.016610	3366	1.234717	0.029385
3454	1.224312	0.016760	3364	1.235924	0.029389
3452	1.224202	0.017029	3362	1.236997	0.028745
3450	1.224206	0.017545	3360	1.237715	0.028095
3448	1.224454	0.017937	3358	1.238264	0.027632
3446	1.224620	0.018067	3356	1.238792	0.026998
3444	1.224681	0.018305	3354	1.238919	0.026231
3442	1.224892	0.018779	3352	1.238768	0.025883
3440	1.225151	0.018787	3350	1.238794	0.026058
3438	1.225175	0.018939	3348	1.239167	0.026065
3436	1.225125	0.019215	3346	1.239478	0.025850
3434	1.225356	0.019865	3344	1.239663	0.025725
3432	1.225797	0.020095	3342	1.239826	0.025767

Table 9. Continued

<u>v, cm⁻¹</u>	<u>n</u>	<u>k'</u>	<u>v, cm⁻¹</u>	<u>n</u>	<u>k</u>
3340	1.240100	0.025863	3250	1.242345	0.013452
3338	1.240505	0.026070	3248	1.242051	0.013795
3336	1.241030	0.026106	3246	1.241803	0.014313
3334	1.241655	0.026220	3244	1.241689	0.014905
3332	1.242444	0.026119	3242	1.241691	0.015468
3330	1.243095	0.025669	3240	1.241839	0.016132
3328	1.243462	0.025248	3238	1.242099	0.016640
3326	1.243842	0.025193	3236	1.242352	0.017114
3324	1.244504	0.025051	3234	1.242708	0.017753
3322	1.245179	0.024592	3232	1.243303	0.018314
3320	1.245640	0.023970	3230	1.243996	0.018672
3318	1.246000	0.023583	3228	1.244740	0.018952
3316	1.246414	0.023076	3226	1.245579	0.019162
3314	1.246778	0.022541	3224	1.246466	0.019082
3312	1.247027	0.021900	3222	1.247318	0.018921
3310	1.247178	0.021389	3220	1.248017	0.018444
3308	1.247251	0.020835	3218	1.248587	0.018110
3306	1.247355	0.020519	3216	1.249108	0.017675
3304	1.247526	0.020080	3214	1.249577	0.017206
3302	1.247657	0.019604	3212	1.249915	0.016706
3300	1.247713	0.019159	3210	1.250255	0.016294
3298	1.247809	0.018799	3208	1.250564	0.015808
3296	1.247918	0.018343	3206	1.250774	0.015225
3294	1.247976	0.017872	3204	1.250891	0.014822
3292	1.247956	0.017394	3202	1.251021	0.014371
3290	1.247972	0.017045	3200	1.251171	0.014010
3288	1.247942	0.016522	3198	1.251308	0.013529
3286	1.247865	0.016130	3196	1.251320	0.013017
3284	1.247798	0.015753	3194	1.251325	0.012716
3282	1.247728	0.015282	3192	1.251363	0.012300
3280	1.247553	0.014849	3190	1.251354	0.011897
3278	1.247357	0.014458	3188	1.251287	0.011548
3276	1.247098	0.014081	3186	1.251255	0.011236
3274	1.246833	0.013785	3184	1.251220	0.010923
3272	1.246576	0.013543	3182	1.251129	0.010533
3270	1.246364	0.013264	3180	1.250963	0.010298
3268	1.246090	0.012949	3178	1.250899	0.010155
3266	1.245677	0.012577	3176	1.250901	0.009947
3264	1.245150	0.012437	3174	1.250861	0.009637
3262	1.244700	0.012440	3172	1.250773	0.009460
3260	1.244286	0.012422	3170	1.250761	0.009273
3258	1.243832	0.012441	3168	1.250786	0.009058
3256	1.243401	0.012644	3166	1.250738	0.008692
3254	1.243018	0.012814	3164	1.250585	0.008458
3252	1.242651	0.013102	3162	1.250462	0.008305

Table 9. Continued

$\nu, \text{ cm}^{-1}$	n	k	$\nu, \text{ cm}^{-1}$	n	k
3160	1.250414	0.008180	2750	1.239748	0.0
3158	1.250386	0.007969	2740	1.239653	0.0
3156	1.250324	0.007776	2730	1.239563	0.0
3154	1.250293	0.007601	2720	1.239474	0.0
3152	1.250219	0.007352	2710	1.239388	0.0
3150	1.250137	0.007142	2700	1.239304	0.0
3140	1.249638	0.006448	2690	1.239223	0.0
3130	1.249373	0.005738	2680	1.239142	0.0
3120	1.248953	0.004938	2670	1.239065	0.0
3110	1.248488	0.004469	2660	1.238988	0.0
3100	1.248165	0.004027	2650	1.238913	0.0
3090	1.247789	0.003417	2640	1.238839	0.0
3080	1.247348	0.003054	2630	1.238767	0.0
3070	1.246975	0.002734	2620	1.238695	0.0
3060	1.246680	0.002409	2610	1.238624	0.0
3050	1.246391	0.002083	2600	1.238554	0.0
3040	1.246034	0.001651	2590	1.238485	0.0
3030	1.245628	0.001426	2580	1.238415	0.0
3020	1.245299	0.001209	2570	1.238347	0.0
3010	1.244977	0.000966	2560	1.238278	0.0
3000	1.244636	0.000754	2550	1.238209	0.0
2990	1.244319	0.000607	2540	1.238139	0.0
2980	1.243988	0.000388	2530	1.238068	0.0
2970	1.243677	0.000311	2520	1.237997	0.0
2960	1.243376	0.000140	2500	1.237848	0.0
2950	1.243022	0.0	2480	1.237689	0.0
2940	1.242668	0.0	2470	1.237602	0.0
2930	1.242397	0.0	2460	1.237510	0.0
2920	1.242155	0.0	2450	1.237409	0.0
2910	1.241938	0.0	2440	1.237297	0.0
2900	1.241735	0.0	2430	1.237169	0.0
2890	1.241549	0.0	2420	1.237020	0.0
2880	1.241373	0.0	2410	1.236836	0.0
2870	1.241209	0.0	2400	1.236602	0.0
2860	1.241053	0.0	2390	1.236275	0.0
2850	1.240907	0.0	2380	1.235773	0.0
2840	1.240766	0.0	2370	1.234847	0.0
2830	1.240634	0.0	2360	1.232361	0.0
2820	1.240506	0.0	2358	1.231136	0.0
2810	1.240386	0.0	2356	1.228785	0.000063
2800	1.240268	0.0	2354	1.225210	0.001988
2790	1.240157	0.0	2352	1.221291	0.007108
2780	1.240049	0.0	2350	1.221402	0.017613
2770	1.239945	0.0	2348	1.232623	0.030273
2760	1.239844	0.0	2346	1.249718	0.027470

Table 9. Continued

<u>v, cm⁻¹</u>	<u>n</u>	<u>k</u>	<u>v, cm⁻¹</u>	<u>n</u>	<u>k</u>
2344	1.257006	0.011125	2230	1.237587	0.0
2342	1.252608	0.001615	2220	1.237503	0.0
2340	1.247051	0.0	2210	1.237424	0.0
2338	1.244399	0.0	2200	1.237351	0.0
2336	1.243066	0.0	2190	1.237279	0.0
2334	1.242191	0.0	2180	1.237212	0.0
2332	1.241544	0.0	2170	1.237146	0.0
2330	1.241062	0.0	2160	1.237082	0.0
2328	1.240673	0.0	2150	1.237018	0.0
2326	1.240365	0.0	2140	1.236956	0.0
2324	1.240102	0.0	2130	1.236892	0.0
2322	1.239880	0.0	2120	1.236830	0.0
2320	1.239696	0.0	2110	1.236764	0.0
2318	1.239542	0.0	2100	1.236697	0.0
2316	1.239391	0.0	2098	1.236681	0.0
2314	1.239253	0.0	2096	1.236668	0.0
2312	1.239151	0.0	2094	1.236652	0.0
2310	1.239046	0.0	2092	1.236638	0.0
2308	1.238957	0.0	2090	1.236620	0.0
2306	1.238919	0.0	2088	1.236605	0.0
2304	1.238796	0.0	2086	1.236586	0.0
2302	1.238726	0.0	2084	1.236568	0.0
2300	1.238659	0.0	2082	1.236546	0.0
2298	1.238578	0.0	2080	1.236521	0.0
2296	1.238541	0.0	2078	1.236483	0.000003
2294	1.238492	0.0	2076	1.236459	0.000039
2292	1.238437	0.0	2074	1.236452	0.000059
2290	1.238390	0.0	2072	1.236440	0.000055
2288	1.238346	0.0	2070	1.236397	0.000066
2286	1.238303	0.0	2068	1.236378	0.000124
2284	1.238263	0.0	2066	1.236397	0.000173
2282	1.238225	0.0	2064	1.236422	0.000161
2280	1.238189	0.0	2062	1.236414	0.000162
2278	1.238153	0.0	2060	1.236391	0.000158
2276	1.238121	0.0	2058	1.236378	0.000209
2274	1.238088	0.0	2056	1.236388	0.000228
2272	1.238058	0.0	2054	1.236415	0.000263
2270	1.238028	0.0	2052	1.236442	0.000253
2268	1.238000	0.0	2050	1.236443	0.000233
2266	1.237972	0.0	2048	1.236441	0.000257
2264	1.237946	0.0	2046	1.236454	0.000258
2262	1.237919	0.0	2044	1.236467	0.000259
2260	1.237895	0.0	2042	1.236478	0.000261
2250	1.237780	0.0	2040	1.236494	0.000260
2240	1.237679	0.0	2038	1.236515	0.000260

Table 9. Continued

<u>$\nu, \text{ cm}^{-1}$</u>	<u>n</u>	<u>k</u>	<u>$\nu, \text{ cm}^{-1}$</u>	<u>n</u>	<u>k</u>
2036	1.236538	0.000240	1770	1.233444	0.0
2034	1.236564	0.000229	1760	1.233136	0.0
2032	1.236594	0.000190	1750	1.232761	0.0
2030	1.236604	0.000123	1740	1.232299	0.0
2028	1.236584	0.000065	1738	1.232189	0.0
2026	1.236535	0.000006	1736	1.232076	0.0
2024	1.236480	0.0	1734	1.231952	0.0
2022	1.235441	0.0	1732	1.231822	0.0
2020	1.236415	0.0	1730	1.231677	0.0
2018	1.236390	0.0	1728	1.231521	0.0
2016	1.236370	0.0	1726	1.231332	0.0
2014	1.236348	0.0	1724	1.231130	0.000033
2012	1.236330	0.0	1722	1.230911	0.000082
2010	1.236311	0.0	1720	1.230662	0.000144
2008	1.236295	0.0	1718	1.230437	0.000322
2006	1.236277	0.0	1716	1.230274	0.000473
2004	1.236262	0.0	1714	1.230125	0.000596
2002	1.236244	0.0	1712	1.229966	0.000718
2000	1.236230	0.0	1710	1.229795	0.000817
1998	1.236213	0.0	1708	1.229572	0.000926
1996	1.236199	0.0	1706	1.229334	0.001099
1994	1.236182	0.0	1704	1.229135	0.001350
1992	1.236169	0.0	1702	1.228969	0.001539
1990	1.236152	0.0	1700	1.228810	0.001796
1980	1.236030	0.0	1698	1.228627	0.001978
1970	1.236005	0.0	1696	1.228486	0.002325
1960	1.235932	0.0	1694	1.228457	0.002611
1950	1.235855	0.0	1692	1.228421	0.002744
1940	1.235779	0.0	1690	1.228267	0.002877
1930	1.235697	0.0	1688	1.228074	0.003119
1920	1.235616	0.0	1686	1.227928	0.003415
1910	1.235529	0.0	1684	1.227904	0.003764
1900	1.235441	0.0	1682	1.227875	0.003882
1890	1.235345	0.0	1680	1.227793	0.004073
1880	1.235248	0.0	1678	1.227638	0.004184
1870	1.235141	0.0	1676	1.227464	0.004366
1860	1.235031	0.0	1674	1.227238	0.004532
1850	1.234910	0.0	1672	1.226958	0.004671
1840	1.234784	0.0	1670	1.226566	0.004909
1830	1.234644	0.0	1668	1.226123	0.005188
1820	1.234495	0.0	1666	1.225618	0.005637
1810	1.234328	0.0	1664	1.225116	0.006164
1800	1.234148	0.0	1662	1.224633	0.006875
1790	1.233941	0.0	1660	1.224173	0.007610
1780	1.233712	0.0	1658	1.223707	0.008530

Table 9. Continued

<u>v, cm⁻¹</u>	<u>n</u>	<u>k</u>	<u>v, cm⁻¹</u>	<u>n</u>	<u>k</u>
1656	1.223212	0.009568	1550	1.240405	0.000405
1654	1.222867	0.011006	1540	1.239879	0.000305
1652	1.222922	0.012668	1530	1.239408	0.000203
1650	1.223168	0.013980	1520	1.239048	0.000197
1648	1.223459	0.015545	1510	1.238679	0.000021
1646	1.223937	0.017177	1500	1.238295	0.0
1644	1.224668	0.018894	1490	1.237971	0.000069
1642	1.225680	0.020726	1480	1.237755	0.000059
1640	1.227119	0.022584	1470	1.237562	0.000120
1638	1.229003	0.024358	1460	1.237375	0.0
1636	1.231554	0.026017	1450	1.237149	0.000054
1634	1.234709	0.027020	1440	1.236937	0.0
1632	1.238153	0.027064	1430	1.236754	0.000101
1630	1.241580	0.026363	1420	1.236638	0.000116
1628	1.244572	0.024474	1410	1.236521	0.000095
1626	1.246773	0.022159	1400	1.236343	0.000048
1624	1.248125	0.019541	1390	1.236170	0.000097
1622	1.248589	0.016915	1380	1.236045	0.000143
1620	1.248376	0.014894	1370	1.235942	0.000147
1618	1.247805	0.013250	1360	1.235794	0.000126
1616	1.246915	0.012179	1350	1.235672	0.000192
1614	1.245851	0.011808	1340	1.235566	0.000199
1612	1.245266	0.012633	1330	1.235468	0.000195
1610	1.246040	0.013996	1320	1.235352	0.000222
1608	1.248437	0.014707	1310	1.235215	0.000160
1606	1.251299	0.013246	1300	1.235083	0.000282
1604	1.253098	0.010180	1290	1.235021	0.000265
1602	1.253082	0.006732	1280	1.234945	0.000291
1600	1.251843	0.004224	1270	1.234831	0.000205
1598	1.250259	0.002807	1260	1.234772	0.000309
1596	1.248815	0.001878	1250	1.234666	0.000095
1594	1.247581	0.001534	1240	1.234474	0.000102
1592	1.246648	0.001281	1230	1.234267	0.000068
1590	1.245890	0.001141	1220	1.234172	0.000168
1588	1.245303	C.001057	1210	1.233985	0.0
1586	1.244736	0.000847	1200	1.233822	0.000108
1584	1.244221	0.000838	1190	1.233632	0.000042
1582	1.243810	0.000815	1180	1.233497	0.000060
1580	1.243442	0.000715	1170	1.233247	0.0
1578	1.243076	0.000737	1160	1.233015	0.0
1576	1.242861	0.000758	1150	1.232763	0.000139
1574	1.242614	0.000608	1140	1.232658	0.000170
1572	1.242324	0.000530	1130	1.232431	0.000151
1570	1.242018	0.000543	1120	1.232301	0.000222
1560	1.241087	C.000451	1110	1.232072	0.000154

Table 9. Concluded

<u>ν, cm⁻¹</u>	<u>n</u>	<u>k</u>	<u>ν, cm⁻¹</u>	<u>n</u>	<u>k</u>
1100	1.231840	0.000094	890	1.217763	0.004434
1090	1.231592	0.000246	880	1.215906	0.005882
1080	1.231346	0.0	870	1.213921	0.008513
1070	1.230989	0.000186	860	1.213961	0.012851
1060	1.230780	0.000134	850	1.216177	0.015736
1050	1.230435	0.000040	840	1.217569	0.014601
1040	1.230035	0.0	830	1.216326	0.014834
1030	1.229577	0.000019	820	1.214976	0.016856
1020	1.229146	0.0	810	1.214441	0.019429
1010	1.228560	0.0	800	1.214231	0.021496
1000	1.228018	0.000094	790	1.213812	0.024338
990	1.227437	0.000245	780	1.213696	0.027561
980	1.226688	0.000089	770	1.214727	0.032260
970	1.225884	0.000638	760	1.217790	0.036196
960	1.225209	0.000784	750	1.221429	0.038196
950	1.224404	0.001125	740	1.224129	0.038658
940	1.223604	0.001583	730	1.225775	0.039930
930	1.222753	0.001907	720	1.227216	0.041262
920	1.221894	0.002505	710	1.227836	0.043175
910	1.220748	0.002720	700	1.229070	0.047315
900	1.219392	0.003525			

Table 10. Optical Constants of 20°K Ar/H₂O

<u>v, cm⁻¹</u>	<u>n</u>	<u>k</u>	<u>v, cm⁻¹</u>	<u>n</u>	<u>k</u>
3700	1.249066	0.005282	3610	1.249494	0.0
3698	1.250708	0.005334	3608	1.249055	0.0
3696	1.251937	0.004303	3606	1.248880	0.0
3694	1.252366	0.003300	3604	1.248784	0.0
3692	1.252415	0.002511	3602	1.248686	0.0
3690	1.252528	0.002083	3600	1.248593	0.0
3688	1.252687	0.001379	3598	1.248505	0.0
3686	1.252374	0.000326	3596	1.248386	0.0
3684	1.251692	0.0	3594	1.248227	0.0
3682	1.251209	0.0	3592	1.248239	0.000256
3680	1.250937	0.0	3590	1.248191	0.0
3678	1.250718	0.0	3588	1.247925	0.0
3676	1.250600	0.000083	3586	1.247751	0.000300
3674	1.250499	0.0	3584	1.247823	0.000415
3672	1.250377	0.0	3582	1.247818	0.000360
3670	1.250262	0.0	3580	1.247782	0.000312
3668	1.250183	0.0	3578	1.247394	0.000060
3666	1.250096	0.0	3576	1.246714	0.000231
3664	1.250031	0.0	3574	1.246701	0.001503
3662	1.249958	0.0	3572	1.247297	0.001593
3660	1.249903	0.0	3570	1.247339	0.001190
3658	1.249839	0.0	3568	1.247155	0.001617
3656	1.249790	0.0	3566	1.247360	0.001929
3654	1.249731	0.0	3564	1.247683	0.001939
3652	1.249686	0.0	3562	1.247768	0.001772
3650	1.249632	0.0	3560	1.247726	0.001743
3648	1.249590	0.0	3558	1.247768	0.001930
3646	1.249538	0.0	3556	1.247889	0.001817
3644	1.249497	0.0	3554	1.247895	0.001781
3642	1.249445	0.0	3552	1.247848	0.001681
3640	1.249406	0.0	3550	1.247731	0.001670
3638	1.249354	0.0	3548	1.247585	0.001680
3636	1.249314	0.0	3546	1.247372	0.001788
3634	1.249260	0.0	3544	1.247335	0.002111
3632	1.249219	0.0	3542	1.247437	0.002320
3630	1.249160	0.0	3540	1.247439	0.002192
3628	1.249116	0.0	3538	1.247615	0.002670
3626	1.249047	0.0	3536	1.247632	0.002110
3624	1.248997	0.0	3534	1.247113	0.002105
3622	1.248905	0.0	3532	1.246690	0.002855
3620	1.248838	0.0	3530	1.247097	0.003690
3618	1.248637	0.0	3528	1.247805	0.003875
3616	1.248215	0.000034	3526	1.247979	0.003213
3614	1.248479	0.001204	3524	1.247806	0.003569
3612	1.249350	0.001042	3522	1.247907	0.003800

Table 10. Continued

<u>v, cm⁻¹</u>	<u>n</u>	<u>k</u>	<u>v, cm⁻¹</u>	<u>n</u>	<u>-k</u>
3520	1.248127	0.003985	3430	1.249133	0.003460
3518	1.248552	0.004365	3428	1.248819	0.003064
3516	1.249057	0.004127	3426	1.248412	0.003542
3514	1.249237	0.003869	3424	1.248569	0.004289
3512	1.249326	0.003869	3422	1.249127	0.004315
3510	1.249785	0.004035	3420	1.249353	0.004056
3508	1.250309	0.003529	3418	1.249407	0.003886
3506	1.250257	0.002649	3416	1.249329	0.003738
3504	1.249813	0.002477	3414	1.249093	0.003522
3502	1.249669	0.002611	3412	1.248760	0.003762
3500	1.249792	0.002552	3410	1.248636	0.004058
3498	1.249746	0.002139	3408	1.248758	0.004482
3496	1.249485	0.001981	3406	1.248967	0.004543
3494	1.249165	0.001913	3404	1.249048	0.004585
3492	1.248909	0.002027	3402	1.249287	0.004854
3490	1.248853	0.002294	3400	1.249490	0.004581
3488	1.248924	0.002254	3398	1.249343	0.004337
3486	1.248821	0.002107	3396	1.249067	0.004561
3484	1.248524	0.002066	3394	1.249018	0.004839
3482	1.248177	0.002271	3392	1.249126	0.005199
3480	1.248055	0.002772	3390	1.249434	0.005396
3478	1.248319	0.003211	3388	1.249753	0.005413
3476	1.248813	0.003281	3386	1.249862	0.005115
3474	1.248810	0.002687	3384	1.249635	0.005071
3472	1.248558	0.002817	3382	1.249452	0.005359
3470	1.248550	0.003142	3380	1.249579	0.005911
3468	1.248558	0.002854	3378	1.249846	0.006045
3466	1.248527	0.003279	3376	1.250243	0.006493
3464	1.248439	0.002993	3374	1.250906	0.006591
3462	1.248109	0.003305	3372	1.251483	0.006230
3460	1.248292	0.004167	3370	1.251700	0.005775
3458	1.249019	0.004334	3368	1.251780	0.005531
3456	1.249455	0.003876	3366	1.251705	0.005193
3454	1.249561	0.003679	3364	1.251609	0.005180
3452	1.249602	0.003421	3362	1.251700	0.005313
3450	1.249623	0.003245	3360	1.251856	0.005089
3448	1.249476	0.002895	3358	1.252043	0.005114
3446	1.249117	0.002757	3356	1.252203	0.004703
3444	1.248642	0.002880	3354	1.251981	0.004208
3442	1.248519	0.003517	3352	1.251546	0.004241
3440	1.248930	0.003964	3350	1.251435	0.004541
3438	1.249368	0.003696	3348	1.251540	0.004616
3436	1.249327	0.003297	3346	1.251554	0.004454
3434	1.249122	0.003343	3344	1.251342	0.004405
3432	1.249062	0.003400	3342	1.251076	0.004573

Table 10. Continued

<u>v, cm⁻¹</u>	<u>n</u>	<u>k</u>	<u>v, cm⁻¹</u>	<u>n</u>	<u>k</u>
3340	1.251014	0.005047	3250	1.253525	0.001865
3338	1.251362	0.005483	3248	1.253326	0.001939
3336	1.251789	0.005416	3246	1.253168	0.001964
3334	1.251914	0.005144	3244	1.253122	0.002182
3332	1.251803	0.005167	3242	1.253176	0.002195
3330	1.251828	0.005410	3240	1.253207	0.002175
3328	1.252038	0.005656	3238	1.253162	0.002089
3326	1.252425	0.005795	3236	1.253048	0.002080
3324	1.252951	0.005817	3234	1.252965	0.002132
3322	1.253335	0.005336	3232	1.252960	0.002267
3320	1.253374	0.004939	3230	1.253014	0.002149
3318	1.253339	0.004793	3220	1.252766	0.002659
3316	1.253344	0.004627	3210	1.253285	0.003241
3314	1.253288	0.004451	3200	1.254012	0.002774
3312	1.253267	0.004503	3190	1.254224	0.002280
3310	1.253312	0.004392	3180	1.254313	0.001911
3308	1.253469	0.004443	3170	1.254332	0.001547
3306	1.253443	0.004039	3160	1.254115	0.000985
3304	1.253272	0.004042	3150	1.253977	0.001160
3302	1.253357	0.004324	3140	1.254002	0.000797
3300	1.253565	0.004035	3130	1.253951	0.000576
3298	1.253447	0.003825	3120	1.253741	0.000270
3296	1.253353	0.003937	3110	1.253475	0.000073
3294	1.253411	0.004010	3100	1.253271	0.000178
3292	1.253495	0.003958	3090	1.253163	0.0
3290	1.253695	0.004100	3080	1.252976	0.0
3288	1.253943	0.003827	3070	1.252844	0.0
3286	1.253930	0.003472	3060	1.252744	0.0
3284	1.253780	0.003382	3050	1.252654	0.0
3282	1.253738	0.003372	3040	1.252575	0.0
3280	1.253712	0.003275	3030	1.252506	0.0
3278	1.253633	0.003212	3020	1.252441	0.0
3276	1.253519	0.003252	3010	1.252384	0.0
3274	1.253471	0.003401	3000	1.252329	0.0
3272	1.253727	0.003748	2990	1.252281	0.0
3270	1.254355	0.003721	2980	1.252234	0.0
3268	1.254645	0.002904	2970	1.252192	0.0
3266	1.254224	0.002230	2960	1.252151	0.0
3264	1.253729	0.002456	2950	1.252115	0.0
3262	1.253675	0.002665	2940	1.252078	0.0
3260	1.253862	0.002768	2930	1.252045	0.0
3258	1.253989	0.002516	2920	1.252013	0.0
3256	1.253980	0.002347	2910	1.251983	0.0
3254	1.253907	0.002152	2900	1.251954	0.0
3252	1.253757	0.001966	2890	1.251927	0.0

Table 10. Continued

<u>v, cm⁻¹</u>	<u>n</u>	<u>k</u>	<u>v, cm⁻¹</u>	<u>n</u>	<u>k</u>
2880	1.251900	0.0	2410	1.251143	0.0
2870	1.251876	0.0	2400	1.251111	0.0
2860	1.251851	0.0	2390	1.251064	0.0
2850	1.251829	0.0	2380	1.251001	0.0
2840	1.251806	0.0	2370	1.250886	0.0
2830	1.251786	0.0	2368	1.250856	0.0
2820	1.251765	0.0	2366	1.250811	0.0
2810	1.251745	0.0	2364	1.250768	0.0
2800	1.251726	0.0	2362	1.250701	0.0
2790	1.251707	0.0	2360	1.250630	0.0
2780	1.251689	0.0	2358	1.250515	0.0
2770	1.251672	0.0	2356	1.250379	0.0
2760	1.251655	0.0	2354	1.250112	0.0
2750	1.251638	0.0	2352	1.249447	0.0
2740	1.251622	0.0	2350	1.248796	0.001049
2730	1.251607	0.0	2348	1.249310	0.002814
2720	1.251591	0.0	2346	1.250755	0.003415
2710	1.251577	0.0	2344	1.252099	0.003018
2700	1.251562	0.0	2342	1.253152	0.002487
2690	1.251548	0.0	2340	1.253490	0.000908
2680	1.251534	0.0	2338	1.252905	0.0
2670	1.251520	0.0	2336	1.252279	0.0
2660	1.251506	0.0	2334	1.252047	0.0
2650	1.251493	0.0	2332	1.251903	0.0
2640	1.251480	0.0	2330	1.251806	0.0
2630	1.251467	0.0	2320	1.251549	0.0
2620	1.251455	0.0	2310	1.251441	0.0
2600	1.251430	0.0	2300	1.251375	0.0
2580	1.251405	0.0	2290	1.251332	0.0
2570	1.251393	0.0	2280	1.251298	0.0
2560	1.251380	0.0	2270	1.251272	0.0
2550	1.251368	0.0	2260	1.251249	0.0
2540	1.251356	0.0	2250	1.251230	0.0
2530	1.251343	0.0	2240	1.251212	0.0
2520	1.251331	0.0	2230	1.251196	0.0
2510	1.251318	0.0	2220	1.251181	0.0
2500	1.251305	0.0	2210	1.251167	0.0
2490	1.251291	0.0	2200	1.251154	0.0
2480	1.251278	0.0	2190	1.251140	0.0
2470	1.251263	0.0	2180	1.251128	0.0
2460	1.251248	0.0	2170	1.251115	0.0
2450	1.251231	0.0	2160	1.251104	0.0
2440	1.251214	0.0	2150	1.251091	0.0
2430	1.251193	0.0	2140	1.251080	0.0
2420	1.251171	0.0	2130	1.251067	0.0

Table 10. Continued

$\nu, \text{ cm}^{-1}$	n	k	$\nu, \text{ cm}^{-1}$	n	k
2120	1.251056	0.0	1694	1.249448	0.0
2110	1.251043	0.0	1692	1.249326	0.000007
2100	1.251033	0.0	1690	1.249227	0.000111
2090	1.251020	0.0	1688	1.249275	0.000297
2080	1.251009	0.0	1686	1.249352	0.000175
2070	1.250997	0.0	1684	1.249165	0.0
2060	1.250985	0.0	1682	1.248931	0.000165
2050	1.250972	0.0	1680	1.248847	0.000405
2040	1.250960	0.0	1678	1.248874	0.000503
2030	1.250946	0.0	1676	1.248973	0.000727
2020	1.250935	0.0	1674	1.249095	0.000586
2010	1.250919	0.0	1672	1.249079	0.000544
2000	1.250908	0.0	1670	1.248971	0.000391
1990	1.250892	0.0	1668	1.248775	0.000414
1980	1.250880	0.0	1666	1.248460	0.000373
1970	1.250863	0.0	1664	1.248315	0.000863
1960	1.250850	0.0	1662	1.248361	0.000993
1950	1.250833	0.0	1660	1.248428	0.001136
1940	1.250819	0.0	1658	1.248491	0.001238
1930	1.250800	0.0	1656	1.248594	0.001192
1920	1.250785	0.0	1654	1.248457	0.000975
1910	1.250765	0.0	1652	1.248087	0.000934
1900	1.250748	0.0	1650	1.247718	0.001252
1890	1.250726	0.0	1648	1.247611	0.001686
1880	1.250708	0.0	1646	1.247530	0.001858
1870	1.250683	0.0	1644	1.247496	0.002269
1860	1.250663	0.0	1642	1.247418	0.002446
1850	1.250636	0.0	1640	1.247357	0.002838
1840	1.250612	0.0	1638	1.247318	0.003261
1830	1.250581	0.0	1636	1.247361	0.003637
1820	1.250553	0.0	1634	1.247475	0.004227
1810	1.250518	0.0	1632	1.247630	0.004548
1800	1.250485	0.0	1630	1.247649	0.005097
1790	1.250443	0.0	1628	1.248062	0.006145
1780	1.250401	0.0	1626	1.249049	0.006851
1770	1.250350	0.0	1624	1.250307	0.007018
1760	1.250297	0.0	1622	1.251186	0.006497
1750	1.250232	0.0	1620	1.251722	0.006138
1740	1.250159	0.0	1618	1.252088	0.005894
1730	1.250069	0.0	1616	1.252375	0.005528
1720	1.249961	0.0	1614	1.252832	0.005736
1710	1.249822	0.0	1612	1.253699	0.005368
1700	1.249626	0.0	1610	1.254160	0.004311
1698	1.249579	0.0	1608	1.253804	0.003327
1696	1.249516	0.0	1606	1.253206	0.003316

Table 10. Continued

<u>v, cm⁻¹</u>	<u>n</u>	<u>k</u>	<u>v, cm⁻¹</u>	<u>n</u>	<u>k</u>
1604	1.253168	0.003750	1410	1.250914	0.0
1602	1.253735	0.003908	1400	1.250888	0.0
1600	1.254253	0.003325	1390	1.250840	0.0
1598	1.253926	0.002412	1380	1.250816	0.0
1596	1.253385	0.002789	1370	1.250769	0.0
1594	1.253887	0.003741	1360	1.250747	0.0
1592	1.255329	0.003537	1350	1.250700	0.0
1590	1.256103	0.001891	1340	1.250678	0.0
1588	1.255522	0.000232	1330	1.250631	0.0
1586	1.254499	0.0	1320	1.250610	0.0
1584	1.253935	0.0	1310	1.250562	0.0
1582	1.253615	0.0	1300	1.250542	0.0
1580	1.253369	0.0	1290	1.250491	0.0
1578	1.253171	0.0	1280	1.250471	0.0
1576	1.253011	0.0	1270	1.250419	0.0
1574	1.252869	0.0	1260	1.250398	0.0
1572	1.252754	0.0	1250	1.250343	0.0
1570	1.252643	0.0	1240	1.250321	0.0
1568	1.252555	0.0	1230	1.250263	0.0
1566	1.252464	0.0	1228	1.250273	0.0
1564	1.252395	0.0	1226	1.250247	0.0
1562	1.252318	0.0	1224	1.250257	0.0
1560	1.252261	0.0	1222	1.250230	0.0
1558	1.252195	0.0	1220	1.250241	0.0
1556	1.252148	0.0	1218	1.250213	0.0
1554	1.252090	0.0	1216	1.250224	0.0
1552	1.252050	0.0	1214	1.250196	0.0
1550	1.251999	0.0	1212	1.250207	0.0
1548	1.251965	0.0	1210	1.250179	0.0
1546	1.251918	0.0	1208	1.250190	0.0
1544	1.251889	0.0	1206	1.250161	0.0
1542	1.251846	0.0	1204	1.250172	0.0
1540	1.251821	0.0	1202	1.250143	0.0
1530	1.251670	0.0	1200	1.250155	0.0
1520	1.251563	0.0	1198	1.250125	0.0
1510	1.251458	0.0	1196	1.250137	0.0
1500	1.251385	0.0	1194	1.250107	0.0
1490	1.251304	0.0	1192	1.250119	0.0
1480	1.251250	0.0	1190	1.250089	0.0
1470	1.251183	0.0	1180	1.250063	0.0
1460	1.251141	0.0	1170	1.249992	0.0
1450	1.251082	0.0	1160	1.249963	0.0
1440	1.251047	0.0	1150	1.249886	0.0
1430	1.250994	0.0	1140	1.249855	0.0
1420	1.250964	0.0	1130	1.249771	0.0

Table 10. Concluded

<u>v, cm⁻¹</u>	<u>n</u>	<u>k</u>	<u>v, cm⁻¹</u>	<u>n</u>	<u>k</u>
1120	1.249736	0.0	852	1.241419	0.004537
1110	1.249643	0.0	850	1.242650	0.007045
1100	1.249605	0.0	848	1.243544	0.007106
1090	1.249502	0.0	846	1.244664	0.007574
1080	1.249458	0.0	844	1.244939	0.007633
1070	1.249343	0.0	842	1.245859	0.007950
1060	1.249292	0.0	840	1.247131	0.008614
1050	1.249161	0.0	838	1.249136	0.007166
1040	1.249102	0.0	836	1.248565	0.004230
1030	1.248953	0.0	834	1.246488	0.003609
1020	1.248883	0.0	832	1.245191	0.005663
1010	1.248709	0.0	830	1.246742	0.007428
1000	1.248625	0.0	828	1.248595	0.006429
990	1.248419	0.0	826	1.249127	0.004235
980	1.248315	0.0	824	1.247127	0.002330
970	1.248064	0.0	822	1.245549	0.003753
960	1.247931	0.0	820	1.245568	0.005333
950	1.247613	0.0	818	1.246528	0.005133
940	1.247437	0.0	816	1.247073	0.005237
930	1.247011	0.0	814	1.247855	0.004134
920	1.246760	0.0	812	1.246683	0.001980
910	1.246121	0.0	810	1.244401	0.001900
900	1.245724	0.0	808	1.243067	0.004216
890	1.244445	0.0	806	1.243806	0.005460
880	1.241515	0.0	804	1.244072	0.005369
878	1.241195	0.001042	802	1.244116	0.005597
876	1.241114	0.001906	800	1.243802	0.006375
874	1.240672	0.001888	790	1.244805	0.006450
872	1.239697	0.002590	780	1.243940	0.006819
870	1.238850	0.004744	770	1.244231	0.010241
868	1.239395	0.006566	760	1.246398	0.011076
866	1.238941	0.008525	750	1.248004	0.010519
864	1.242225	0.013065	740	1.248717	0.010100
862	1.251549	0.016886	730	1.249084	0.009408
860	1.254026	0.0	720	1.248452	0.008370
858	1.247662	0.0	710	1.246375	0.008336
856	1.243620	0.000873	700	1.244410	0.010819
854	1.242590	0.002689			

Table 11. Optical Constants of 20°K CO/CO₂

<u>v, cm⁻¹</u>	<u>n</u>	<u>k</u>	<u>v, cm⁻¹</u>	<u>n</u>	<u>k</u>
3700	1.243539	0.001550	3610	1.243449	0.000958
3698	1.242298	0.001074	3608	1.243405	0.001122
3696	1.241527	0.001264	3605	1.243450	0.001028
3694	1.240888	0.001003	3604	1.243268	0.000871
3692	1.240200	0.001390	3602	1.242978	0.001015
3690	1.239624	0.001740	3600	1.243028	0.001507
3688	1.239123	0.002275	3598	1.243526	0.001691
3686	1.238828	0.003213	3596	1.243797	0.001114
3684	1.238985	0.004011	3594	1.243631	0.000789
3682	1.239127	0.004521	3592	1.243471	0.000786
3680	1.239010	0.005020	3590	1.243259	0.000506
3678	1.239044	0.006404	3588	1.243025	0.000662
3676	1.240180	0.008036	3586	1.243058	0.000865
3674	1.242461	0.008888	3584	1.243059	0.000579
3672	1.244501	0.007617	3582	1.242920	0.000647
3670	1.245190	0.005960	3580	1.242900	0.000652
3668	1.245079	0.005011	3578	1.242867	0.000506
3666	1.244782	0.004310	3576	1.242683	0.000381
3664	1.244389	0.004014	3574	1.242519	0.000435
3662	1.244157	0.004092	3572	1.242392	0.000417
3660	1.244220	0.004197	3570	1.242271	0.000421
3658	1.244282	0.004061	3568	1.242106	0.000423
3656	1.244278	0.004102	3566	1.241935	0.000456
3654	1.244447	0.004353	3564	1.241795	0.000609
3652	1.244936	0.004456	3562	1.241727	0.000680
3650	1.245494	0.004231	3560	1.241654	0.000781
3648	1.245981	0.003757	3558	1.241667	0.000887
3646	1.246203	0.003085	3556	1.241719	0.000880
3644	1.246096	0.002366	3554	1.241604	0.000644
3642	1.245816	0.002042	3552	1.241382	0.000707
3640	1.245651	0.001796	3550	1.241181	0.000727
3638	1.245451	0.001509	3548	1.240954	0.000787
3636	1.245271	0.001358	3546	1.240788	0.001041
3634	1.245151	0.001252	3544	1.240603	0.001092
3632	1.245041	0.000965	3542	1.240500	0.001469
3630	1.244797	0.000807	3540	1.240559	0.001733
3628	1.244669	0.000715	3538	1.240608	0.001721
3626	1.244553	0.000524	3536	1.240609	0.001997
3624	1.244179	0.0	3534	1.240719	0.001996
3622	1.243408	0.0	3532	1.240819	0.002079
3620	1.242639	0.000361	3530	1.240711	0.001779
3618	1.242692	0.001706	3528	1.240442	0.001930
3616	1.243524	0.001957	3526	1.240317	0.002171
3614	1.243993	0.001321	3524	1.240310	0.002321
3612	1.243746	0.000886	3522	1.240277	0.002419

Table 11. Continued

<u>v, cm⁻¹</u>	<u>n</u>	<u>k</u>	<u>v, cm⁻¹</u>	<u>n</u>	<u>k</u>
3520	1.240203	0.002558	3422	1.242965	0.005266
3510	1.239928	0.003341	3420	1.243027	0.005222
3508	1.240011	0.003593	3418	1.243116	0.005402
3506	1.239922	0.003613	3416	1.243351	0.005362
3504	1.239871	0.003943	3414	1.243349	0.005073
3502	1.239774	0.004172	3412	1.243281	0.005153
3500	1.239728	0.004541	3410	1.243291	0.005201
3498	1.239771	0.005161	3408	1.243456	0.005202
3496	1.240145	0.005707	3406	1.243454	0.005002
3494	1.240705	0.006191	3404	1.243350	0.004859
3492	1.241618	0.006461	3402	1.243118	0.004932
3490	1.242368	0.006017	3400	1.243085	0.005083
3488	1.242827	0.005508	3398	1.243024	0.005203
3486	1.242971	0.005011	3396	1.243136	0.005339
3484	1.242857	0.004372	3394	1.243149	0.005374
3482	1.242401	0.004220	3392	1.243214	0.005344
3480	1.242234	0.004455	3390	1.243080	0.005436
3478	1.242354	0.004662	3388	1.243154	0.005562
3476	1.242427	0.004353	3386	1.243110	0.005733
3474	1.242384	0.004524	3384	1.243319	0.005808
3472	1.242531	0.004466	3382	1.243353	0.005977
3470	1.242462	0.004178	3380	1.243675	0.005785
3468	1.242299	0.004237	3370	1.243795	0.006333
3466	1.242262	0.004376	3368	1.243618	0.006301
3464	1.242255	0.004264	3366	1.243807	0.006594
3462	1.242097	0.004358	3364	1.243941	0.006809
3460	1.242046	0.004524	3362	1.244369	0.006895
3458	1.242150	0.004793	3360	1.244649	0.006876
3456	1.242283	0.004728	3358	1.244962	0.006639
3454	1.242335	0.004827	3356	1.244978	0.006453
3452	1.242544	0.004938	3354	1.245105	0.006425
3450	1.242697	0.004695	3352	1.245115	0.006271
3448	1.242632	0.004492	3350	1.245154	0.006216
3446	1.242404	0.004441	3348	1.245217	0.006326
3444	1.242223	0.004565	3346	1.245361	0.006135
3442	1.242120	0.004815	3344	1.245371	0.006120
3440	1.242202	0.005061	3342	1.245421	0.006041
3438	1.242327	0.005231	3340	1.245379	0.005986
3436	1.242543	0.005342	3338	1.245473	0.006135
3434	1.242731	0.005362	3336	1.245562	0.006030
3432	1.242888	0.005251	3334	1.245624	0.006011
3430	1.242914	0.005204	3332	1.245755	0.006122
3428	1.242982	0.005178	3330	1.245974	0.005933
3426	1.242956	0.005115	3328	1.246009	0.005727
3424	1.242948	0.005139	3326	1.245955	0.005567

Table 11. Continued

<u>$\nu, \text{ cm}^{-1}$</u>	<u>n</u>	<u>k</u>	<u>$\nu, \text{ cm}^{-1}$</u>	<u>n</u>	<u>k</u>
3324	1.245791	0.005486	3226	1.247980	0.004886
3322	1.245711	0.005618	3224	1.248032	0.004730
3320	1.245725	0.005751	3222	1.248047	0.004660
3310	1.246393	0.005628	3220	1.248079	0.004619
3308	1.246414	0.005468	3218	1.248211	0.004625
3306	1.246409	0.005425	3216	1.248295	0.004431
3304	1.246430	0.005372	3214	1.248312	0.004316
3302	1.246405	0.005268	3212	1.248351	0.004314
3300	1.246383	0.005323	3210	1.248460	0.004148
3298	1.246509	0.005389	3208	1.248485	0.004011
3296	1.246608	0.005202	3206	1.248434	0.003774
3294	1.246588	0.005093	3204	1.248283	0.003738
3292	1.246557	0.005070	3202	1.248245	0.003771
3290	1.246552	0.005008	3200	1.248227	0.003814
3288	1.246510	0.004978	3190	1.248419	0.003471
3286	1.246531	0.005026	3180	1.248482	0.003209
3284	1.246570	0.004974	3170	1.248493	0.002960
3282	1.246575	0.004909	3160	1.248588	0.002687
3280	1.246529	0.004892	3150	1.248604	0.002364
3278	1.246502	0.004905	3140	1.248497	0.001898
3276	1.246598	0.005030	3130	1.248358	0.001827
3274	1.246678	0.004849	3120	1.248235	0.001443
3272	1.246546	0.004706	3110	1.248011	0.001341
3270	1.246499	0.004945	3100	1.247919	0.001327
3268	1.246557	0.004890	3090	1.247978	0.001217
3266	1.246551	0.004901	3080	1.247914	0.000856
3264	1.246572	0.005028	3070	1.247625	0.000615
3262	1.246732	0.005058	3060	1.247502	0.000763
3260	1.246848	0.004972	3050	1.247486	0.000558
3258	1.246804	0.004768	3040	1.247317	0.000275
3256	1.246707	0.004881	3030	1.247071	0.000340
3254	1.246747	0.004959	3020	1.246928	0.000206
3252	1.246844	0.004987	3010	1.246863	0.000381
3250	1.246881	0.004920	3000	1.246793	0.000087
3248	1.246869	0.004931	2990	1.246654	0.000157
3246	1.246891	0.005014	2980	1.246492	0.000000
3244	1.246952	0.005042	2970	1.246384	0.000097
3242	1.247030	0.005107	2960	1.246284	0.000029
3240	1.247122	0.005134	2950	1.246194	0.000002
3238	1.247222	0.005165	2940	1.246058	0.0
3236	1.247415	0.005251	2930	1.245986	0.000008
3234	1.247606	0.005108	2920	1.245887	0.0
3232	1.247627	0.004929	2910	1.245818	0.0
3230	1.247651	0.005021	2900	1.245726	0.0
3228	1.247819	0.005020	2890	1.245664	0.0

Table 11. Continued

<u>v, cm⁻¹</u>	<u>n</u>	<u>k</u>	<u>v, cm⁻¹</u>	<u>n</u>	<u>k</u>
2880	1.245580	0.0	2430	1.241556	0.000114
2870	1.245521	0.0	2420	1.241361	0.000078
2860	1.245443	0.0	2410	1.241162	0.000122
2850	1.245386	0.0	2400	1.240892	0.000026
2840	1.245312	0.0	2390	1.240550	0.000038
2830	1.245256	0.0	2380	1.240137	0.000065
2820	1.245185	0.0	2370	1.239505	0.000048
2810	1.245129	0.0	2368	1.239393	0.000117
2800	1.245060	0.0	2366	1.239276	0.000202
2790	1.245005	0.0	2364	1.239168	0.000130
2780	1.244937	0.0	2362	1.238934	0.000118
2770	1.244881	0.0	2360	1.238616	0.000064
2760	1.244814	0.0	2358	1.238208	0.000175
2750	1.244757	0.0	2356	1.237698	0.000235
2740	1.244689	0.0	2354	1.236962	0.000480
2730	1.244631	0.0	2352	1.235078	0.000727
2720	1.244563	0.0	2350	1.233319	0.003967
2710	1.244503	0.0	2348	1.236576	0.010602
2700	1.244432	0.0	2346	1.243309	0.010054
2690	1.244367	0.0	2344	1.246004	0.003693
2680	1.244302	0.000013	2342	1.244356	0.001092
2670	1.244242	0.0	2340	1.242749	0.000413
2660	1.244166	0.0	2338	1.241891	0.000129
2650	1.244095	0.0	2336	1.241273	0.000091
2640	1.244020	0.0	2334	1.240863	0.000033
2630	1.243946	0.0	2332	1.240526	0.000076
2620	1.243866	0.0	2330	1.240295	0.000082
2610	1.243789	0.000002	2328	1.240102	0.000093
2600	1.243704	0.0	2326	1.239924	0.000056
2590	1.243621	0.0	2324	1.239740	0.000051
2580	1.243528	0.0	2322	1.239586	0.000052
2570	1.243433	0.0	2320	1.239432	0.000021
2560	1.243346	0.000023	2318	1.239266	0.000000
2550	1.243257	0.0	2316	1.239098	0.0
2540	1.243148	0.0	2314	1.238945	0.0
2530	1.243036	0.0	2312	1.238791	0.0
2520	1.242922	0.0	2310	1.238642	0.0
2510	1.242800	0.0	2308	1.238488	0.0
2500	1.242671	0.0	2306	1.238337	0.0
2490	1.242534	0.0	2304	1.238178	0.0
2480	1.242383	0.0	2302	1.238016	0.0
2470	1.242200	0.0	2300	1.237825	0.0
2460	1.242045	0.000075	2298	1.237656	0.000059
2450	1.241912	0.000093	2296	1.237523	0.000109
2440	1.241745	0.000062	2294	1.237366	0.000071

Table 11. Continued

<u>ν, cm⁻¹</u>	<u>n</u>	<u>k</u>	<u>ν, cm⁻¹</u>	<u>n</u>	<u>k</u>
2292	1.237186	0.000138	2202	1.229384	0.008309
2290	1.237053	0.000174	2200	1.228693	0.008274
2288	1.236899	0.000159	2198	1.229259	0.008061
2286	1.236696	0.000163	2196	1.228432	0.007727
2284	1.236507	0.000245	2194	1.228745	0.007339
2282	1.236372	0.000303	2192	1.227535	0.006920
2280	1.236255	0.000325	2190	1.227566	0.006611
2278	1.236097	0.000270	2188	1.226059	0.006290
2276	1.235901	0.000267	2186	1.225976	0.006131
2274	1.235663	0.000224	2184	1.224399	0.005898
2272	1.235387	0.000244	2182	1.224281	0.005518
2270	1.235133	0.000335	2180	1.222332	0.005038
2268	1.234921	0.000403	2178	1.221840	0.004565
2266	1.234722	0.000457	2176	1.219288	0.003931
2264	1.234507	0.000456	2174	1.218196	0.003449
2262	1.234197	0.000424	2172	1.214983	0.003021
2260	1.233875	0.000563	2170	1.213298	0.002399
2258	1.233602	0.000665	2168	1.208981	0.001901
2256	1.233359	0.000762	2166	1.206138	0.001497
2254	1.233123	0.000864	2164	1.200314	0.001245
2252	1.232870	0.000869	2162	1.195816	0.001170
2250	1.232544	0.000906	2160	1.187502	0.001318
2248	1.232167	0.000901	2158	1.179490	0.001935
2246	1.231754	0.001014	2156	1.165594	0.004163
2244	1.231343	0.001173	2154	1.151506	0.010685
2242	1.230549	0.001207	2152	1.133629	0.022710
2240	1.230347	0.001388	2150	1.117938	0.039256
2238	1.229208	0.001643	2148	1.097293	0.059488
2236	1.229156	0.001841	2146	1.064531	0.089090
2234	1.228573	0.002361	2144	0.975806	0.140012
2232	1.227850	0.003053	2142	1.046830	0.427410
2230	1.227915	0.003829	2140	1.357008	0.558077
2228	1.227123	0.004674	2138	1.549678	0.215395
2226	1.227495	0.005580	2136	1.499450	0.100639
2224	1.227171	0.006321	2134	1.432747	0.033736
2222	1.227912	0.006953	2132	1.393136	0.010363
2220	1.227610	0.007411	2130	1.355911	0.002580
2218	1.228332	0.007802	2128	1.339369	0.000044
2216	1.228007	0.008161	2126	1.321837	0.0
2214	1.228810	0.008478	2124	1.314686	0.0
2212	1.228552	0.008664	2122	1.304824	0.0
2210	1.229354	0.008671	2120	1.300834	0.0
2208	1.228932	0.008636	2118	1.294129	0.0
2206	1.229564	0.008508	2116	1.291502	0.0
2204	1.228903	0.008382	2114	1.286606	0.000243

Table 11. Continued

<u>v, cm⁻¹</u>	<u>n</u>	<u>k</u>	<u>v, cm⁻¹</u>	<u>n</u>	<u>k</u>
2112	1.285056	0.000320	1770	1.248668	0.0
2110	1.281297	0.000066	1760	1.248507	0.0
2108	1.279846	0.0	1750	1.248340	0.0
2106	1.276475	0.000002	1740	1.248157	0.0
2104	1.275187	0.000199	1730	1.247950	0.0
2102	1.272259	0.000462	1728	1.247901	0.0
2100	1.270948	0.000797	1726	1.247851	0.0
2098	1.267317	0.001339	1724	1.247794	0.0
2096	1.265161	0.004208	1722	1.247728	0.0
2094	1.265766	0.010460	1720	1.247631	0.000004
2092	1.271968	0.012123	1718	1.247546	0.000079
2090	1.275079	0.007070	1716	1.247513	0.000174
2088	1.274915	0.002911	1714	1.247525	0.000219
2086	1.272071	0.000840	1712	1.247528	0.000236
2084	1.270423	0.0	1710	1.247503	0.000215
2082	1.268291	0.0	1708	1.247480	0.000252
2080	1.267631	0.0	1706	1.247451	0.000221
2070	1.263601	0.0	1704	1.247373	0.000205
2060	1.261570	0.0	1702	1.247342	0.000301
2050	1.259549	0.0	1700	1.247343	0.000267
2040	1.258391	0.0	1698	1.247241	0.000193
2030	1.257083	0.0	1696	1.247150	0.000326
2020	1.256307	0.0	1694	1.247179	0.000391
2010	1.255385	0.0	1692	1.247203	0.000322
2000	1.254816	0.0	1690	1.247116	0.000241
1990	1.254132	0.0	1688	1.246944	0.000209
1980	1.253690	0.0	1686	1.246833	0.000368
1970	1.253163	0.0	1684	1.246828	0.000432
1960	1.252803	0.0	1682	1.246809	0.000410
1950	1.252388	0.0	1680	1.246730	0.000400
1940	1.252083	0.0	1678	1.246634	0.000401
1930	1.251750	0.0	1676	1.246501	0.000407
1920	1.251482	0.0	1674	1.246348	0.000464
1900	1.250971	0.0	1672	1.246243	0.000604
1880	1.250526	0.0	1670	1.246195	0.000678
1870	1.250323	0.0	1668	1.246123	0.000698
1860	1.250131	0.0	1666	1.245987	0.000718
1850	1.249949	0.0	1664	1.245782	0.000761
1840	1.249774	0.0	1662	1.245584	0.000942
1830	1.249607	0.0	1660	1.245426	0.001118
1820	1.249444	0.0	1658	1.245255	0.001303
1810	1.249286	0.0	1656	1.245073	0.001587
1800	1.249130	0.0	1654	1.245047	0.002006
1790	1.248977	0.0	1652	1.245147	0.002263
1780	1.248823	0.0	1650	1.245130	0.002322

Table 11. Continued

$\nu, \text{ cm}^{-1}$	n	k	$\nu, \text{ cm}^{-1}$	n	k
1648	1.244967	0.002573	1558	1.249776	0.000003
1646	1.244848	0.002987	1556	1.249684	0.000058
1644	1.244778	0.003437	1554	1.249651	0.000051
1642	1.244894	0.004172	1552	1.249586	0.000032
1640	1.245459	0.004933	1550	1.249522	0.000004
1638	1.246384	0.005240	1548	1.249431	0.0
1636	1.247111	0.004898	1546	1.249363	0.0
1634	1.247485	0.004576	1544	1.249247	0.0
1632	1.247716	0.004363	1542	1.249211	0.000107
1630	1.247915	0.004055	1540	1.249254	0.000165
1628	1.247982	0.003791	1538	1.249235	0.0
1626	1.247975	0.003506	1536	1.249145	0.000072
1624	1.247959	0.003354	1534	1.249138	0.000071
1622	1.247849	0.002941	1532	1.249070	0.0
1620	1.247461	0.002599	1530	1.249047	0.000100
1618	1.246747	0.002367	1528	1.249041	0.000043
1616	1.245796	0.002545	1526	1.249017	0.0
1614	1.244737	0.003226	1524	1.248931	0.0
1612	1.243808	0.004529	1522	1.248922	0.0
1610	1.243512	0.006644	1520	1.248844	0.0
1608	1.243857	0.008741	1510	1.248570	0.000024
1606	1.244752	0.011220	1508	1.248609	0.000121
1604	1.248435	0.015268	1506	1.248657	0.000152
1602	1.255131	0.015658	1504	1.248707	0.000060
1600	1.259668	0.009576	1502	1.248643	0.0
1598	1.259305	0.004155	1500	1.248590	0.0
1596	1.257085	0.001856	1498	1.248548	0.000019
1594	1.255405	0.000927	1496	1.248533	0.000012
1592	1.254197	0.000411	1494	1.248512	0.000027
1590	1.253304	0.000231	1492	1.248495	0.0
1588	1.252650	0.000158	1490	1.248460	0.0
1586	1.252141	0.000069	1488	1.248433	0.0
1584	1.251723	0.000105	1486	1.248407	0.0
1582	1.251427	0.000114	1484	1.248383	0.0
1580	1.251127	0.000061	1482	1.248358	0.0
1578	1.250899	0.000185	1480	1.248336	0.000002
1576	1.250782	0.000210	1478	1.248312	0.0
1574	1.250692	0.000172	1476	1.248290	0.0
1572	1.250525	0.000084	1474	1.248261	0.0
1570	1.250385	0.000122	1472	1.248229	0.0
1568	1.250247	0.000086	1470	1.248223	0.000043
1566	1.250172	0.000134	1468	1.248211	0.0
1564	1.250103	0.000104	1466	1.248185	0.000018
1562	1.250024	0.000020	1464	1.248159	0.000008
1560	1.249881	0.000013	1462	1.248117	0.0

Table 11. Concluded

<u>v, cm⁻¹</u>	<u>n</u>	<u>k</u>	<u>v, cm⁻¹</u>	<u>n</u>	<u>k</u>
1460	1.248034	0.000024	1090	1.245687	0.0
1458	1.248069	0.000188	1080	1.245544	0.0
1456	1.248182	0.000177	1070	1.245459	0.000047
1454	1.248212	0.000033	1060	1.245348	0.0
1452	1.248138	0.000011	1050	1.245230	0.0
1450	1.248100	0.000019	1040	1.245074	0.0
1440	1.247996	0.0	1030	1.244953	0.0
1430	1.247893	0.0	1020	1.244778	0.0
1420	1.247851	0.000099	1010	1.244636	0.0
1410	1.247822	0.0	1000	1.244429	0.0
1400	1.247731	0.0	990	1.244257	0.0
1390	1.247648	0.0	980	1.244002	0.0
1380	1.247573	0.0	970	1.243784	0.0
1370	1.247530	0.000043	960	1.243438	0.0
1360	1.247479	0.0	950	1.243064	0.0
1350	1.247411	0.0	940	1.242745	0.000307
1340	1.247341	0.0	930	1.242387	0.000112
1330	1.247286	0.0	920	1.241817	0.000310
1320	1.247220	0.0	910	1.241277	0.000486
1310	1.247169	0.0	900	1.240409	0.000459
1300	1.247102	0.0	890	1.239242	0.001066
1290	1.247050	0.0	880	1.237651	0.001952
1280	1.246983	0.0	870	1.236399	0.004478
1270	1.246931	0.0	860	1.237189	0.008387
1260	1.246863	0.0	850	1.240715	0.010543
1250	1.246811	0.0	840	1.243175	0.008523
1240	1.246740	0.0	830	1.242536	0.006441
1230	1.246687	0.0	820	1.242590	0.009110
1220	1.246611	0.0	810	1.243925	0.007899
1210	1.246558	0.0	800	1.243215	0.006310
1200	1.246472	0.0	790	1.242124	0.008092
1190	1.246403	0.0	780	1.242068	0.008698
1180	1.246344	0.000057	770	1.242727	0.010505
1170	1.246304	0.0	760	1.244175	0.011285
1160	1.246198	0.0	750	1.245739	0.010816
1150	1.246087	0.0	740	1.246217	0.009966
1140	1.246004	0.000094	730	1.246069	0.009155
1130	1.246027	0.000145	720	1.245261	0.009189
1120	1.245975	0.000024	710	1.244690	0.009611
1110	1.245850	0.0	700	1.243171	0.010179
1100	1.245752	0.000069			

Table 12. Optical Constants of 20°K Simulated Plume Mixture

<u>v, cm⁻¹</u>	<u>n</u>	<u>k</u>	<u>v, cm⁻¹</u>	<u>n</u>	<u>k</u>
3700	1.215081	0.009275	3610	1.213824	0.002032
3698	1.214256	0.009380	3608	1.212661	0.003538
3696	1.214063	0.009621	3606	1.213268	0.006475
3694	1.214346	0.009739	3604	1.215957	0.008318
3692	1.214828	0.010045	3602	1.219005	0.007255
3690	1.215359	0.009547	3600	1.220177	0.004940
3688	1.215395	0.009361	3598	1.220133	0.003480
3686	1.215791	0.009714	3596	1.219712	0.002621
3684	1.216436	0.009600	3594	1.219717	0.002153
3682	1.217035	0.009137	3592	1.219344	0.001112
3680	1.217369	0.008861	3590	1.218823	0.000623
3678	1.217597	0.008261	3588	1.218094	0.000469
3676	1.217712	0.008261	3586	1.217848	0.000494
3674	1.218106	0.008047	3584	1.217645	0.000600
3672	1.218494	0.007761	3582	1.217652	0.000186
3670	1.218925	0.007354	3580	1.217224	0.0
3668	1.219112	0.006709	3570	1.216023	0.0
3666	1.219143	0.006231	3560	1.215293	0.000500
3664	1.219091	0.005943	3550	1.214859	0.0
3662	1.219212	0.005687	3540	1.214160	0.000800
3660	1.219301	0.005389	3530	1.213027	0.0
3658	1.219563	0.005081	3520	1.212422	0.002700
3656	1.219629	0.004480	3510	1.212988	0.003100
3654	1.219473	0.003867	3500	1.213587	0.003800
3652	1.219317	0.003800	3490	1.214070	0.004100
3650	1.219412	0.003346	3480	1.214878	0.004300
3648	1.219052	0.002651	3470	1.215099	0.003700
3646	1.218756	0.002716	3460	1.215283	0.003900
3644	1.218649	0.002533	3450	1.215440	0.003800
3642	1.218620	0.002141	3440	1.215659	0.003600
3640	1.218251	0.001805	3430	1.215579	0.003600
3638	1.217901	0.001545	3420	1.215671	0.003600
3636	1.217522	0.001630	3410	1.215852	0.003900
3634	1.217257	0.001400	3400	1.216100	0.003600
3632	1.216806	0.001514	3390	1.216137	0.003700
3630	1.216697	0.001785	3380	1.216365	0.003800
3628	1.216543	0.001736	3370	1.216733	0.003800
3626	1.216505	0.001854	3360	1.217120	0.003600
3624	1.216500	0.001934	3350	1.217338	0.003200
3622	1.216403	0.001488	3340	1.217493	0.003000
3620	1.215900	0.001521	3330	1.217620	0.002600
3618	1.215666	0.001756	3320	1.217743	0.002300
3616	1.215449	0.001859	3310	1.217672	0.001700
3614	1.215306	0.001916	3300	1.217346	0.001300
3612	1.214791	0.001875	3290	1.216983	0.001200

Table 12. Continued

<u>v, cm⁻¹</u>	<u>n</u>	<u>k</u>	<u>v, cm⁻¹</u>	<u>n</u>	<u>k</u>
3280	1.216813	0.001200	2830	1.211457	0.0
3270	1.216478	0.000900	2820	1.211285	0.0
3260	1.216159	0.001200	2810	1.211095	0.0
3250	1.216029	0.001400	2800	1.210907	0.0
3240	1.216197	0.001700	2790	1.210705	0.0
3230	1.216442	0.001700	2780	1.210508	0.0
3220	1.216709	0.001500	2770	1.210284	0.0
3210	1.216747	0.001200	2760	1.210056	0.0
3200	1.216697	0.000900	2750	1.209824	0.0
3190	1.216598	0.000800	2740	1.209590	0.0
3180	1.216533	0.000500	2730	1.209321	0.0
3170	1.216312	0.000300	2720	1.209006	0.0
3160	1.216117	0.000200	2710	1.208768	0.0
3150	1.215917	0.000100	2700	1.208431	0.0
3140	1.215715	0.0	2690	1.208154	0.0
3130	1.215489	0.0	2680	1.207780	0.0
3120	1.215334	0.0	2670	1.207468	0.0
3110	1.215175	0.0	2660	1.207041	0.0
3100	1.215047	0.0	2650	1.206697	0.0
3090	1.214904	0.0	2640	1.206271	0.0
3080	1.214788	0.0	2630	1.205822	0.0
3070	1.214655	0.0	2620	1.205176	0.0
3060	1.214544	0.0	2610	1.204818	0.0
3050	1.214415	0.0	2600	1.204292	0.0
3040	1.214307	0.0	2590	1.203655	0.0
3030	1.214180	0.0	2580	1.203162	0.0
3020	1.214072	0.0	2570	1.202288	0.0
3010	1.213946	0.0	2560	1.201524	0.0
3000	1.213836	0.0	2550	1.200659	0.0
2990	1.213709	0.0	2540	1.199741	0.0
2980	1.213597	0.0	2530	1.198680	0.0
2970	1.213467	0.0	2520	1.197517	0.0
2960	1.213351	0.0	2510	1.196220	0.0
2950	1.213218	0.0	2500	1.194758	0.0
2940	1.213098	0.0	2490	1.193076	0.0
2930	1.212960	0.0	2480	1.191149	0.0
2920	1.212834	0.0	2470	1.188900	0.0
2910	1.212691	0.0	2460	1.186220	0.000000
2900	1.212558	0.0	2458	1.185599	0.000000
2890	1.212409	0.0	2456	1.184963	0.000056
2880	1.212268	0.0	2454	1.184367	0.000145
2870	1.212110	0.0	2452	1.183763	0.000114
2860	1.211961	0.0	2450	1.183084	0.000116
2850	1.211794	0.0	2448	1.182348	0.000112
2840	1.211633	0.0	2446	1.181611	0.000160

Table 12. Continued

$\nu, \text{ cm}^{-1}$	n	k	$\nu, \text{ cm}^{-1}$	n	k
2444	1.180854	0.000210	2352	0.694267	0.540940
2442	1.180087	0.000222	2350	0.808144	0.745030
2440	1.179262	0.000271	2348	1.021717	0.931720
2438	1.178431	0.000301	2346	1.379764	1.030800
2436	1.177594	0.000378	2344	1.776525	0.877880
2434	1.176759	0.000345	2342	1.930187	0.415660
2432	1.175774	0.000234	2340	1.803969	0.138500
2430	1.174710	0.000244	2338	1.653760	0.078657
2428	1.173592	0.000255	2336	1.572210	0.029726
2426	1.172471	0.000294	2334	1.506116	0.012437
2424	1.171285	0.000331	2332	1.458468	0.008348
2420	1.168764	0.000266	2330	1.428012	0.010091
2418	1.167330	0.000245	2328	1.408325	0.008914
2416	1.165835	0.000252	2326	1.391024	0.002972
2414	1.164240	0.000246	2324	1.374095	0.000001
2412	1.162547	0.000234	2320	1.347470	0.0
2410	1.160693	0.000226	2310	1.310493	0.0
2408	1.158752	0.000254	2300	1.289457	0.0
2406	1.156635	0.000303	2290	1.274252	0.000000
2404	1.154426	0.000354	2288	1.270584	0.000001
2402	1.152013	0.000468	2286	1.265558	0.001166
2400	1.149488	0.000566	2284	1.261706	0.006881
2398	1.146756	0.000743	2282	1.265238	0.016040
2396	1.143923	0.000862	2280	1.274066	0.015936
2394	1.140792	0.000932	2278	1.277600	0.006289
2392	1.137430	0.000953	2276	1.273477	0.000265
2390	1.133573	0.000900	2274	1.268815	0.000001
2388	1.129388	0.000958	2270	1.264272	0.0
2386	1.124715	0.001038	2260	1.257555	0.0
2384	1.119621	0.000964	2250	1.252687	0.0
2382	1.113664	0.000907	2240	1.248827	0.0
2380	1.107068	0.000887	2230	1.245501	0.0
2378	1.099310	0.000814	2220	1.242633	0.0
2376	1.090501	0.000763	2210	1.239920	0.0
2374	1.079812	0.000761	2200	1.237371	0.0
2372	1.067416	0.001003	2190	1.234590	0.0
2370	1.051959	0.001502	2180	1.231487	0.0
2368	1.033479	0.002682	2170	1.226790	0.0
2366	1.009559	0.004943	2160	1.216233	0.000000
2364	0.979234	0.008995	2158	1.211524	0.000646
2362	0.936442	0.018013	2156	1.205086	0.004471
2360	0.882099	0.039828	2154	1.200090	0.012115
2358	0.812599	0.085186	2152	1.198679	0.022256
2356	0.723610	0.158950	2150	1.200304	0.030764
2354	0.668587	0.340720	2148	1.200479	0.037437

Table 12. Continued

<u>v, cm⁻¹</u>	<u>n</u>	<u>k</u>	<u>v, cm⁻¹</u>	<u>n</u>	<u>k</u>
2146	1.200132	0.050521	1740	1.223461	0.0
2144	1.211075	0.073367	1730	1.223211	0.0
2142	1.241948	0.089953	1720	1.222941	0.0
2140	1.277483	0.076495	1710	1.222637	0.0
2138	1.294404	0.044058	1700	1.222290	0.0
2136	1.289880	0.017328	1690	1.221871	0.0
2134	1.277281	0.004191	1680	1.221339	0.0
2132	1.266084	0.000001	1670	1.220587	0.0
2130	1.259112	0.0	1662	1.219627	0.000000
2120	1.246832	0.0	1660	1.219234	0.000000
2110	1.242194	0.0	1658	1.218736	0.000097
2100	1.239455	0.0	1656	1.218217	0.000396
2090	1.237612	0.0	1654	1.217799	0.000812
2080	1.236184	0.0	1652	1.217458	0.001241
2070	1.235066	0.0	1650	1.217095	0.001646
2060	1.234108	0.0	1648	1.216723	0.002222
2050	1.233306	0.0	1646	1.216464	0.002922
2040	1.232585	0.0	1644	1.216318	0.003626
2030	1.231958	0.0	1642	1.216250	0.004371
2020	1.231380	0.0	1640	1.216285	0.005174
2010	1.230865	0.0	1638	1.216415	0.005971
2000	1.230382	0.0	1636	1.216721	0.006877
1990	1.229945	0.0	1634	1.217343	0.007768
1980	1.229532	0.0	1632	1.218171	0.008266
1970	1.229152	0.0	1630	1.219135	0.008580
1960	1.228790	0.0	1628	1.219971	0.008241
1950	1.228453	0.0	1626	1.220239	0.007498
1940	1.228132	0.0	1624	1.219739	0.006934
1930	1.227830	0.0	1622	1.218622	0.006826
1920	1.227540	0.0	1620	1.217096	0.007696
1900	1.227000	0.0	1618	1.215804	0.009838
1880	1.226502	0.0	1616	1.215607	0.013266
1870	1.226265	0.0	1614	1.217222	0.017068
1860	1.226036	0.0	1612	1.220834	0.020352
1850	1.225813	0.0	1610	1.226051	0.021861
1840	1.225596	0.0	1608	1.231624	0.020756
1830	1.225382	0.0	1606	1.236077	0.017308
1820	1.225173	0.0	1604	1.238452	0.012666
1810	1.224965	0.0	1602	1.238752	0.008129
1800	1.224759	0.0	1600	1.237593	0.004591
1790	1.224552	0.0	1598	1.235867	0.002229
1780	1.224345	0.0	1596	1.233941	0.000709
1770	1.224134	0.0	1594	1.232242	0.000001
1760	1.223919	0.0	1590	1.229902	0.0
1750	1.223695	0.0	1580	1.227531	0.0

Table 12. Concluded

<u>v, cm⁻¹</u>	<u>n</u>	<u>k</u>	<u>v, cm⁻¹</u>	<u>n</u>	<u>k</u>
1570	1.226382	0.0	1130	1.219088	0.0
1560	1.225638	0.0	1120	1.218940	0.0
1550	1.225118	0.0	1110	1.218790	0.0
1540	1.224708	0.0	1100	1.218632	0.0
1530	1.224384	0.0	1090	1.218468	0.0
1520	1.224104	0.0	1080	1.218298	0.0
1510	1.223869	0.0	1070	1.218121	0.0
1500	1.223654	0.0	1060	1.217935	0.0
1490	1.223466	0.0	1050	1.217739	0.0
1480	1.223289	0.0	1040	1.217536	0.0
1470	1.223129	0.0	1030	1.217318	0.0
1460	1.222975	0.0	1020	1.217092	0.0
1450	1.222834	0.0	1010	1.216846	0.0
1440	1.222696	0.0	1000	1.216594	0.0
1430	1.222568	0.0	990	1.216313	0.0
1420	1.222440	0.0	980	1.216025	0.0
1410	1.222321	0.0	970	1.215700	0.0
1400	1.222200	0.0	960	1.215366	0.0
1390	1.222087	0.0	950	1.214978	0.0
1380	1.221972	0.0	940	1.214581	0.0
1370	1.221863	0.0	930	1.214101	0.0
1360	1.221751	0.0	920	1.213608	0.0
1350	1.221645	0.0	910	1.212972	0.0
1340	1.221535	0.0	900	1.212310	0.0
1330	1.221431	0.0	890	1.211289	0.0
1320	1.221322	0.0	880	1.209555	0.0
1310	1.221218	0.0	870	1.207913	0.002200
1300	1.221110	0.0	860	1.208694	0.005100
1290	1.221005	0.0	850	1.211262	0.005800
1280	1.220897	0.0	840	1.210937	0.001700
1270	1.220792	0.0	830	1.208871	0.002900
1260	1.220681	0.0	820	1.207997	0.003800
1250	1.220573	0.0	810	1.207365	0.003200
1240	1.220460	0.0	800	1.206484	0.004700
1230	1.220349	0.0	790	1.205145	0.003300
1220	1.220234	0.0	780	1.202433	0.004600
1210	1.220120	0.0	770	1.201271	0.007700
1200	1.219999	0.0	760	1.201720	0.008900
1190	1.219879	0.0	750	1.201752	0.008700
1180	1.219755	0.0	740	1.200085	0.007300
1170	1.219631	0.0	730	1.196445	0.006400
1160	1.219499	0.0	720	1.191063	0.006500
1150	1.219366	0.0	710	1.184139	0.007700
1140	1.219228	0.0	700	1.174786	0.009705